Biomaterials 320 (2025) 123288

Contents lists available at ScienceDirect

Biomaterials

journal homepage: www.elsevier.com/locate/biomaterials

# Force-electric biomaterials and devices for regenerative medicine

Shuncheng Yao [a,b,1], Xi Cui [b,d,1], Chao Zhang [d,*], Wenguo Cui [a,**], Zhou Li [b,c,***]

[a] Department of Orthopaedics, Shanghai Key Laboratory for Prevention and Treatment of Bone and Joint Diseases, Shanghai Institute of Traumatology and Orthopaedics, Ruijin Hospital, Shanghai Jiao Tong University School of Medicine, Shanghai, 200025, China
[b] Beijing Institute of Nanoenergy and Nanosystems, Chinese Academy of Sciences, Beijing, 101400, China
[c] School of Nanoscience and Engineering, Chinese Academy of Sciences, Beijing, 100049, China
[d] School of Biomedical Engineering, Shenzhen Campus of Sun Yat-Sen University, Shenzhen, 518107, China

ARTICLE INFO

*Keywords:*
Force-electric conversion
Piezoelectric
Triboelectric
Electroactive
Regenerative medicine

ABSTRACT

There is a growing recognition that force-electric conversion biomaterials and devices can convert mechanical energy into electrical energy without an external power source, thus potentially revolutionizing the use of electrical stimulation in the biomedical field. Based on this, this review explores the application of force-electric biomaterials and devices in the field of regenerative medicine. The article focuses on piezoelectric biomaterials, piezoelectric devices and triboelectric devices, detailing their categorization, mechanisms of electrical generation and methods of improving electrical output performance. Subsequently, different sources of driving force for electroactive biomaterials and devices are explored. Finally, the biological applications of force-electric biomaterials and devices in regenerative medicine are presented, including tissue regeneration, functional modulation of organisms, and electrical stimulation therapy. The aim of this review is to emphasize the role of electrical stimulation generated by force-electric conversion biomaterials and devices on the regulation of bioactive molecules, ion channels and information transfer in living systems, and thus affects the metabolic processes of organisms. In the future, physiological modulation of electrical stimulation based on force-electric conversion is expected to bring important scientific advances in the field of regenerative medicine.

## 1. Introduction

As human society continues to develop, human concern for their own health is increasing. However, the rapid ageing of the population, unhealthy diets and the occurrence of accidents have placed a heavy burden on the socio-economic system. The emergence of regenerative medicine not only provides personalized treatment options, but also leads to innovative treatments such as cell therapy [1,2], tissue engineering [3,4] and stem cell technology [5,6]. At the same time, these therapeutic processes can integrate material science and biological engineering approaches [7,8], which is expected to revolutionize the existing medical model and bring better treatment outcomes and quality of life to patients. Bioelectricity, as a fundamental feature of biological systems [9], plays a crucial role in the development of regenerative medicine. The generation of bioelectricity is related to the segregation of biofilm formation as well as the distribution and flow of ions on both sides of these membranes, and the resulting bioelectricity can be involved in the regulation of gene expression, intercellular information transfer, and cell growth and differentiation. Therefore, electrical stimulation has attracted great attention as a way to effectively regulate bioelectricity. It has been found that electrical stimulation can effectively modulate cellular life activities, such as cell survival, migration, proliferation, or differentiation downstream of cells, leading to advances in wound healing [10,11], stem cell differentiation [12,13], nerve regeneration [14,15], tumor therapy [16,17], and bone repair [18,19]. However, the conventional electrical stimulation application process has the problems of temporal and spatial limitations of complex power supply devices, poor patient compliance, and the risk of surgical

This article is part of a special issue entitled: Regenerative Bioelectronics published in Biomaterials.

* Corresponding author.
** Corresponding author.
*** Corresponding author. Beijing Institute of Nanoenergy and Nanosystems, Chinese Academy of Sciences, Beijing 101400, China.
*E-mail addresses:* wgcui@sjtu.edu.cn (C. Zhang), zhchao9@mail.sysu.edu.cn (W. Cui), zli@binn.cas.cn (Z. Li).
[1] These authors contributed equally to this work.

https://doi.org/10.1016/j.biomaterials.2025.123288
Received 13 December 2024; Received in revised form 2 March 2025; Accepted 23 March 2025
Available online 24 March 2025

infections, which limit the further development of electrical stimulation in the field of regenerative medicine.

The human body generates a large amount of biomechanical energy during physical activity, cardiopulmonary exercise, and blood circulation. In addition, the introduction of external stimuli such as ultrasound (US), light and magnetic fields can also cause changes in mechanical energy [20]. Force-electric converting biomaterials and devices with piezoelectric and triboelectric effects can convert these mechanical energies into electrical energies, thus getting rid of the problems associated with conventional power supply devices [21,22]. Since piezoelectric materials not only respond to subtle mechanical force changes and generate electrical signals, but also have good biocompatibility and degradability. Meanwhile, piezoelectric nanogenerators (PENGs) can achieve reversible conversion of mechanical and electrical energy, thus realizing efficient electromechanical coupling and fast response. In recent years, with the emergence of piezoelectric biomaterials and the development of new processing technologies, PENGs have developed rapidly and made significant progress in the fields of biomedicine and nanotechnology [23,24]. In addition, triboelectric nanogenerators (TENGs) based on the contact electrification (CE) and electrostatic induction coupling effects, as a rapidly developing energy harvesting device, can convert ambient mechanical energy into electrical energy. TENG has attracted the attention of many researchers due to its many advantages such as low cost, light weight, high charge density, wide range of material choices, and flexible structure [25,26]. In the past five years, there are three main categories of applications of TENG as a kind of electrical stimulator in the field of regenerative medicine. The first category is the direct generation of electrical stimulation by TENG [27]; the second category is the self-driven devices or microsystems performing interventional therapeutic tasks [28]; and the third category is the implantable microsystems based on TENG to drive the long-term operation of implantable medical devices in vivo [29]. However, the weak and uncertain nature of the ambient mechanical forces results in weak electrical output of TENG/PENG. With the emergence of new materials and the development of processing techniques, some parameter adjustments can effectively enhance the output performance of PENG/TENG, thus promoting the development of PENG/TENG in the field of regenerative medicine.

This review paper aims to overview various applications of force-electric biomaterials and devices based on piezoelectric and triboelectric effects in the field of regenerative medicine (Fig. 1). In order to better promote the development of piezoelectric and triboelectric biomaterials and devices in the field of regenerative medicine, this review will firstly introduce typical piezoelectric and triboelectric biomaterials as well as their force-electric conversion mechanisms, which will provide ideas for the preparation of electrostimulation devices and the enhancement of electrical output performance. Subsequently, the power generation modes and generator mechanisms of PENG/TENG electrostimulation devices will be introduced so as to expand their potential applications in the field of regenerative medicine. Based on the force-electric conversion properties possessed by electroactive materials and devices, different force-driven modes (biological movement, cellular traction and physical signals) required for the application of electroactive materials and devices in the field of regenerative medicine will be discussed in the next section, which is expected to expand the in vivo and ex vivo application scenarios of force-electric biomaterials and devices. The next section summarizes the applications of biomaterials and devices with force-electric conversion effects in the field of regenerative medicine, mainly in the regeneration and functional modulation of tissues such as nerves, bones, skin and muscles, as well as in the treatment

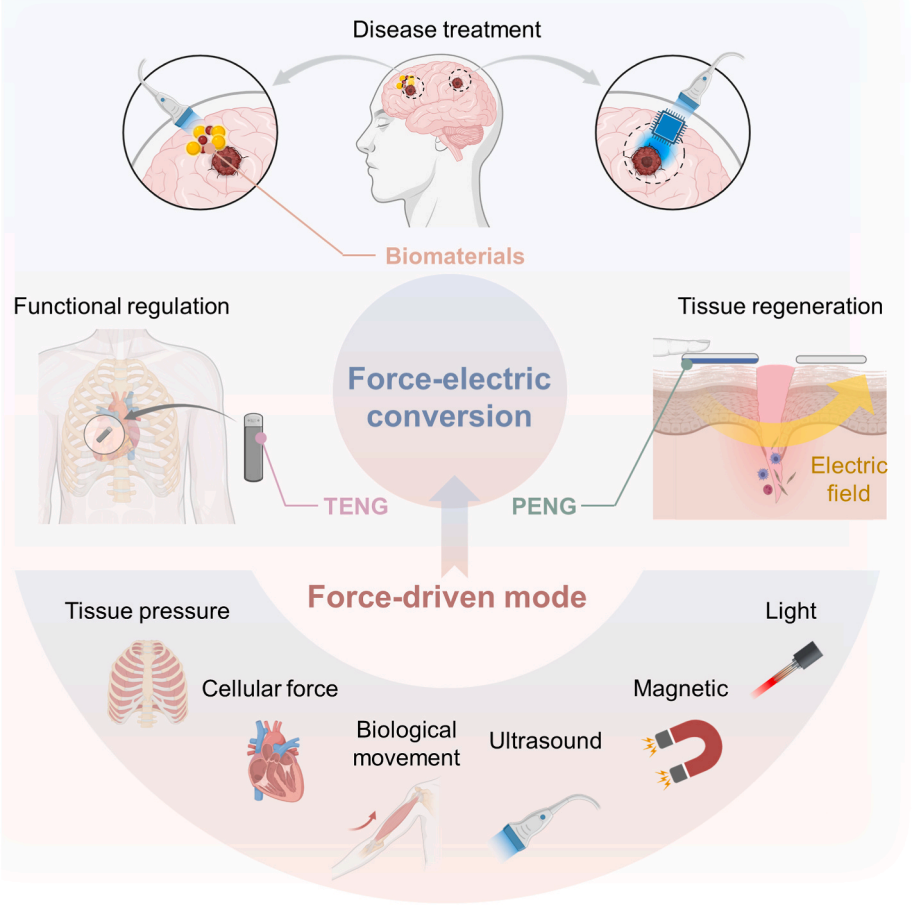


**Fig. 1.** Force-electric biomaterials and devices for regenerative medicine under different force-driven modes.

of diseases. Finally, challenges and opportunities in the application of force-electric biomaterials and devices in the field of regenerative medicine are overviewed.

## 2. Piezoelectric biomaterials based on force-electric conversion

In 1880, the Curie brothers revealed the piezoelectric effect in piezoelectric materials for the first time in their published paper [30], which laid the fundamental working principle of piezoelectric materials. The piezoelectric effect is specifically described as follows: When certain specific dielectrics undergo deformation along a certain direction due to external force, polarization occurs internally, resulting in the accumulation of opposite charges on the two opposite surfaces of the material. Once the external force is removed, the material will revert to its initial uncharged state, a phenomenon termed the direct piezoelectric effect. Conversely, if an electric field is applied in the polarization direction of these dielectrics, they will also undergo deformation, and the deformation will disappear when the electric field is removed, known as the converse piezoelectric effect [31]. Based on the direction of applied stress, two primary piezoelectric modes can be distinguished: longitudinal mode ($d_{33}$) and transverse mode ($d_{31}$) [32]. Specifically, when stress/strain is applied parallel to the 3-axis direction of the piezoelectric material, if the generated potential also occurs along the same axis direction, this design mode is referred to as the $d_{33}$ mode; if the potential is perpendicular to the direction of applied stress/strain (i.e., the 1-direction), it is termed the $d_{31}$ mode. Additionally, a special piezoelectric direction, namely $d_{14}$, has been observed in piezoelectric polymers. In this scenario, when stress is applied in the shear direction (1-direction), a potential is generated in a specific polarization direction (4-direction). Notably, when piezoelectric materials are subjected to shear forces, another known shear mode exists, namely $d_{15}$ mode. These different piezoelectric modes and directions not only enrich the application fields of piezoelectric materials but also provide an important theoretical basis for scientific research in related fields.

Piezoelectric materials are a direct manifestation of the force-electric conversion effect and are crucial components in many modern devices, such as sonar [33], medical US [34], sensors, actuators [35], and vibration-driven electronic equipment [36,37]. Their piezoelectric effect is attributed to their non-centrosymmetric structure, where the positive and negative charge centers do not coincide. Based on the properties of piezoelectric materials, they can be classified into: piezoelectric ceramics, piezoelectric polymers, piezoelectric hydrogels, piezoelectric biomolecules, and composite piezoelectric materials. As shown in Fig. 2, we have summarized here the types of piezoelectric materials and their common processing in order to enhance piezoelectricity.

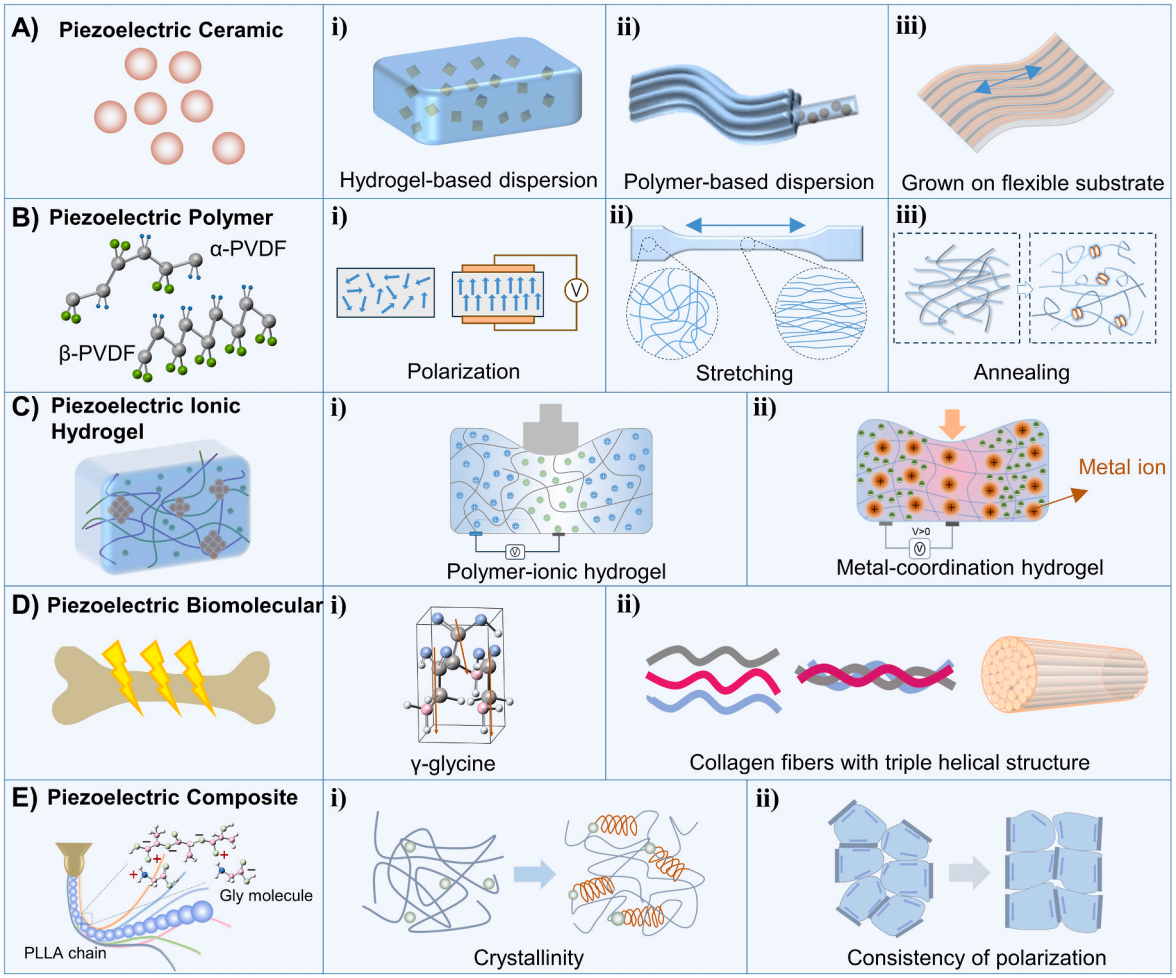


**Fig. 2.** Types of piezoelectric materials and their common forms or processing methods to enhance piezoelectricity. A) Piezoelectric ceramic. i) piezoelectric ceramic particles distributed in hydrogels; ii) piezoelectric ceramic particles distributed in polymers; iii) oriented growth of piezoelectric ceramics on flexible substrates. B) Piezoelectric polymers. i) high-voltage electric field polarization; ii) molecular orientation by stretching; iii) crystallinity increase by high temperature annealing. C) Piezoelectric ionic hydrogel. i) polymer-ionic hydrogel; ii) metal-coordination hydrogel. D) Piezoelectric biomolecular. i) γ-glycine, ii) Triple helix piezoelectric collagen fibers. E) Piezoelectric composites. i) improvement of piezoelectricity by increasing crystallinity, ii) improvement of piezoelectricity by increasing the degree of polarization.

### 2.1. Piezoelectric ceramics

Piezoelectric ceramics are primarily composed of ferroelectric grains. Due to the polycrystalline nature of ceramics, with grains randomly oriented, the spontaneous polarization vectors of individual ferroelectric grains are also randomly oriented. To exhibit macroscopic piezoelectric properties, the ceramics undergo polarization treatment after sintering and electrode application. This process involves exposing the ceramics to a strong direct current electric field, causing the originally disordered spontaneous polarization vectors to align preferentially along the electric field direction. After polarization treatment, even when the electric field is removed, the ceramics retain a certain macroscopic residual polarization intensity, thereby acquiring piezoelectric properties.

Piezoelectric ceramics can be classified into lead-based and lead-free categories. Lead-based ceramics, such as lead zirconate titanate (PZT), Pb $(Mg_{1/3}Nb_{2/3})$ $O_3$ (PMN), and $Pb_{0.96}Sr_{0.04}(Zr_x,\ Ti_{1-x})_{0.7}(Zn_{1/3}Nb_{2/3})_{0.3}O_3$ (PNZT), composed mainly of lead, zirconium, and titanium, exhibit high piezoelectric coefficients and good stability, making them widely used in sensors and electro-acoustic devices. However, the toxicity of lead limits their application in biology. Lead-free piezoelectric ceramics, on the other hand, include barium titanate ($BiTiO_3$-based), sodium bismuth titanate (BNT-based), potassium sodium niobate [(K, Na) $NbO_3$-based] (KNN-based), and bismuth-layered structures (such as bismuth titanate $Bi_4Ti_3O_{12}$, calcium bismuth titanate $CaBi_4Ti_4O_{15}$, and strontium bismuth titanate $SrBi_4Ti_4O_{15}$). Lead-free piezoelectric ceramics exhibit excellent sintering stability, with surfaces that are easy to process and adhere well to other materials.

Most traditional piezoelectric ceramic materials are bulky and fragile, limiting their application in regenerative medicine. In response, researchers have conducted extensive studies on the flexibilization of piezoelectric ceramics while ensuring sufficient electromechanical conversion efficiency. Two common strategies are employed: one involves preparing ceramics into nano- or micrometer-sized particles and doping them into flexible materials or dispersing them in hydrogel systems (Fig. 2A ⓘ-ii). For instance, Zhu et al. processed tetragonal $BaTiO_3$ nanoparticles (BTO NPs) into an injectable system for ultrasonic piezoelectric generation of internal electric fields, catalyzing the production of reactive oxygen species (ROS) to achieve tumor eradication [38]. Shan et al. processed BTO particles into polylactic acid (PLA) nanofibers to create flexible implantable sensors for monitoring neural repair after injury [39]. As shown in Fig. 2A iii, the other strategy involves processing ceramics onto the surface of flexible substrates using methods such as chemical lift-off, laser lift-off [40], wet etching [41], liquid-phase synthesis [42], and gravity sintering [43] to create discontinuous microstructures, thereby enhancing flexibility. For example, Xu et al. employed a biomimetic soft-rigid hybrid strategy to fabricate droplet-shaped ceramics with damage-resistant properties on a superhydrophobic surface using the freeze-casting method. As rigid components, their unique arched surfaces and rounded corners effectively disperse stress during deformation, preventing fracture. Liquid metal (gallium-indium eutectic, EGaIn) was patterned into customized soft circuits to maintain nearly constant resistance during high-level deformation and form direct, stable electrical connections with the piezoelectric ceramics, achieving excellent sensitivity and durability [44]. Additionally, Liu et al. prepared high-piezoelectric-effect PZT films (piezoelectric charge constant $d_{33} \approx 271$ pC $N^{-1}$) on flexible zirconia ribbon ceramics (ZRC) substrates using a low-cost one-step sol-gel method [45]. Yuvasree et al. prepared lead-free (K, Na)$NbO_3$-based piezoelectric ceramics textured along the (001) direction using $NaNbO_3$ (NN) seeds and investigated the variation in dielectric and piezoelectric properties of KNN-xNN (x = 0, 3, 5, 7 wt%) materials with sintering temperature and texturing degree [46]. In this strategy of fabricating ceramics into micro- or nanostructures, the nanostructures further enhance the effective piezoelectric constant due to the size effect [47]. Meanwhile, researchers have also turned their attention to piezoelectric polymers.

### 2.2. Piezoelectric polymers

The piezoelectric polymers, despite exhibiting a lower piezoelectric coefficient compared to piezoelectric ceramics, offer significant advantages in regenerative medicine due to their flexible processing methods, adjustable elastic moduli, excellent biocompatibility, abundant availability, and low cost. Unlike ceramics, which possess a well-defined crystalline structure, polymers are composed of long molecular chains. These chains can form small crystalline regions surrounded by amorphous areas. Piezoelectric polymers also possess a non-centrosymmetric structure. Regarding the contribution of either the crystalline or amorphous regions to polymer piezoelectricity, there exist contradictory model theories (molecular models). While most studies attribute the piezoelectricity of polymers to their crystalline regions, research by Katsouras et al. has shown that some piezoelectric polymers exhibit significant relaxation near the glass transition temperature, a characteristic of amorphous polymers, thus confirming that amorphous polymer chains have a certain degree of influence on the piezoelectricity of these polymers [31,48,49].

Polyvinylidene fluoride (PVDF) was the first synthetic polymer discovered to possess good piezoelectric properties (first discovery). Subsequently, the confirmation of its pyroelectric and ferroelectric behaviors (pyroelectricity, ferroelectricity) quickly garnered the attention of many researchers. Following this, piezoelectric behavior was identified in several other polymer families (discovery of piezoelectric polymers). PVDF exhibits a planar conformation of its polymer chains, making it insufficient for the simple arrangement of molecules to eliminate the non-centrosymmetric center (Fig. 2B). However, it can exhibit ferroelectric behavior under a strong electric field through polarization, ultimately demonstrating piezoelectricity in both normal and shear directions. Poly(L-lactic acid) (PLLA) differs from PVDF in that it does not require polarization but only simple alignment of its polymer chains to eliminate the symmetric center. Due to its asymmetric carbon distribution, PLLA exhibits piezoelectricity only in the shear direction ($d_{14}$), which explains the origin of natural piezoelectric materials in organisms [50]. These materials possess piezoelectricity in vivo without being polarized or stretched, relying solely on the ordered arrangement of molecules.

The piezoelectric properties of piezoelectric polymers are closely dependent on their processing methods, which commonly include annealing, stretching, and polarization (Fig. 2B ⓘ-iii). These processes are interrelated to some extent, and performing one process may affect the outcome of another.

Polarization is the process of aligning dipoles in a material by applying an external strong electric field, which is only applicable to ferroelectric materials. This is because spontaneous residual polarization exists only in ferroelectric materials and can be switched by a strong electric field. In polycrystalline ferroelectric materials, the polarization of individual grains may be randomly oriented, and even in single-crystalline ferroelectric materials, there may be multiple domains with random orientations. This random orientation results in isotropy of the material, manifesting macroscopically as non-piezoelectric behavior. In such cases, fully aligning the dipole moments through polarization is necessary for piezoelectricity [51–54]. The polarization process can be achieved by directly applying a high-voltage electric field to the material surface or using electrical needle corona polarization. It should be noted that piezoelectric electrets and voided charged polymers also exhibit surface charges induced by polarization, but this is distinct from the piezoelectric behavior of piezoelectric materials [55].

Stretching is a common method in polymer processing that ensures the formation of strong alignments of polymer chains along the stretching direction, achieving anisotropy. The parallel alignment of certain polymer chains is a sufficient condition for their piezoelectricity, including PLLA, Poly-β-hydroxybutyrate-co-β-hydroxyvalerate,

Polyhydroxybutyrate, cellulose, and collagen chains. Their piezoelectric coefficients generally increase with the stretching ratio [49]. For PVDF, stretching leads to transitions between its crystalline phases. PVDF encompasses five polymorphs: α-phases, β-phases, γ-phases, σ-phases, and ε-phases [56]. During stretching, the α-phase of PVDF transforms into the β-phase with the strongest polar moment, which determines the piezoelectric potential of the polymer. The copolymer of PVDF, P (VDF-TrFE), can spontaneously crystallize into the polar β-phase, indicating that stretching is not the sole condition for obtaining the polar phase.

Annealing, a heat treatment process, serves to increase the crystallinity of polymers, i.e., to elevate the proportion of crystalline regions within the polymer. Annealing is a common processing step for piezoelectric polymer materials. Several studies have investigated the relationship between annealing time, temperature, and the crystallinity and piezoelectricity of polymers [57–59], typically with annealing temperatures ranging from 80 to 140 °C and durations varying from minutes to hours [60]. However, annealing is not always beneficial in polymers. For instance, nylon requires a rapid quenching process to obtain a disordered intermediate crystalline structure, which is necessary for the rotation and switching of its dipoles. The ordered polymer chains induced by annealing can inhibit dipole rotation, thereby reducing its ferroelectric and piezoelectric properties [61,62]. To achieve macroscopic piezoelectric properties, it is essential to maintain the anisotropy of the polymer crystalline units, which necessitates processing steps beyond annealing.

### 2.3. Piezoelectric hydrogel

Unlike doping piezoelectric ceramics or polymers into hydrogels to achieve a piezoelectric effect, the piezoelectric hydrogels discussed here share similarities with the mechanism of gated ion migration in skin nerves. They are ionic hydrogels that convert pressure stimuli into piezoelectric ion signals due to the different diffusion coefficients of ions in the charged matrix. This occurs either through the flow of ions of a single polarity or through the polymer matrix preferentially carrying ions of one polarity, resulting in a net charge imbalance. As shown in Fig. 2C, the piezoelectric coefficient depends on the type of ions and the properties of the hydrogel matrix.

Dobashi and colleagues conducted in-depth research on the mechanism of piezoelectric hydrogels, which exhibit a built-in potential difference caused by a fixed charge concentration difference between poly (acrylic acid) (polyAA, charged) and polyacrylamide (pAAM, neutral) [63]. They proposed a single-ion-driven hydrogel that converts pressure into ionic currents like Fig. 2C i, mimicking the somatosensory network in humans to stimulate movement in rodent limbs. Pressure on the charged side generates the flow of solvent and protons, thereby enhancing this potential difference. In the piezoelectric ion matrix prepared from hydrogel ion conductors, the open-circuit voltage is proportional to the applied pressure, with the piezoelectric ion coefficient typically ranging from 0.01 to 100 nV $Pa^{-1}$. According to this study, when the diffusion coefficients of the two ions are approximately equal, the generated voltage is zero, while maximizing the difference in ion size can yield a larger induced voltage. Under conditions of high salt concentration (>1.0 M), the ionic conductivity of the polymer gel exceeds that of bulk electrolytes. Raquez et al. used high-resolution stereolithography printing to stack piezoelectric ion touch sensors integrated onto fingertips, providing tactile feedback for object recognition applications [64]. Similarly, Jong Ik Lee and colleagues utilized this piezoelectric ion effect in luminescent electronic skin to enhance the luminous intensity of the device, and combined with the viscoelasticity of the polymer matrix, they also achieved spatial mapping of tactile stimulation [65].

To enhance the performance of ion-piezoelectric hydrogels, Wang et al. and colleagues incorporated Poly(3,4-ethylenedioxythiophene): poly(styrene sulfonate), significantly altering the intermolecular forces between cations and anions, achieving a voltage of up to 700 mV and a current of 7 mA [66]. Furthermore, they conducted a theoretical analysis of the nonlinear phenomena observed in ion-piezoelectricity, demonstrating the role of ion-ion interactions in nonlinear responses, which provides support for the theoretical basis of piezoelectric hydrogels. Kai Yang and team proposed a strategy using crown ethers as differential amplifiers for ion-selective mobility to enhance the pressure-induced voltage response in ion-conducting polyvinyl alcohol (PVA) hydrogels [67]. The crown ether-grafted PVA hydrogels achieved a 30-fold amplification within the 0–1 kPa range, with a piezoelectric coefficient reaching 1490 nV $Pa^{-1}$.

Notably, metal-coordination hydrogels exhibit a similar effect, as illustrated in Fig. 2C ii. Their primary components include hydrogel polymers, central metal ions, and corresponding ligand ions (such as $Cl^-$, $NO_3^-$). When metal ions crosslink with polymers, only the ligand ions are free to move. Therefore, under external pressure stimulation, the reallocation of ligand ion channels through stretching and compression of the internal hydrogel polymer structure generates electrical signals. Inspired by spider webs, Xiaoyu Guan and colleagues developed a metal-coordination hydrogel with significantly improved tensile, compressive, and fatigue resistance properties [68]. This hydrogel was evaluated as a pressure sensor in applications aimed at protecting the tactile nervous system of patients experiencing pain.

### 2.4. Piezoelectric bimolecular

In 1950, wood was first reported to exhibit piezoelectricity, and subsequently, this phenomenon was also discovered in collagen tissues such as bone and tendon, hair, and even Deoxyribonucleic Acid [69,70]. To date, natural piezoelectric biomaterials, ranging from the microscopic to the macroscopic scale, can be categorized into several types, including amino acids, peptides, collagen, polysaccharides (chitin, chitosan), and tissues and organs (bone, skin, cornea) (Fig. 2D). The piezoelectric signals generated by these piezoelectric biomolecules play crucial roles in various vital biological activities, including cell communication, neural electrical signal conduction, cell migration and differentiation, embryonic development, and tissue healing. Natural piezoelectric biomolecules possess the advantages of high biocompatibility and degradability, but they generally exhibit relatively low piezoelectric performance, which is the main factor limiting their applications.

Glycine, as a monomer composing peptides and proteins, was investigated for its piezoelectric properties along with 19 other amino acids and their isomers in 1970. The structure revealed that 19 of these amino acids theoretically exhibit piezoelectric properties, with different amino acid structures demonstrating different piezoelectric performances [71]. Among them, glycine shows strong piezoelectric properties and has been extensively studied. The three crystal forms of glycine: α, β, and γ, exhibit distinct piezoelectric performances. Specifically, α-glycine, which adopts an antiparallel conformation, does not exhibit piezoelectricity macroscopically and is the most stable crystalline phase. β-glycine possesses a certain shear piezoelectric coefficient $d_{16}$, but it is metastable and spontaneously converts into the more stable α and γ phases in air. Additionally, the piezoelectric properties in the shear direction are not as widely applied as those in the longitudinal direction. Therefore, more attention has been given to the piezoelectric properties of γ-glycine. γ-glycine, with dipoles oriented along the axial helix, exhibits excellent longitudinal piezoelectric coefficient $d_{33}$, approximately 9.93 p.m. $V^{-1}$, demonstrating a significant advantage (Fig. 2D i). In piezoelectric applications, to simultaneously satisfy the macroscopic piezoelectric properties and flexible preparation of γ-glycine, a strategy designed by Yang et al., involving PVA-induced self-assembly of γ-glycine into films, has been widely developed. The formation of hydrogen bonds between PVA and glycine at the interface leads to the formation and self-alignment of γ-glycine crystals, resulting in a $d_{33}$ piezoelectric coefficient of 5.3 pC $N^{-1}$ [72,73]. In addition, L-leucine

[74], L-valine [75], and DL-alanine [76] all exhibit piezoelectricity in specific directions and have achieved preliminary applications in sensors.

Peptides, consisting of two or more amino acids linked by peptide bonds, can self-assemble into nanostructures with piezoelectric properties, such as diphenylalanine ($NH_2$-Phe-Phe-COOH, FF). The self-assembly and growth of FF can be controlled to orient its polarization direction through substrate interactions or applied electric fields. The asymmetry in its molecular arrangement enables the effective conversion of force into piezoelectric signals [77]. PENG prepared from FF peptides can generate an output voltage of up to 3.4 V [78]. However, challenges such as controlling the molecular arrangement of amino acids and peptides, poor stability, the need for encapsulation due to water solubility, and difficulties in flexible fabrication remain to be addressed. Further theoretical research is needed to clarify these issues.

Proteins are large organic compounds composed of amino acid polymers. Common piezoelectric proteins include collagen, keratin, and silk fibroin. Natural collagen features a stable triple-helix structure formed by three interwoven α-helical peptide chains (Fig. 2D U60; i). The strong dipolar moment along the peptide chain axis and the interaction of hydrogen bonds are the sources of piezoelectricity. When external mechanical force is applied, the direction and magnitude of the dipolar moment in collagen molecules change, altering the dipolar moment vector and thereby inducing the piezoelectric effect, with bone collagen fibers being the most classic example. Researchers [79,80] used high-resolution piezo-response force microscopy (PFM) to study the piezoelectricity of isolated collagen fibers from bovine tendon, revealing a shear piezoelectric coefficient of approximately 1 pm $V^{-1}$ for single collagen fibers and unipolar axial polarization along their length. Keratin has a repetitive amino acid block structure with elastic α-helix and β-sheet configurations, tightly organized through intramolecular and intermolecular hydrogen bonds, and exhibits strong mechanical strength due to the presence of disulfide bonds. Researchers [81] used $d_{33}$ piezoelectric measurement instruments to measure the piezoelectric coefficient of chicken feather fibers, which was found to be approximately 1.6–2.1 pC $N^{-1}$. Piezoelectric energy harvesting devices made from these fibers exhibited excellent electrical performance output. Silk fibroin obtained from silkworm silk [82] or spider silk [83] has also been fabricated into energy harvesters for use in electronic medical devices.

Polysaccharides are natural high-molecular-weight carbohydrates composed of various monosaccharides, widely found in plants, animals, and microorganisms, existing as storage polysaccharides and structural polysaccharides. In 1955, researchers first measured the piezoelectric effect of wood, proposing that the piezoelectric response of wood could be generated by the uniaxial arrangement and monoclinic symmetry of cellulose crystals [84]. Subsequent studies have investigated the piezoelectric properties of chitin, chitosan, and cellulose [85–87].

### 2.5. Piezoelectric composites

Combining flexible piezoelectric polymers with rigid piezoelectric ceramics represents a potentially effective strategy to address the challenges of the difficult processing of piezoelectric ceramics and the low piezoelectric coefficient of piezoelectric polymers. However, this discussion will not reiterate simple composites but will instead focus on composites that exhibit additional effects during this process, particularly those that enhance the crystallinity and polarization of piezoelectric polymers through fillers (Fig. 2E).

The piezoelectric coefficient of piezoelectric polymers is closely related to their crystallinity, and increasing crystallinity through various methods is a crucial direction for enhancing their piezoelectricity, including the high-temperature annealing mentioned earlier (Fig. 2E i). Here, we mainly review cases where the crystallinity of polymers is increased by adding fillers. Hydrogen bonding is ubiquitous in polymers. Li et al. utilized electrospinning technology to fabricate core/shell nanofibers (NFs) composed of PLLA and glycine. They investigated the technique of interfacial anchoring. The self-assembled core/shell structure facilitated strong intermolecular interactions between the –OH groups on glycine and the C═O groups on PLLA, which in turn promoted the crystallization of oriented PLLA polymer chains, stabilized the β-phase structure, and significantly enhanced the piezoelectric properties of PLLA [88]. Su et al. used phase-field simulations and molecular dynamics calculations to find that the –OH surface terminals on $Ti_3C_2T_x$ nanosheets provided hydrogen bonding with the fluoropolymer matrix, resulting in dipolar alignment and enhanced net spontaneous polarization in the polymer-ceramic composites [89]. By further introducing $Ti_3C_2T_x$ MXene nanosheets, a simple and effective method was proposed to enhance the local dipolar moment and β-phase content of piezoelectric polymer composites. Adding an appropriate amount (2.5 wt%) of $Ti_3C_2T_x$ nanosheets below the percolation threshold effectively enhanced the polarization efficiency and interface coupling between inorganic nanofillers and the organic polymer matrix, resulting in a 160 % increase in the piezoelectric effect compared to the undoped material. Liu et al. used liquid metal nanodroplets as nanofillers in a PVDF matrix, and the formed liquid-solid/conductive-dielectric interface significantly improved the piezoelectric output and reliability of the piezoelectric composites [90]. Significant performance improvements were achieved, with an increase in output voltage by nearly 1000 % (up to 212 V) and a 270 % increase in the piezoelectric coefficient ($d_{33} \approx 51.1$ pC $N^{-1}$). Cui et al. doped zoledronic acid, a drug used to treat osteoporosis, as a nucleation agent in PLLA to prepare spun coatings with higher piezoelectric output [91]. These coatings were applied to the surface of titanium implants to effectively prevent aseptic loosening of the implants, providing a direction and reference for drug-modified piezoelectric polymers.

For piezoelectric polymers with effects ferroelectric, their piezoelectric coefficient can also be enhanced by improving the polarization process (Fig. 2E U60; i). Zhang et al. proposed a nanoscale confinement polarization pinning effect, providing theoretical support for the application of heterojunctions composed of metal-organic frameworks and conductors or semiconductors in enhancing the piezoelectricity of piezoelectric polymers [56]. The formation of a heterojunction between the metal-organic framework UIO-66(Hf)–$NO_2$ and $MoS_2$ allows the porous metal-organic frameworks to securely anchor $MoS_2$ onto the molecular chains of PVDF-HFP. During the polarization process, $MoS_2$, which is highly responsive to the electric field, facilitates the movement of PVDF-HFP's molecular chains via UIO-66(Hf)–$NO_2$. Consequently, the molecular chains of PVDF-HFP align with the electric field, resulting in a more organized arrangement of the electric domains within the material and amplifying the piezoelectric effect, with the $d_{33}$ value rising from 8 pC $N^{-1}$ to 27 pC $N^{-1}$.

To increase the interfacial polarization effect, Yoojeong et al. prepared alternating soft/hard layered multilayer materials, which caused stress concentration and increased effective stress-induced polarization and interfacial polarization between organic and inorganic materials, resulting in a dielectric constant higher than that of pure PVDF-TrFE films [92].

In summary, the introduction of fillers and the construction of heterojunctions have proven to be effective strategies in enhancing the piezoelectric properties of piezoelectric polymer and piezoelectric ceramic composites, addressing the processing and performance limitations of traditional materials. In the future, with a deeper understanding of the interaction mechanisms between fillers and polymer matrices, as well as the development of novel fillers, the performance of piezoelectric composites is expected to further improve [93]. Meanwhile, exploring more fillers with special functions, such as drug molecules and liquid metals, will open up new applications for piezoelectric composites. Additionally, optimizing the polarization process and enhancing the interface polarization effect will also be important pathways to achieving high-performance piezoelectric composites.

## 3. Triboelectric biomaterials based on force-electric conversion

CE represents one of the oldest scientific phenomena, dating back over 2600 years, yet its physical underpinnings remain elusive. Despite the ongoing mystery surrounding the precise mechanism of CE, its effects have long been recognized. This phenomenon is rooted in the charge transfer process that ensues when two dissimilar materials make contact. When dissimilar materials contact each other, charge transfer occurs as a result of varying electron-gaining and electron-losing capabilities at the material interface [94]. Upon separation, this leads to the generation of opposing electrostatic charges on the surfaces, balancing the surface potential and consequently facilitating charge accumulation. Triboelectric materials, pivotal to CE, play a critical role in shaping the efficiency of energy conversion and the potential applications of related devices. Consequently, research in this area has garnered considerable attention in recent years. Subsequently, we will delve into the CE mechanisms exhibited by various triboelectric materials, namely inorganic triboelectric materials, polymer triboelectric materials, and triboelectric composite materials (Fig. 3). Furthermore, we will explore their utilization in augmenting electrical output characteristics.

### 3.1. Inorganic triboelectric materials

The CE mechanism of metal triboelectric materials, within the realm of inorganic triboelectric materials, has been thoroughly examined. Research on the CE process between two metals suggests that electron transfer serves as the fundamental mechanism underlying surface charging [94]. The charge generated through CE is directly proportional to the variance in work functions between the metals in contact [95,96]. Surfaces with lower work functions acquire a positive charge, whereas surfaces with higher work functions develop a negative charge, resulting in the transfer of electrons from surfaces with lower work function to those with higher work function. Considering the work function characteristics of metal triboelectric materials, several studies have explored adjusting the work function of these materials by incorporating metallic NPs [97–99]. This approach aims at boosting the electrical output performance of these materials. Beyond manipulating the variance in material work function, alternative strategies involve the selection of suitable triboelectric materials, as well as incorporating chemical and physical modifications like adjusting stretchability, dielectric constants, and surface roughness [100,101]. Wang et al. augmented the polyethyleneimine/PVA (PEI/PVA) matrix by incorporating Au NPs, consequently decreasing the composite's work function and facilitating a higher electron transfer rate (Fig. 4A) [98]. As a result, the composites demonstrated elevated surface charge density and manifested a substantial surface potential difference. Additionally, the introduction of Au NPs by Wang et al. bolstered the dielectric properties of the material, thereby enhancing the device output. In equation (1), σ' represents the total transferred charge density on the Au/PEI/PVA material, with $\varepsilon_1$ and $\varepsilon_2$ denoting the dielectric constants of polyethylene terephthalate (PET) and Au/PEI/PVA, $d_1$ and $d_2$ representing their respective thicknesses, $d'$ indicating the air-gap distance, and σ representing the triboelectric charge density at equilibrium. Equation (1) suggests that an increase in $\varepsilon_2$ corresponds to a heightened transferred charge density.

$$\sigma' = \frac{\sigma d'}{d_1/\varepsilon_1 + d' + d_2/\varepsilon_2} \tag{1}$$

Chun et al. employed Au NPs to fill mesoporous polydimethylsiloxane (PDMS) films [99]. The dipoles produced from the interaction of PDMS with Au NPs within the pores influence the surface potential energy of the mesoporous film, consequently amplifying the charge transfer density on the PDMS surface (Fig. 4B). Lai et al. created

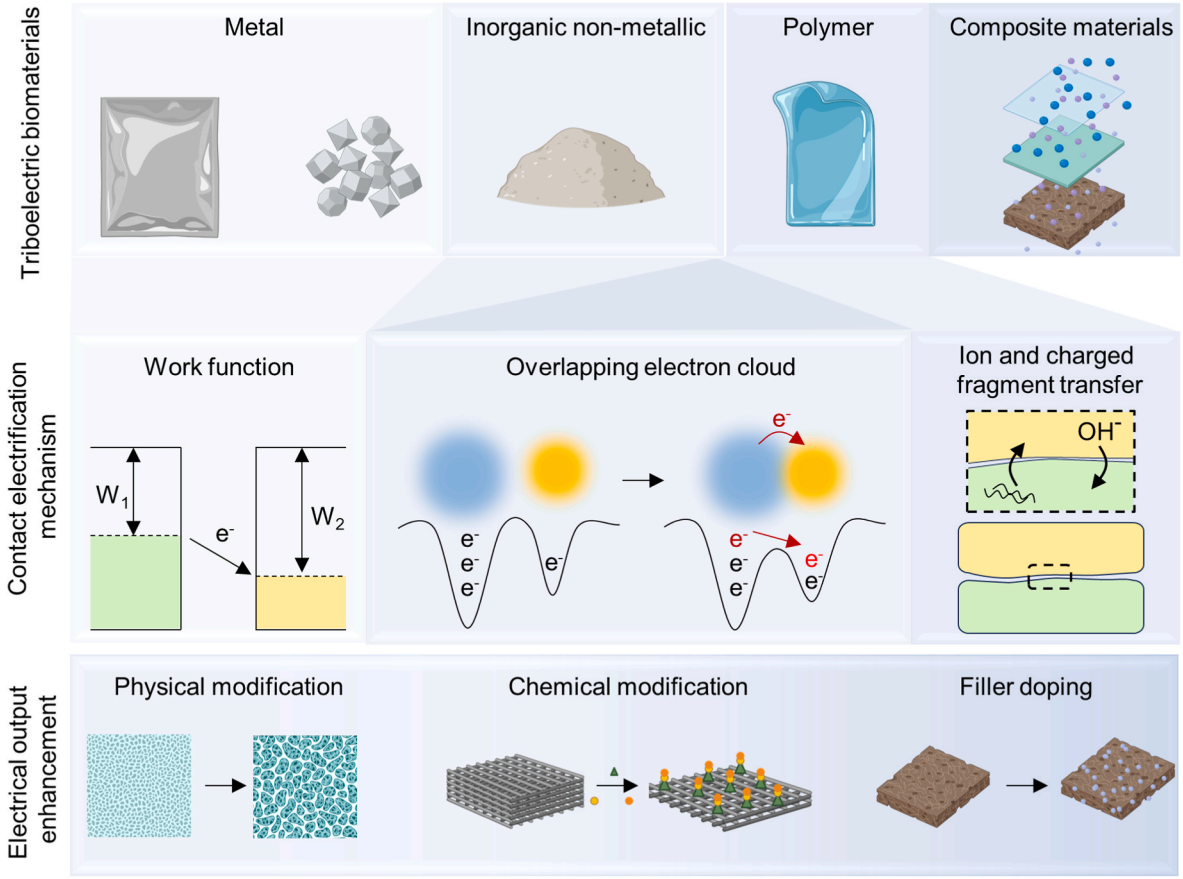


**Fig. 3.** CE mechanisms and electrical output enhancement methods of metal, inorganic non-metallic, polymer and composites triboelectric materials.

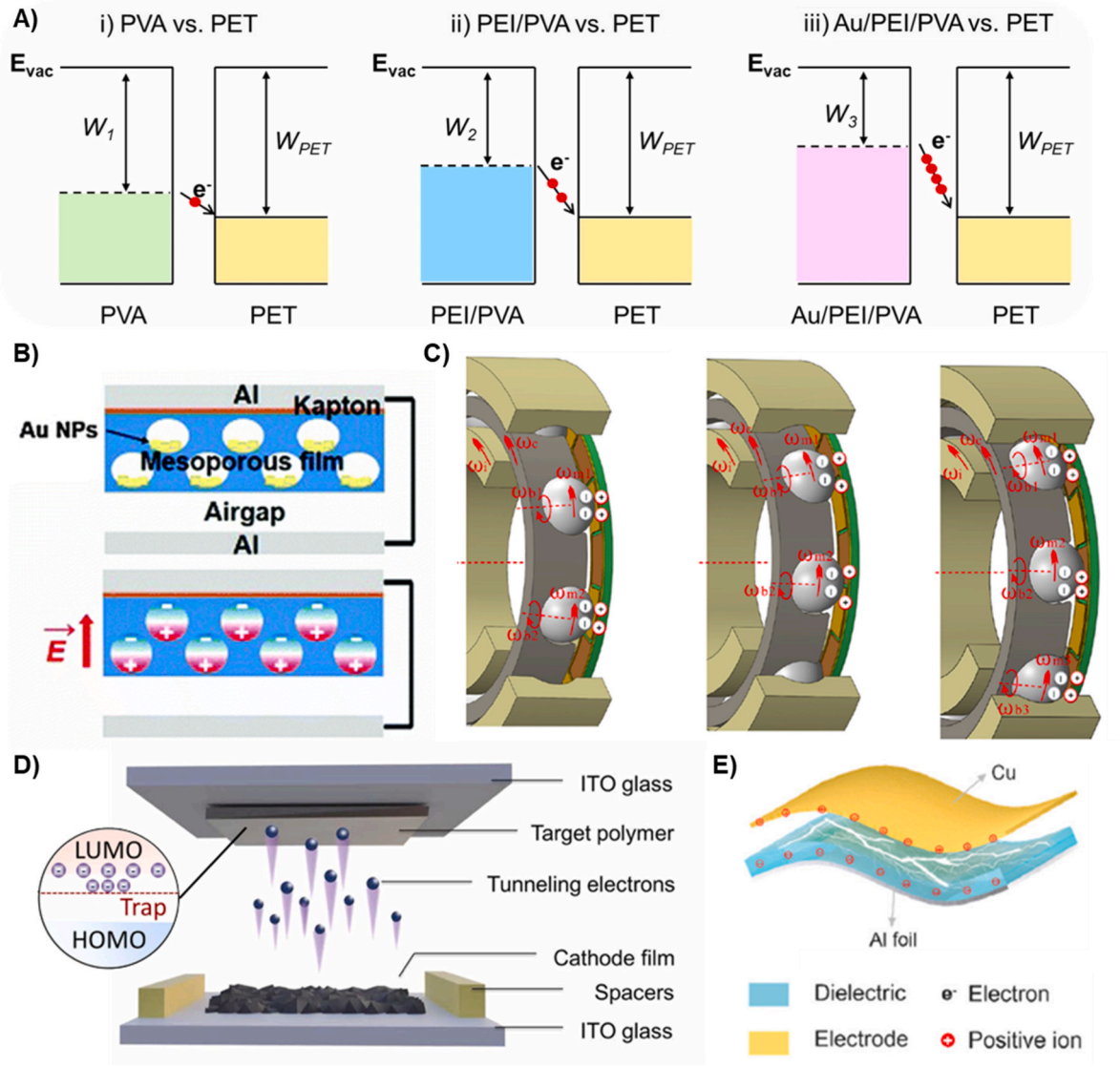


**Fig. 4.** A) A schematic energy band diagram illustrating the mechanism of the increased charge transfer due to the decrease of work function of the positive triboelectric material. Reproduced with permission from Ref. [98]. Copyright 2018. Published by Elsevier Ltd. B) Schematic diagrams of the net electric field in mesoporous films along the direction from PDMS to the top electrode and the contact between positive charges and the bottom electrode. Reproduced with permission from Ref. [99]. Copyright 2015. Published by Royal Society of Chemistry. C) Schematic diagram of working principle of ultra-high-speed ceramic triboelectric bearing with floating spinning-sliding freestanding mode. Reproduced with permission from Ref. [102]. Copyright 2022. Published by Elsevier Ltd. D) Diagram of the process of a tunneling electron injection (TEI). Reproduced with permission from Ref. [103]. Copyright 2024. Published by Elsevier Ltd. E) Schematic illustration of the P(VDF–TrFE–CFE) films. Reproduced with permission from Ref. [104]. Copyright 2024. Published by Royal Society of Chemistry.

internal space charge zones by integrating grooves and furrows in the longitudinal and transversal Au layer adjacent to the surface of the tribological layer, thereby augmenting the material's charge transfer density [101].

Inorganic nonmetallic triboelectric materials entail a complex CE mechanism, sparking ongoing debate among researchers. To elucidate the CE phenomenon, Wang and colleagues introduced a comprehensive overlapping electron cloud model [94]. The model involves two surfaces that are far apart. In this case, the electron clouds of atoms on one surface are separated from those of atoms on the other surface. Thus, the electrons remain localized. Upon contact, CE ensues, potentially leading to overlapping electron clouds of atoms from both surfaces, engendering an asymmetric double-well potential. With a reduced energy barrier in the overlapping electron cloud, electrons can shift from a higher energy state of an atom on one surface to a lower energy state of an atom on the other surface. This electron exchange results in the charging of both surfaces. When the surfaces part ways, the electron clouds no longer overlap, preventing electron transfer back to the original surfaces. Consequently, the separated surfaces retain a permanent charge originating from the electron transfer process.

Ceramic materials, among inorganic non-metallic triboelectric materials, are employed to enhance device performance and usability owing to their exceptional durability and dielectric properties [105–108]. Addressing the durability aspect, Chi et al. utilized commercially available porous $Al_2O_3$ ceramic flakes as triboelectric materials in a liquid-solid triboelectric device, complemented by a straightforward sprayed electrode layer [109]. The use of ceramic triboelectric material made the device robust, easy to fabricate, low cost and stable in performance. In another study, Gao engineered an ultra-high-speed ceramic triboelectric bearing for monitoring real-time dynamic behavior and stability (Fig. 4C) [102]. The use of ceramic triboelectric material enables this triboelectric bearing to operate stably at ultra-high speeds up to 16000 rpm. Furthermore, Manpreet et al. harnessed micro-fibrous ceramics with a composition of 54 % $SiO_2$ and

46 % $Al_2O_3$ as triboelectric material combined with a sodium chloride aqueous solution for power generation purposes [110]. This microfiber ceramic not only thrives in corrosive, high-temperature, or high-pressure environments but also resolves current loss issues linked to the innate conductivity of certain triboelectric materials.

In addition, ceramic materials possess impressive dielectric properties that guarantee stable output of the device. Nevertheless, their inherent rigidity hampers their application in flexible energy harvesting systems. Researchers have tackled this rigidity concern by integrating ceramic triboelectric materials into polymer films. Concurrently, they have capitalized on ceramic materials' high dielectric traits to augment charge accumulation on material surfaces [111,112]. Punnarao et al. employed a solid-state reaction process to synthesize a dielectric calcium copper titanate ($CaCu_3Ti_4O_{12}$ (CCTO)) ceramic material [113]. These particles were incorporated into PDMS polymer to create a CCTO/PDMS-based flexible composite film (FCF). The addition of CCTO particles significantly enhanced the dielectric properties, surface charge density, and electrical conductivity of the FCF. From a material point of view, the temperature fluctuations can notably impact the dielectric constant of ceramic triboelectric materials, influencing their surface electrical properties. To mitigate this challenge, Xie et al. utilized ceramic powders based on $Ba(Cu_{0.5}W_{0.5})O_3$ (BCW) to engineer temperature-stabilized materials with elevated dielectric constants [103]. BCW ceramics, initially employed as sintering auxiliaries, exhibit substantial dielectric constants facilitating charge storage in electric fields while demonstrating robust electrothermal stability. Integrating these materials into polymer substrates effectively boosts charge accumulation and enhances the energy conversion efficiency of the materials.

### 3.2. Polymer triboelectric materials

In recent years, the high dielectric constants of inorganic materials have been regarded theoretically as optimal triboelectric materials. However, due to their high leakage properties and limited contact potential difference with metal electrodes, achieving high tribo-charge densities has proven challenging. Polymeric materials offer a promising solution by enabling the incorporation of high dielectric nanofillers or even conductive NPs. Additionally, polymer materials stand out as ideal choices for triboelectric applications because of their superior charge density, flexibility, low processing temperatures, and potential for structural and chemical modifications [114–116].

An electron cloud/potential model based on fundamental electron cloud interactions elucidates the specific CE processes in polymer triboelectric materials [114]. Upon the application of an external force bringing two materials into contact, their electron clouds merge, leading to the formation of either an ionic or covalent bond. Consequently, the potential barrier between the materials diminishes, the minimum required energy for electron liberation is lower than the energy level the electron occupies. Therefore, electrons leap from atoms of one material to atoms of another. The efficiency and extent of electron transfer hinge upon the "charge affinity" of the triboelectric material, influenced by various factors such as electron acceptance or donation capabilities, surface roughness, and local morphology. Nonetheless, these correlations are not universally applicable to all polymers, necessitating theories that can be universally applied to all polymerization reactions.

Indeed, polymer adhesion plays a key role in the CE process, and the cross-linking, chain entanglement, network topology, and non-covalent structural domain interactions brought about by the adhesion processes result in the formation of new polymer chains [117,118]. Simple modeling of a polymer undergoing vertical segregation reveals that polymer bonds break at a given strain or distance. This bond cleavage is due to the rearrangement of the polymer chains that occurs during contact, suggesting that the CE mechanism in the polymer arises from cleavage and transfer of charged polymer fragments. The dissociation of these covalent bonds can be either homolytic, where two free radicals are formed, or heterolytic, where anion-cation pairs are formed. Homolytic cleavage leads to the generation of identical free radicals at the termini of each broken chain within the macromolecule, whereas heterolytic cleavage results in the production of both cations and anions (mechano-ions). As a result, mechano-ions dominate the net charge density measured on each contact surface. During surface separation, charged organic ion fragments undergo material transfer. On repeated contact separations, these charged fragments move between surfaces, undergo neutralization reactions, and form new charged fragments. This means that while polymer fragment transfer is considered to be the dominant effect of polymer-polymer CE, the role of ions and electrons transferring between radicals and mechano-ions should not be neglected. As mentioned above, the main mechanisms of polymer CE are electron transfer, ion transfer, and charged fragment transfer of macromolecules. Since the factors affecting the charge formation during polymer CE are as follows: i) contact time and contact force; ii) morphology (surface roughness, patterning); iii) bulk (macromolecular ordering, degree of cross-linking); and iv) surface chemistry (functional groups). Therefore, chemical and structural modifications of polymer triboelectric materials are further investigated to improve the output performance of the devices [119–121].

Chemical modification of polymer materials includes various methods such as introduction of electron adsorption functional groups, injection of ions or charges, and continuous gas permeation [104,122,123]. Structural modification of polymer materials refers to the formation of morphological features and roughness with regular or irregular shapes on the surface of the friction electric material [124]. The main purpose of structural modification is to increase the active surface area in contact with the opposing triboelectric medium or to increase the effective force on the polymer medium. Therefore, the modification of polymer materials to achieve high CE capability of polymer triboelectric materials has been widely investigated.

Polymer triboelectric materials with high tribocharge density are essential for expanding the range of applications of triboelectric devices. Direct charge injection is an effective strategy to increase the charge density of materials. However, it traditionally requires high voltages (~10 kV) and injection times of several minutes or more. In this work, Wu et al. demonstrate an effective and simple method for charge injection into polymer triboelectric materials using TEI technique (Fig. 4D) [122]. In terms of chemical modification, Liu et al. developed a method for producing triboelectric polymers based on repeated rheological forging [123]. The fluorinated ethylene-propylene films prepared by the repeated forging method not only have excellent mechanical properties and good light transmission, but also maintain ultra-high tribocharge density. This performance enhancement is attributed to the fact that the iterative forging process effectively modulates the surface functional group composition, crystallinity, and dielectric constant of the fluorinated ethylene propylene.

However, conventional polymer triboelectric materials limit further improvements in charge density due to the inevitable air breakdown under high charge density conditions. Liu et al. prepared a novel triboelectric polymer (P(VDF-TrFE-CFE)) [104]. The very thin thickness of the P(VDF-TrFE-CFE) film has a high dielectric constant, which effectively suppresses air breakdown (Fig. 4E). In addition, the mechanical mismatch problem at the interface between the polymer substrate and the electrode limits the further application of polymer triboelectric materials in practical applications. Shao et al. prepared a tough monolithically integrated triboelectric bioplastic by exploiting the chemo-selectivity and site specificity of mercaptosilylation reaction as well as thiol-disulfide exchange reaction [125]. The stresses were dissipated by covalent bonding adapted to interfacial interactions, which resulted in good interfacial adhesion (220.55 kPa) between the polymer dielectric layer and the electrode conductive layer. Even when subjected to 10,000 times tensile force (compared to weight), it maintains a stable triboelectric output with no visible cracks. In conclusion, these studies provide new insights into the design of polymer

triboelectric materials with excellent CE capability, which is important for the output performance enhancement of triboelectric devices.

### 3.3. Composite triboelectric materials

Composites have been utilized as an excellent class of triboelectric materials due to their excellent chemical stability, multiphase structure with composite effects, excellent designability, and multiple functionalities [126–128]. Researchers have optimized the mechanical, durability and electrical properties of composite triboelectric materials by tuning the surface composition and processing parameters of the composites [129,130]. Zhang et al. prepared PVDF @ Mxene ($Ti_3C_2Tx$) composite films with a spherical multiple physical network structure by controlling the Rayleigh Instability deformation of the spinning jet and vapor-induced phase separation during the electrostatic spinning process and used them as triboelectric materials (Fig. 5A) [130]. The structure of the composite film and the high conductivity of $Ti_3C_2Tx$ provided high output performance and output stability for the triboelectric devices. In terms of material modification, Wang et al. developed a porous triboelectric material by grafting trimethoxy (1H,1H,2H, 2H-heptadecafluorodecyl) silane (THS) on the surface of cellulose/-graphene oxide aerogel (Fig. 5B) [129]. The grafting of THS enhanced the charge transfer capability of the material. Therefore, direct modification of triboelectric composites is a method to produce high-performance triboelectric devices. However, there are currently limited composite material options available, so material selection and modification alone can provide only a small amount of design flexibility for the preparation of high-performance triboelectric layers.

Heterogeneous polymeric materials (polymer-metal nanocomposites, polymer-carbon-based nanocomposites, ferroelectric polymer-inorganic nanocomposites, and flexible/stretchable composites), as a typical class of composite triboelectric materials, have more interfaces and defects than homogeneous polymer materials, which can provide more sites for charge accumulation and storage. The moderate introduction of nanofillers into the polymer matrix is a direct approach to generate heterogeneous interfaces and defects to enhance the triboelectric properties, hence it has attracted much attention [131–134]. Three main types of fillers commonly used in triboelectric polymer materials are as follows: (1) NPs with high dielectric constants [133], (2) carbon-based materials [135,136], and (3) ionic fillers [137].

High dielectric constant NPs with polarization properties can generate interfacial polarization, which enhances the CE properties of composites. Based on this, Wu et al. developed a simple low-temperature process for the preparation of high-performance ceramic powder-based triboelectric composites, which consisted of electrospun fibers based on PVDF-hexafluoropropylene (PVDF-HFP) and $Eu_2O_3$-doped BTO nanofillers [139]. The incorporation of modified BTO nanofillers resulted in the triboelectric device having a maximum output voltage of up to 1004 V and a corresponding current density of 9.9 $\mu A\ cm^{-2}$. The improvement in the triboelectric properties was attributed to the large amount of interfacial polarization and transferred charges generated by the doping of the NPs, which indicated the improvement in triboelectric electron trapping and storage. Based on the same principle, Wang et al. developed cellulose-based composites with excellent negative triboelectric properties by incorporating modified barium titanate (MBT) and PVDF into trimethoxy (1H,1H,2H,2H-heptadecafluorodecyl) silane-grafted cellulose aerogels (Fig. 5C) [133]. The composites fully utilize the synergistic effect of the complex network structure of cellulose aerogel, the excellent charge transfer capability of PVDF and the strong charge trapping capability of MBT.

The introduction of carbon-based materials can produce charge accumulation and charge confinement interfaces. Therefore, Fang et al. modulated the triboelectric properties of chitosan films by adding single-walled carbon nanotubes to them [136]. It was found that proper carbon nanotube addition improved the dielectric properties of the composites and the balance with the leakage current effect (Fig. 5D). At the same time, triboelectric trap states were provided at the composite interface, ultimately leading to a charge density of 262 $\mu C\ m^{-2}$, which is 2.45 times higher than that of the pure chitosan film. The researchers also found that the introduction of carbon-based materials was able to adjust the surface charge as well as the work function of the composites, ultimately enhancing the output performance of the triboelectric devices. In addition, the doping of ionic fillers in the composites also affects the triboelectric properties. Zhao et al. fabricated a PDMS composite using embedded ionic liquid coated single-walled carbon nanotubes (SWCNT) [137]. By adjusting the ratio of ionic liquids to single-walled carbon nanotubes, the desired material properties of triboelectric devices could be realized. The composite exhibited relatively high electrical conductivity (0.004 S/m) and enhanced triboelectric output compared to unmodified PDMS. However, good dispersion of nanofillers in the developed composites remains a challenge.

Excessive concentration and poor dispersion of fillers in polymers can lead to aggregation, which can cause dielectric breakdown and charge leakage in composites. To address this issue, Puran et al. were able to achieve excellent dispersion of BTO into PVDF matrix by introducing Nafion (Fig. 5E) [138]. The excellent dispersion enhanced the effective stress transfer at the interface between BTO and PVDF, which significantly increased the surface potential of the homogeneous composite nanofibers. Compared with the pristine PVDF nanofibers, the doped nanofibers increased the output voltage, current density and power density of the triboelectric devices by 6.3, 7.1 and 3.7 times, respectively. Overall, the reasons for the filler-enhanced CE capability of composites are categorized into three main points: dielectric effect, interface effect, and double electron layer effect, which tend to coexist in complex composites.

## 4. Devices based on force-electric conversion

### 4.1. Piezoelectric devices

Since its initial discovery in 2006, the PENG has made significant progress as a force-electricity conversion device based on piezoelectric materials (Fig. 6A) [140]. It efficiently converts mechanical energy generated by irregular or regular human movements, such as heartbeats, muscle contractions, and diaphragm movements, into electrical energy. Notably, its application in pacemakers demonstrates the tremendous potential of PENG in the biomedical field (Fig. 6). However, to achieve a self-powered system for PENG in functional devices and meet the goals of maintenance-free and sustainable operation, the key lies in preparing piezoelectric materials with high piezoelectric output.

We have detailed the methods to enhance the piezoelectric performance of PENG from the perspective of piezoelectric materials in Chapter 2. Briefly, inorganic piezoelectric materials improve their piezoelectric coefficients by controlling the size and arrangement of piezoelectric particles. In contrast, organic piezoelectric polymers enhance their piezoelectric properties through stretching to align molecules, annealing to increase crystallinity, polarization to orient dipoles, and the addition of nanofillers. However, ideal bio-piezoelectric devices not only require excellent piezoelectric performance but also meet specific structural characteristics, such as suitable hydrophilicity, roughness, porosity, as well as good mechanical properties, biocompatibility, and biodegradability [141–143]. PENG was first realized in 2010 for harvesting the mechanical energy generated by an organism's heartbeat and respiration into electrical energy (Fig. 6B). Given that many piezoelectric materials struggle to meet these requirements simultaneously, surface modification and engineering of piezoelectric materials are particularly important.

Biocompatibility and biosafety are paramount for biomedical applications. Researchers have attempted to encapsulate toxic lead-based high-piezoelectric-coefficient ceramics and conducted animal experiments, achieving certain verification results. As shown in Fig. 6C, Kim

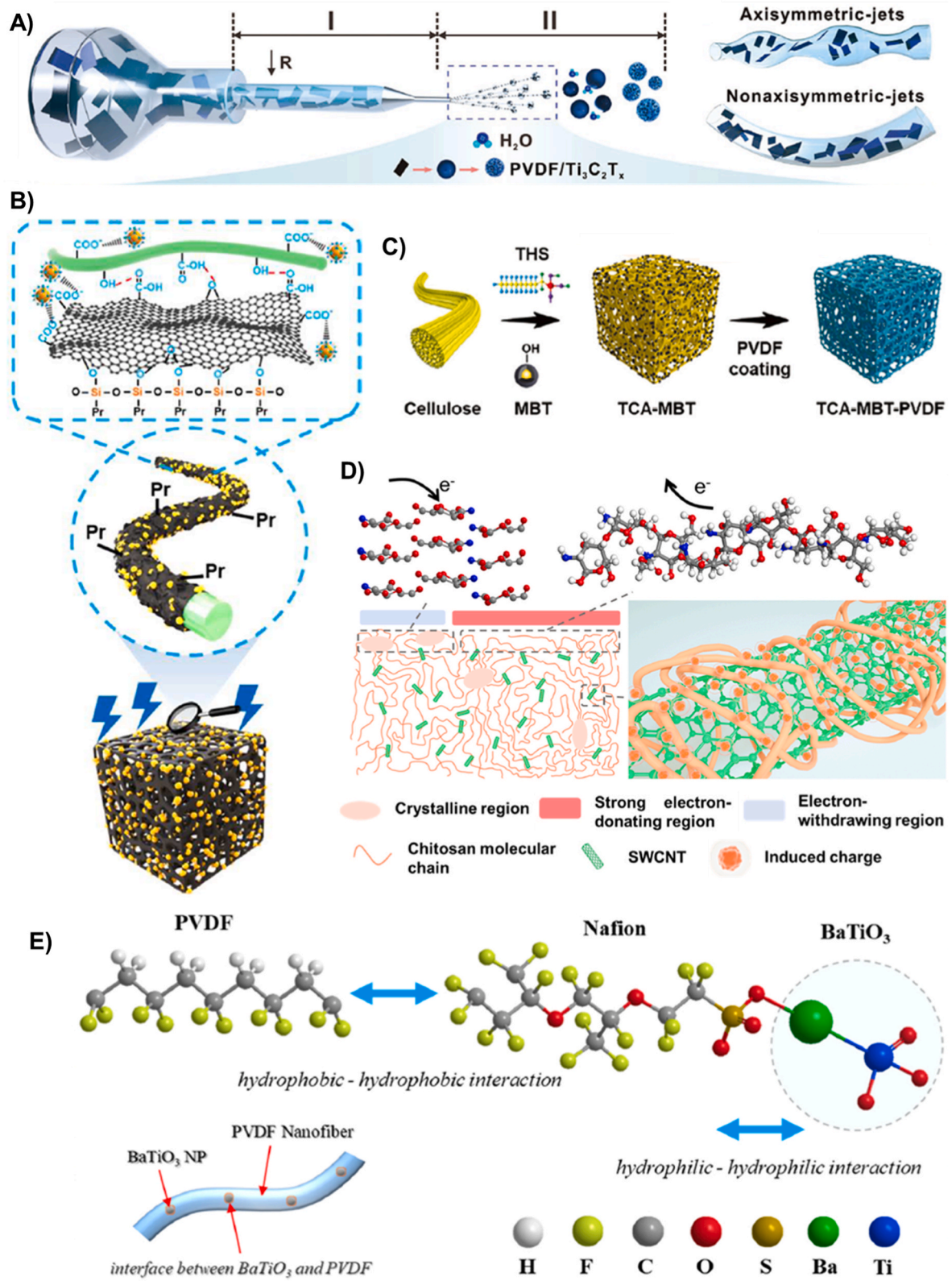


**Fig. 5.** A) Spinning fluid forms an axisymmetric jet and their further transformation into porous spheres. The figure on the right shows the instability model of the charged jet. Reproduced with permission from Ref. [130]. Copyright 2022. Published by Wiley-VCH. B) Schematic diagram of the modification for cellulose/-graphene oxide aerogel porous triboelectric materials. Reproduced with permission from Ref. [129]. Copyright 2024. Published by American Chemical Society. C) Preparation process of the composite cellulose aerogels triboelectric materials based on modified barium titanate nanofiller doping. Reproduced with permission from Ref. [135]. Copyright 2024. Published by Wiley-VCH. D) Schematic illustration of the mechanism of performance improvements. Reproduced with permission from Ref. [137]. Copyright 2023. Published by Elsevier Ltd. E) Mechanism of Nafion functionalized BTO NPs dispersion in PVDF/DMF solution with their chemical structure. Reproduced with permission from Ref. [138]. Copyright 2023. Published by Elsevier Ltd.

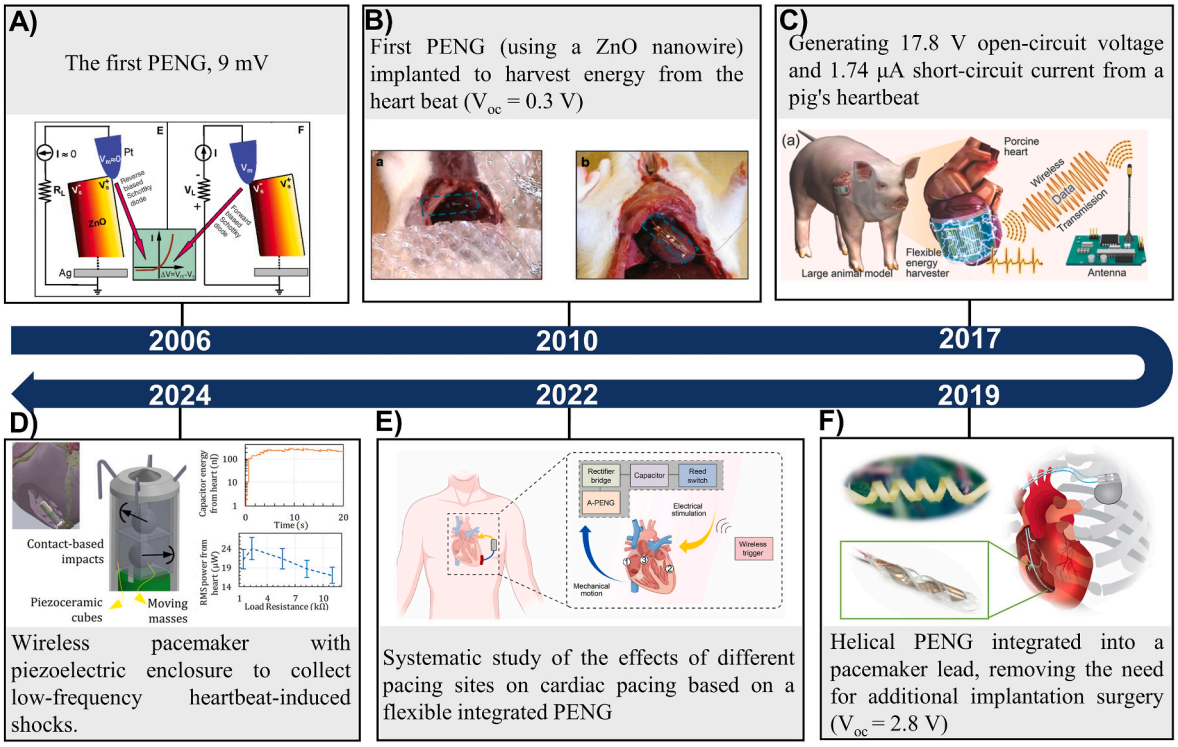


**Fig. 6.** Examples of PENG applications in pacemakers. A) First PENG discovered in 2006. Reproduced with permission from Ref. [140]. Copyright 2006. Published by AAAS. B) First PENG used to harvest energy generated by a beating heart. Reproduced with permission from Ref. [144] Copyright 2010. Published by Wiley-VCH. C) First PENG energy harvesting in a large animal. Reproduced with permission from Ref. [145] Copyright 2017. Published by Wiley-VCH.D) First non-invasively implanted PENG pacemaker. Reproduced with permission from Ref. [146] Copyright 2019. Published by Elsevier. E) The efficiency of PENG in different parts of the heart was studied for the first time. Reproduced with permission from Ref. [147] Copyright 2022. Published by Elsevier.

et al. encapsulated lead-based high-performance single-crystal PMN-PZT films with inert epoxy resin, resulting in an energy harvester that generated high open-circuit voltage and short-circuit current from pig heartbeats, demonstrating excellent biocompatibility [145]. However, the application of toxic materials in organisms still faces challenges such as encapsulation material failure, risks of secondary surgery, and regulatory approval difficulties. Therefore, enhancing the piezoelectric performance of materials with good biosafety is more promising.

The structural design of piezoelectric materials is also crucial. There are mainly two forms of design: direct contact of piezoelectric materials with cells or tissues, and the use of piezoelectric materials as energy harvesting devices to collect electrical energy and then transmit it to tissues through wired or wireless methods. The direct contact approach reduces the requirements for piezoelectric performance and is suitable for piezoelectric NPs, surface-nanostructured materials, and piezoelectric microfiber membrane structures, which have been widely validated in tissue repair. For example, Marc A. et al. implanted PVDF microfibers into injured tendons of rats, effectively promoting tendon repair, with new tissue directly attaching to the microfiber membrane and exhibiting three-dimensional growth trends [148]. However, this approach places higher demands on the surface cell adhesion, biodegradability, and long-term effectiveness of the materials. In contrast, the energy harvesting and subsequent application approach offers advantages such as strong electrical controllability, high power of energy harvesting devices, and a wide range of material choices. However, it requires consideration of implantation site, encapsulation layer materials, circuit conduction, fatigue resistance, and potential secondary surgeries [149]. Addressing these challenges through the overall structural design of the device is also a research direction. For example, in Fig. 6D, Lin et al., inspired by biological structures, prepared piezoelectric materials into a spiral structure and implanted them through wires, avoiding open-chest surgery and enabling seamless connection of the energy harvesting device to the current wires, while also extending the device's lifespan [146]. In Fig. 6E, the researchers further systematically investigated the effects of different pacing sites on cardiac pacing, including the right atrium, left ventricle, and His bundle [147].

In the design of piezoelectric devices, the biodegradability of piezoelectric materials cannot be ignored. This primarily involves biodegradable piezoelectric polymers and piezoelectric biomolecules. By controlling the molecular weight, microstructure, and adding modifiers of polymers, their degradation time can be adjusted to meet early piezoelectric output and degradation metabolism within a certain period. Among them, PLLA, as a mature green renewable energy source, has received widespread attention. Its degradation products are harmless to the body and have more controllable metabolism times [60,150]. Additionally, piezoelectric biomolecules such as β-glycine have also received extensive attention, but their strong water solubility and rapid degradation remain key issues to be addressed [72].

In summary, PENG has broad application prospects in the biomedical field. However, to achieve efficient, safe, and sustainable operation in practical applications, many challenges still need to be addressed. In terms of piezoelectric material preparation, new synthesis and modification strategies should be explored to enhance material piezoelectric performance and meet the structural characteristics required for biomedical applications. At the same time, improving biocompatibility and biosafety is also crucial. In structural design, the advantages and disadvantages of direct contact between piezoelectric materials and cells or tissues, and energy harvesting followed by application should be comprehensively considered for targeted design. Furthermore, the biodegradability of piezoelectric materials is an important direction for future research. By deeply studying material degradation mechanisms and optimizing degradation times, safer and more effective piezoelectric materials can be provided for biomedical applications.

### 4.2. Triboelectric devices

As one of the most promising platforms for power generation, TENGs were first invented and proposed by Zhong Lin Wang in 2012 [151]. The abundance of wasteful mechanical energy, the wide availability and selectivity of triboelectric materials, the relatively simple device configuration and low-cost processing, among many other advantages, have allowed TENGs to gain momentum. Since the invention in 2012, significant experimental and theoretical results have been achieved in understanding the basic principles and applications of TENG. The operating mechanism of TENG is a combination of the tribo-electrification effects and electrostatic induction. The tribo-electrification effects provides a static polarized charge, while the electrostatic induction is the primary mechanism for converting mechanical energy into electrical energy. In addition, the theoretical model of TENG is constructed based on the displacement current of Maxwell's system of equations. On this basis, TENG derives four operating modes: contact-separation (CS) mode, single-electrode (SE) mode, relative-sliding (RS) mode, and freestanding (FS) mode (Fig. 7).

The CS model TENG was proposed by Wang and co-workers in 2012. In the initial stage, the surfaces of two tribological layers with thicknesses of $d_1$ and $d_2$ are uncharged. On the outer surface of these two tribological layers, two metal layers are deposited as two electrodes. The distance (x) between the two tribological layers can be changed by mechanical force. Upon forced contact with each other, based on the CE effect, the inner surfaces of the two tribological layers will generate opposite electrostatic charges (tribocharges) of density σ, which remain stably on the surfaces (Fig. 7A). When the two tribological layers start to separate, the charge on the surfaces will be introduced to the top electrodes, where the charge flows between the two electrodes and eventually converts mechanical energy into electrical energy. This TENG mode has been studied under weak low-frequency mechanical contact as well as under high-frequency mechanical contact [152–155]. Hui et al. found that the CS mode TENG has an advantage over piezoelectric

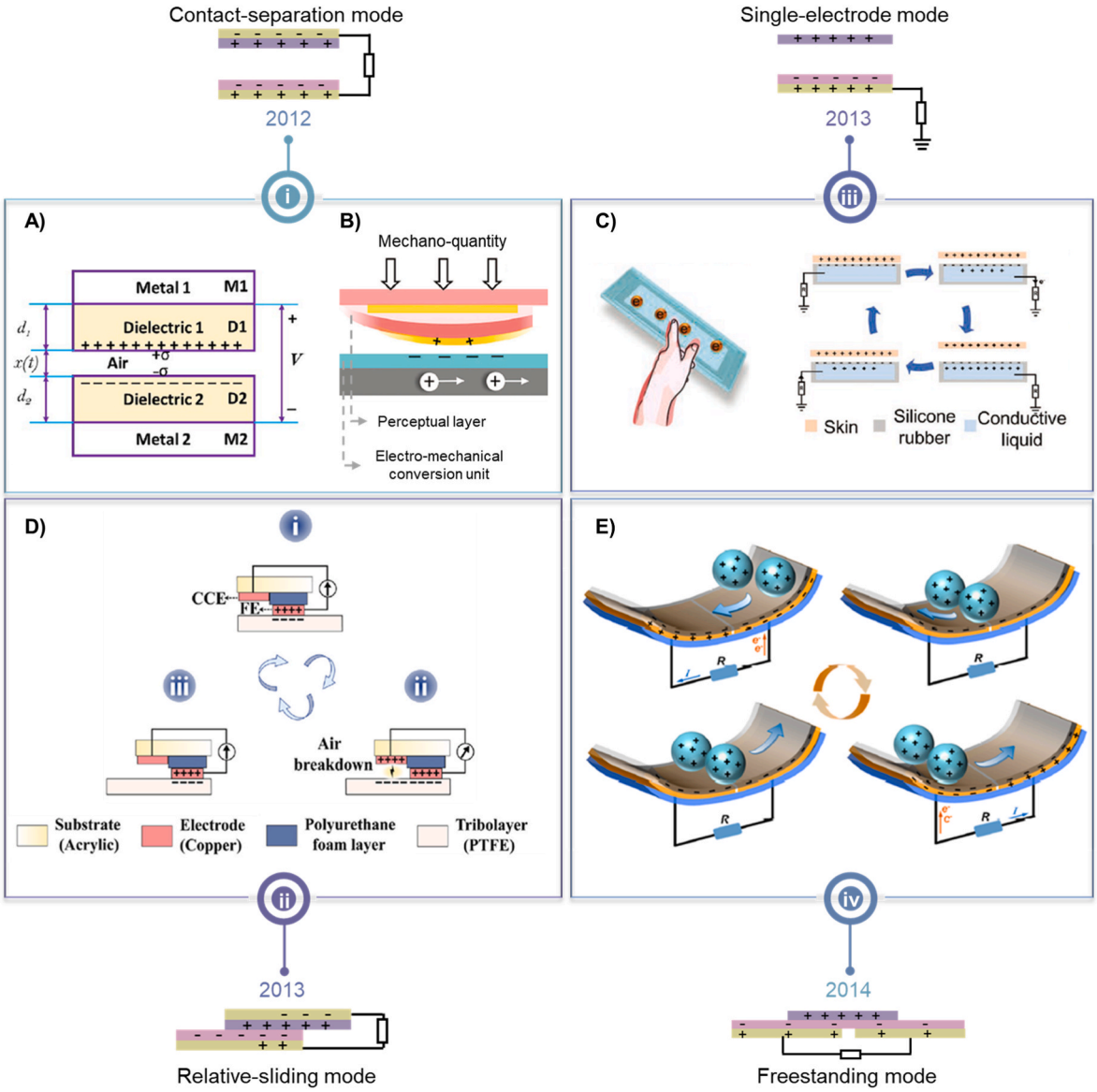


**Fig. 7.** A) Schematic diagram showing the working principle of the vertical contact-separation fundamental mode. Reproduced with permission from Ref. [94]. Copyright 2023. Published by American Chemical Society. B) Schematic illustration of the coupling mode between mechanical quantity, device, and electric output of TENG. Reproduced with permission from Ref. [156]. Copyright 2024. Published by Wiley-VCH. C) Schematic diagram of electricity generation when fingers are in contact with wsTENG. Reproduced with permission from Ref. [158]. Copyright 2022. Published by Wiley-VCH. D, E) Schematic diagram of the working mechanism of TENG. Reproduced with permission from Refs. [159,160]. Copyright 2024. Published by Elsevier Ltd. Copyright 2021. Published by American Chemical Society.

sensors in sensing low-intensity and low-frequency heart sounds [156]. This is due to the fact that, with increasing deformation, the electrical output of the TENG shows a constitutive property of rapid saturation. This saturation effect becomes faster when the tribological layer is thinner. In this case, even small deformations can be translated into high electrical output, thus ensuring high sensitivity to low-intensity mechanical quantities. Second, unlike piezoelectric devices, the direct sensing layer and the electromechanical conversion unit in TENG are relatively independent (Fig. 7B). As a result, TENG has a more flexible design capability to optimally couple low-frequency mechanical information without sacrificing the electromechanical coefficients, which further improves the sensitivity of heart sound sensing. Under the same test conditions, the triboelectric sensor achieves a sensitivity of 1215 mV $Pa^{-1}$ in the 50–80 dB sound pressure range, which is 60 times that of the piezoelectric sensor. In the case of high-frequency mechanical contact, Ronan et al. demonstrated a thin implantable triboelectric device capable of efficiently harvesting the mechanical energy of US-induced high-frequency vibrations [157]. US induces micrometer-scale displacements in polymer films, which generate electrical energy through CE. Under porcine tissue, US energy transfer in vivo produced voltages and currents of 2.4 V and 156 μA, respectively, allowing US to be harvested in vivo and to power medical implants.

The SE mode was invented by Zhang et al., in 2013 [161]. In the SE mode TENG, only one electrode is connected to (or acts as) the tribological layer (called the main electrode). The other electrode serves as an electric potential reference (called the reference electrode). The generator mechanism of the SE mode TENG shows almost the same characteristics as that of the CS mode TENG [133,162,163]. The SE mode TENG has the advantages of simple structure and suitable for single-sided application. Based on this, Yao et al. prepared a self-driven, wearable and stretchable SE-mode TENG (wsTENG), which was attached to a human finger to obtain energy from finger movement for glioma gas therapy (Fig. 7C) [158]. The peak open-circuit voltage ($V_{oc}$) reached about 395 V and the short-circuit current ($I_{sc}$) reached about 2.3 μA when the frequency of finger movement was 1 Hz. In addition, the output of the wsTENG remained almost unchanged after 21 d, suggesting that the wsTENG has a good stability and a long lifetime. In addition, the wsTENG is able to stabilize the output voltage well around 410 V at a non-constant strain rate.

In 2013, Wang's group developed the RS mode TENG, which differs from the CS mode in that the device operates in a horizontal direction, where two tribological layers start to overlap [164]. Based on the CE effect, this overlapping region will cause charge redistribution on the electrodes, thus realizing the energy conversion from mechanical to electrical [165,166]. The most attractive advantage of the RS-mode TENG is that it is suitable for high-frequency applications, and then produces a continuous output of electricity. Based on this, Li et al. fabricated a TENG that generates pulsed direct current (DC) power by coupling the CE effect and the electrostatic breakdown effect (Fig. 7D) [159]. TENG can generate up to 30 pulsed DC peaks with a peak current output of approximately 35 μA in a single slide, providing energy for triboelectric immunotherapy. However, this relative sliding mode of operation also poses a serious challenge of tribological damage to the tribological layer. Although some studies have reported considerable reliability of RS-mode TENG, long-term stability in practical applications remains a major issue. Different from traditional rolling triboelectric energy generation, Wang et al. proposed a novel stacked-disk rolling TENG (SDR-TENG) based on rolling triboelectricity generation to minimize material wear during operation [167]. The output current of the basic unit of the SDR-TENG decays by less than 5 % after 860,000 consecutive operating cycles, demonstrating excellent device durability. The FS mode TENG was proposed by Wang's group in 2014 [168]. The working principle is similar to the RS mode TENG, except that it utilizes continuous sliding friction [160,169]. Inspired by this mode of operation, Liu et al. developed a nodding duck-structured multi-track independent tribological layer nanogenerator (NDM-FTENG) oriented towards blue energy harvesting [160]. By sliding nylon balls on a curved dielectric composite film, the NDM-FTENG is able to convert low-frequency ocean wave energy into electrical energy, and ultimately obtain a stable and efficient power output (Fig. 7E).

Although TENG devices have made great progress in structural design and technological applications, the development of TENG applications in the biomedical field is still at an embryonic stage, and some key issues need to be further clarified. For example, the electrical output process of TENG cannot be separated from the mechanical force drive, and these mechanical forces directly determine the output performance, application scenarios and application effects of TENG. The complexity of biological organisms leads to the fact that the sources of mechanical forces are often complex, variable and uncertain, which hinders the further development of TENGs. Therefore, it is particularly important to understand the driving force patterns during the application of TENG in the biomedical field.

### 4.3. Force-driven mode

Clarifying the force driving modes can guide the application scenarios of electroactive materials and devices both in vivo and ex vivo, improve the electrical output performance and application effect. Currently, the force driving modes of electroactive materials and devices during its use in the biomedical field mainly include biological movement [170,171], tissue pressure [172–177], cellular force [175–177], US [178–180], and other driving modes [181–183] (Fig. 8).

Therefore, further understanding of the driving characteristics, driving scenarios, as well as advantages and limitations of these force driving modes is particularly important for advancing the application of electroactive materials and devices in the biomedical field. Based on this, we will next summarize the application scenarios and application characteristics of the different driving modes of force in the biomedical field, and clarify the advantages and limitations they have and face.

#### 4.3.1. Biological movement

The concept of self-powered electricity has been proposed in the past decade. Based on Maxwell's theory of displacement current, TENG, which can convert mechanical energy generated by body movement into electrical energy, has attracted much attention as a potential biomechanical energy harvester. Meanwhile, the presence of piezoelectric effect endows PENG with good force-electric conversion characteristics. Therefore, at the beginning of the application of TENG/PENG in the

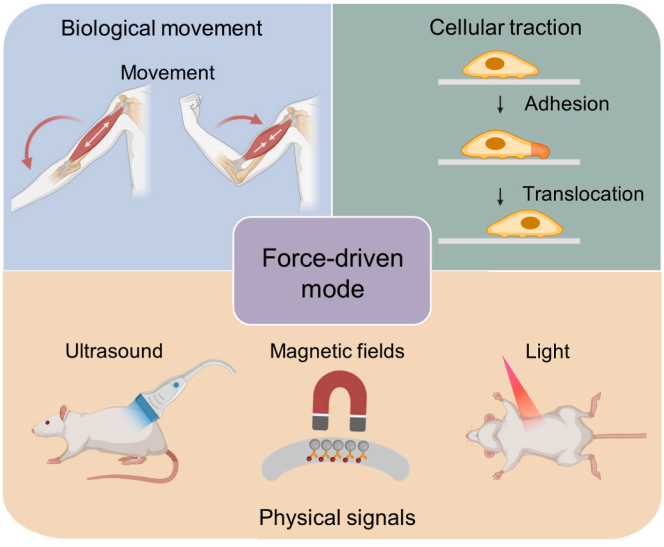


**Fig. 8.** Force-driven modes for driving electroactive materials and devices in the biomedical field.

biomedical field, its force driving method mainly focuses on the direct driving of the movement of the organism (joint movement, muscle stretching, breathing and heartbeat, etc.). TENG/PENG with an output frequency of a few Hz can be used directly during the movement of an organism and has the safety of high voltage and low current output without the need of an external energy transmitter. In addition, the alternating pulsed electrical signals generated by the TENG/PENG are physiologically synchronized under the drive of the organism's movement, which can effectively inhibit the inertia of physiological electrical stimulation that is commonly seen in clinical practice. The above advantages promote the application of TENG/PENG in the biomedical field.

Based on this, Qin et al. developed a wearable triboelectric stimulator, which consists of a flexible TENG (F-TENG) and a triboelectric responsive drug-delivery hydrogel for the healing of bacterial infected wounds [184]. In the F-TENG, a PET-indium tin oxide (PET-ITO) conductive film is used as a flexible top electrode and tribological layer, and a PVA-phytanic acid (PVA-PA) hydrogel-based bottom electrode is wrapped in an elastic silicone rubber tribological layer. The F-TENG can generate pulsed electrical stimulation for wounds by converting the

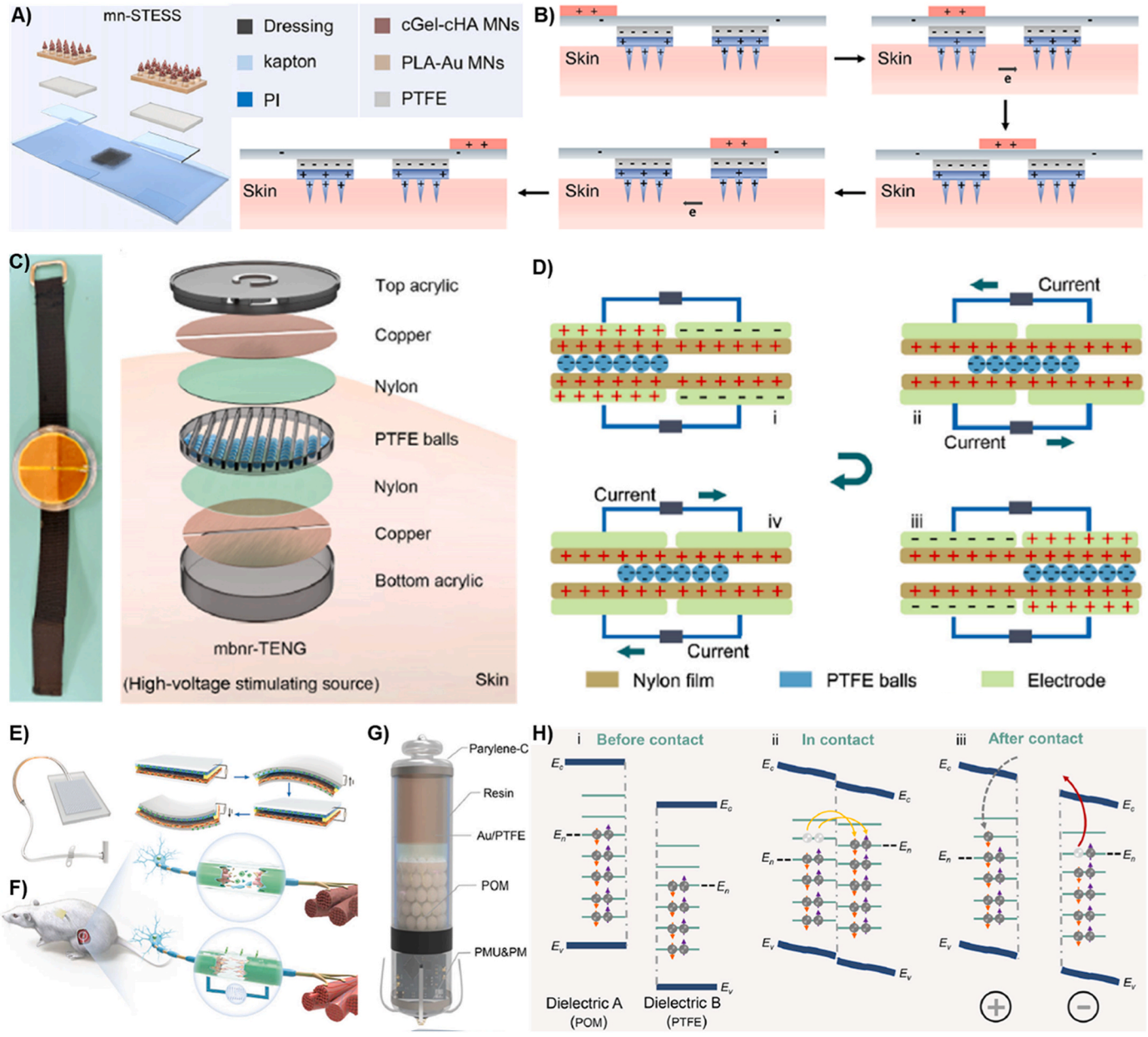


**Fig. 9.** A) Three-dimensional structure of the microneedle-based self-powered transcutaneous electrical stimulation system. Reproduced with permission from Ref. [185]. Copyright 2022. Published by Springer Nature. B) Schematic of the working principle of sf-TENG. C) Optical picture and schematic of mbnr-TENG. Reproduced with permission from Ref. [186]. Copyright 2024. Published by Elsevier Ltd. D) Schematic of the working principle of mbnr-TENG. E) Schematic illustration of the structure of Cs-TENG and its application by the energy-scavenging process. When two layers of dielectric films contact each other and are separated by external force, the inductive potential difference is formed between the two electrodes. Electrons flow from one aluminum electrode to another through a load, creating an inverse potential difference to balance the electrostatic field. Reproduced with permission from Ref. [186]. Copyright 2022. Published by Wiley-VCH. F) Schematic representation of electrode implantation solution. The skin is incised, electrical stimulation cuff is introduced on the rat's left side sciatic nerve. The Cs-TENG worked as an energy harvester has been placed on the rat's lumbar area and connected the electrode with capsulated Pt wire. G) Internal perspective structure of the device. Reproduced with permission from Ref. [187]. Copyright 2023. Published by Springer Nature. H) Charge transfer (i) before contact, (ii) in contact, and (iii) after contact between two different dielectrics-polyformaldehyde (POM) and PTFE.

mechanical energy generated by body movements. When attached to the wrist, arm, or knee, the F-TENG can reach 15–20 V by flexing the joint area. Yang et al. develop a microneedle-based self-powered transcutaneous electrical stimulation system (mn-STESS) by integrating a sliding free-standing TENG (sf-TENG) with a microneedle (MN) patch (Fig. 9A) [185]. sf-TENG converts the mechanical energy generated by sliding a finger into electrical energy and delivers transcutaneous electrical stimulation through a microneedle (Fig. 9B). The TENG consists of a tribological layer, a dielectric layer and an electrode layer. A polyimide film was used as the tribological layer, a polytetrafluoroethylene film covered with Kapton tape was used as the dielectric layer, and polylactic acid (PLA)-coated gold microelectrode array patches were used as the electrodes. When the TENG was actuated by a finger with a sliding frequency of 2 Hz, the obtained open-circuit voltage, short-circuit current, and short-circuit transfer charge were about 20 V, 1 μA, and 11 nC, respectively. In addition, Liu et al. prepared a multi-ball nimble-rolling TENG (mbnr-TENG) consisting of polytetrafluoroethylene balls and nylon film (Fig. 9C) [186]. The mbnr-TENG can convert the mechanical energy generated by the oscillation of an organism into electrical energy, which is used as an electrical stimulation device. The mbnr-TENG consists of a tribological layer, a dielectric layer and an electrode layer. The nylon film was used as the dielectric layer, and the two layers of nylon film were filled with polytetrafluoroethylene balls as the tribological layer (Fig. 9D). The TENG device reached its optimal performance ($V_{oc}$ = 143 V, $I_{sc}$ = 0.62 μA, and $Q_{sc}$ = 46.84 nC) at a swing angle of 90°. This is due to the fact that this angle makes the PTFE balls parallel to the direction of the electrodes, resulting in maximum displacement and highest efficiency. PENG, as another electroactive device, not only has the same energy conversion as TENG, but also has the advantages of simple structural design and sensitivity to mechanical forces. Fu et al. prepared a wearable DC pulsed PENG based on P(VDF-TrFE) [170]. This PENG converted the rat's movement into an electric field and provided electrical stimulation to the wound edge tissue. The PENG was immobilized to the back of the rat, and the output voltages of the PENG were 420, 1320, and 2630 mV under different movement states (anesthetized/awake/jumping).

In additional to the above, special tissues such as the heart beating, breathing, or muscles stretching during exercise generate a certain mechanical force, and converting this force into an electrical signal is also an effective form of electrical stimulation.

Based on this, Zhou et al. selected PDMS and polyamide 6 (PA6) films with different tribological polarity to prepare a contact-separated TENG (Cs-TENG) driven by respiratory motion and regular activity to maximize the triboelectric effect (Fig. 9E) [188]. This TENG was implanted into the subcutaneous site of the rat's lumbar region and generated biphasic electrical pulses during abdominal respiratory movements (Fig. 9F). Four weeks after implantation, the TENG was able to maintain a voltage output of 2.18 ± 0.79 V, thus ensuring its effectiveness in neuroelectric stimulation. Zhong et al. prepared a micro-vibratory TENG with PTFE and PA6 films as tribological layers, also based on the respiratory motor drive in rats. This TENG could collect the micromechanical energy generated by respiration and convert it into a pulsed signal (current value of 0.83 ± 0.23 μA) for phrenic nerve stimulation. Meanwhile, the output of this TENG was stable within 4 weeks of subcutaneous implantation in rats, and the energy harvesting effect was remarkable. In addition, the heart beat induced by the contractile force of cardiomyocytes has gained attention in driving electroactive devices. Liu et al. reported a self-powered intracardiac pacemaker (SICP) with a capsule structure for harvesting biomechanical energy from cardiac beats (Fig. 9G) [187]. The SICP consists of an energy harvesting unit (EHU), a power management unit (PMU), a pacemaker module (PM), a hook, and a radiopaque marker. The SICP is subsequently integrated with a customized delivery catheter system and implanted into the heart via an intravenous route. The SICP is anchored to the endocardium of the right ventricle by a hook-like structural design that converts biomechanical energy generated by cardiac beats into electrical energy. The EHU is fabricated using POM particles and gold electrodes deposited in PTFE film. With the heart beating, the POM particles are rolled back and forth between the two electrodes, resulting in an alternating current based on CE and electrostatic induction (Fig. 9H). At a volume ratio ($V_{pellets}/V_{cavity}$) of 40 %, the maximum value of $V_{oc}$ was approximately 21.8 V. The output performance of the SICP was further validated on a porcine model. The results showed that the average voltage and current of the SICP in vivo could reach 4 V and 0.2 μA, respectively.

In terms of PENG, Liu et al. proposed a piezoelectric conductive scaffold whose piezoelectricity was achieved by assembling diphenylalanine on the surface of the holes, while the conductivity of the scaffold was achieved by adding poly(3,4-ethylenedioxythiophene) [173]. During joint movement, mechanical forces compress the scaffold, which in turn creates a potential difference. The output voltage and current of the piezoelectric hydrogel were about 20 mV and 0.8 μA, respectively, under a cyclic compression force of about 2 N. In addition, the piezoelectric conductive scaffold was implanted into the rabbit knee joint site, and the electrical output was measured during the knee joint movement. The results showed that the deformation induced by joint motion produced a stable voltage output (1 mV) with minimal abnormal fluctuations. Although the PENG had good output stability driven by tissue pressure, its output performance was limited. Wang et al. present an unusual flexible hybrid friction/PENG (HTP-NG) [189]. At the core of the HTP-NG are triboelectric and piezoelectric modules that capture knee motion energy to generate electrical energy. The piezoelectric module consists primarily of a commercially polarized PVDF film and two silver (Ag) electrode layers. Due to the large difference in electronegativity between PTFE and Ag, the PTFE layer and Ag layer are used as negatively and positively charged tribological layers, respectively. The HTP-NG has better force-electricity conversion capability than a single triboelectric or piezoelectric module, and the $V_{oc}$, $I_{sc}$, and corresponding $Q_{sc}$ of the HTP-NG under simulated biomechanical motions are about 35 V, 3.7 μA, and 23 nC, respectively. The designed HTP-NG device is implanted into the subcutaneous tissue of the thigh and generates biphasic electrical impulses driven by knee motion, which are then conducted to the area of the heel defect for electrical stimulation therapy. The researchers mentioned above have used the mechanical force generated by biological movement to directly drive electroactive devices, thereby generating electrical stimulation for biomedical applications. However, due to the direct drive of mechanical forces, most electroactive devices can only be fixed at specific tissue sites in vivo or joints in vitro, which makes the process of applying electrical stimulation complicated in terms of lead connection, unclear stimulation range, and low efficiency of electrical stimulation delivery. This provision of mechanical force is not favorable to organisms with difficulties in locomotion and muscle contraction, thus limiting the further application of electroactive materials and devices in the biomedical field.

#### 4.3.2. Cellular traction

Cellular traction, an innovative force-driven mode, demonstrates unique advantages in driving electroactive materials and devices to produce efficient electrical output. This mode does not need to rely on joint movement or muscle extension of the organism, thus avoiding the potentially detrimental effects of early electrical stimulation on cell spreading and adhesion, while simplifying the complex process of inducing material transformation or external stimulus triggering. In recent years, cardiomyocytes have received close attention from researchers as the quintessential representative of cell force generation. [190]. Zheng et al. designed and fabricated a homogeneous and well-aligned InGaN/GaN nanopillar array, named PLNA array, for detecting the cellular contraction force generated by cardiomyocytes [175]. When the cardiomyocytes are located at the top of the InGaN/GaN nanopillars, the piezoelectric effect of the multiple quantum wells at the top of the nanopillars is extremely sensitive to the internal piezoelectric potential. The small external force generated by the cardiomyocyte can change the intrinsic strain of the InGaN/GaN

nanopillar, leading to the redistribution of the piezoelectric potential, which in turn regulates the spot emission of the PLNA. Therefore, the cellular force of cardiomyocytes in resting and contracted states can be directly derived and visualized by PLNA arrays. The cellular force, as a force-driven mode, can not only drive the electroactive material to generate electrical output, but also this electrical output can counteract the cell itself, thus realizing in situ electrical stimulation.

As shown in Fig. 10A and B, Murillo et al. investigated the proliferation and differentiation of osteoblast-like Saos-2 living cells on piezoelectric zinc oxide nanosheets, verifying the possibility of self-electrical stimulation and modulation of cellular activity driven by cellular traction, enabling in situ electrical stimulation [191]. Similarly, Kitsara et al. achieved in situ electrical stimulation of proliferation by growing Saos-2 cells on piezoelectric PVDF nanofibers [192]. In the work of Polak et al. it was also verified that osteoblast-like cells, G-63 cells, grown on the surface of piezoelectric PLLA fibers were able to feel the PLLA fiber providing a favorable charge environment, and the level of skeleton, filamentous pseudopods and adhesion spot development of the cells was significantly enhanced [193]. Further, the work of Liu et al. provides more visual evidence for in situ electrical stimulation of cells, as shown in Fig. 10C and D, where a smart piezoelectric scaffold with collagen-like stiffness was visualized in real-time monitoring to cause fibers to produce deformation during the growth of living cells [194]. Further, Cui et al. applied this in situ electrical stimulation to rats for the first time, and piezoelectric PLLA fibers were used as coatings for bone implants to rapidly achieve osseointegration of the implants with the organisms, and this work is undoubtedly a strong validation of in situ electrical stimulation induced by cellular traction (Fig. 10E and F) [91].

In addition to the above researches, Sun et al. constructed a three-dimensional multifunctional structure (3DMA) consisting of a titanium dioxide nanotube layer and an electrospun piezoelectric PVDF nanofiber layer [195]. When 3DMA was applied to the wound infection site, macrophages tended to adhere to the piezoelectric PVDF layer. Mechanical interactions between macrophages and piezoelectric PVDF fibers generate a self-excited electric field that modulates the anti-inflammatory phenotype. Therefore, piezoelectric materials can be used to establish in situ electrical stimulation networks for macrophage-based anti-inflammation. Meanwhile, Guo et al. also found that the in situ electrical stimulation network established by piezoelectric materials can not only modulate cellular phenotypes, but also manipulate cellular activities, including alignment and proliferation [177].

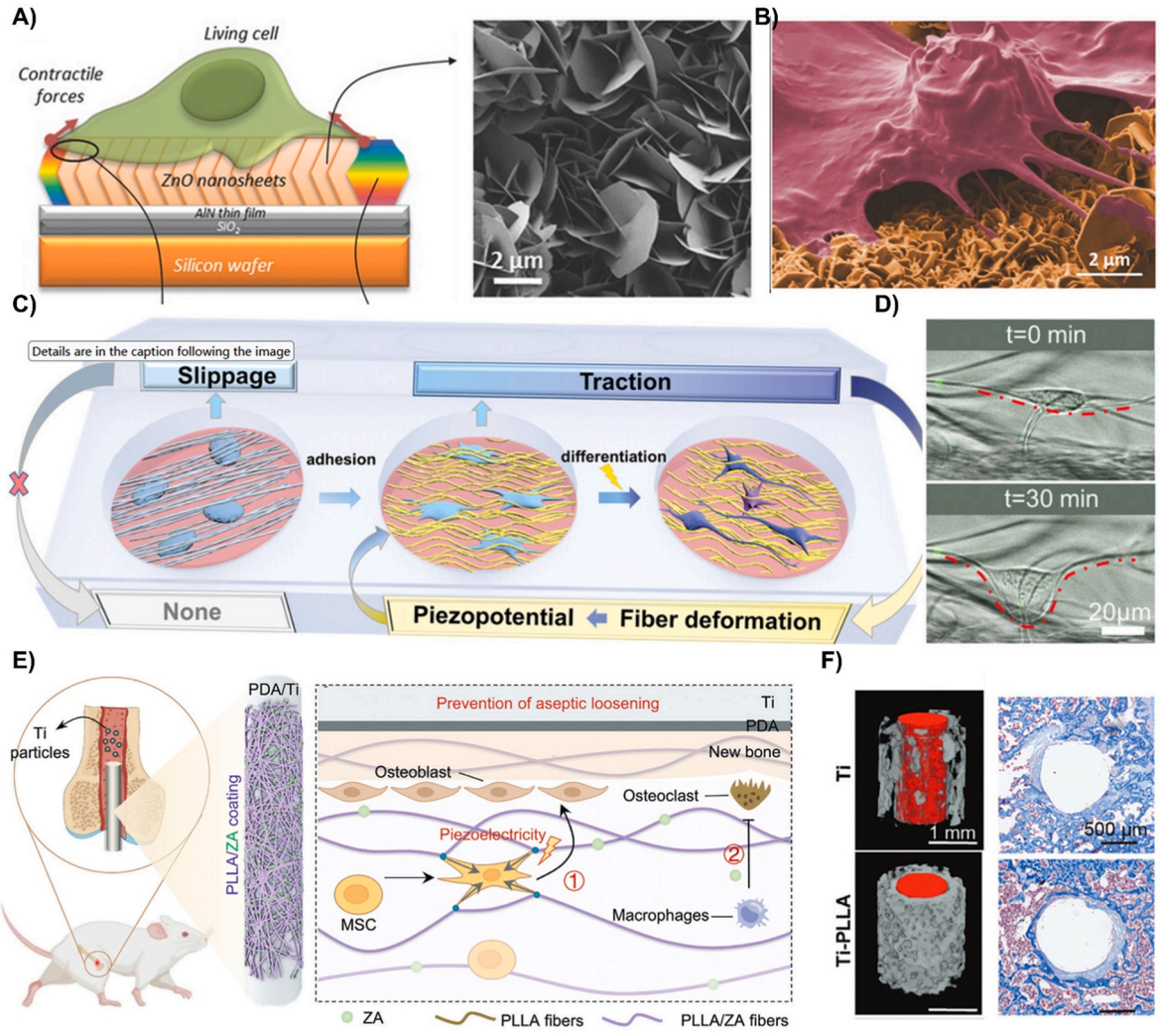


**Fig. 10.** A) Saos-2 living cells grown on piezoelectric zinc oxide nanosheets. B) Cellular traction induced deformation of nanosheets. Reproduced with permission from Ref. [191] Copyright 2017. Published by Wiley-VCH. C) Dynamic mechanical interactions between cells and bionic extracellular matrix. D) The deformation along the nanofibers caused by cell traction. Reproduced with permission from Ref. [194] Copyright 2023. Published by Wiley-VCH. E) Piezoelectric fibers as a surface coating for bone implants. F) Piezoelectric fiber coating enabled rapid osseointegration. Reproduced with permission from Ref. [91] Copyright 2024. Published by Wiley-VCH.

Despite the many advantages of the cellular traction force self-driven in situ electrical stimulation modality, the problem of too small cellular traction force also limits its application. Therefore, the design and optimization of materials or devices for tiny structures to improve their sensitivity to cellular traction is an important direction of current research.

#### 4.3.3. Physical signals

Although some electroactive materials and devices driven by the above mentioned forces can somewhat solve the problems of time and space limitation, poor spatial resolution, low efficiency of electric field transfer, and frequent replacement of power sources that are associated with conventional power supply devices. However, harvesting sufficient energy in the constrained environment of the human body remains a challenge. Mechanical energy generated through organism movement and cellular traction is low, resulting in low electrical output energy. Physical signals (sound, light, electricity, magnetism, heat), as non-invasive external energy sources, can provide stable and sufficient mechanical energy for electroactive materials and devices, especially the ultrasound (US). In the driving process of electroactive materials,

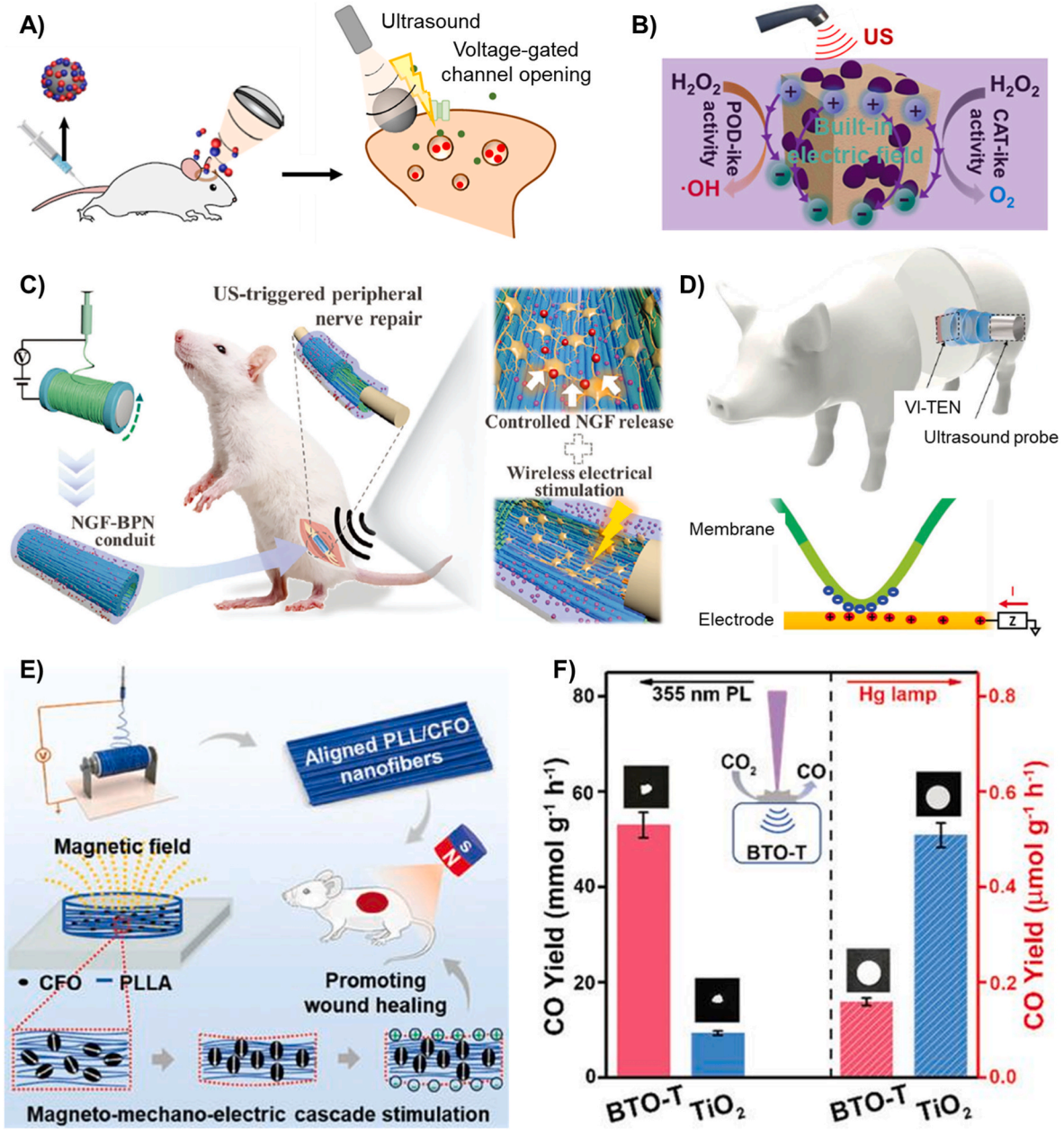


**Fig. 11.** A) Schematic illustration of neural electric stimulation with NPs under US. Reproduced with permission from Ref. [196]. Copyright 2022. Published by Springer Nature. B) Piezoelectric enhanced NPs catalytic activity under US. Reproduced with permission from Ref. [197]. Copyright 2022. Published by American Chemical Society. C) Schematic diagram of the US-responsive aligned piezoelectric nanofibers derived hydrogel conduits for peripheral nerve regeneration. Reproduced with permission from Ref. [198]. Copyright 2024. Published by Wiley-VCH. D) Schematic of the porcine ex vivo (showing the location of the implanted VI-TEG) and the generator mechanism of VI-TEG. Reproduced with permission from Ref. [157]. Copyright 2019. Published by American Association for the Advancement of Science. E) Schematic illustration of the design and possible mechanism of MME cascade stimulation system. Note: MF and EMF are abbreviations of magnetic field and external magnetic field. Reproduced with permission from Ref. [181]. Copyright 2024. Published by Wiley-VCH. F) Photocatalytic $CO_2$ reduction performances of BTO-T and $TiO_2$ under the irradiation of 355 nm pulsed lasers (PL) and Hg lamp, respectively. The inset shows a schematic diagram of laser-triggered piezoelectric photocatalytic reaction on BTO-T. Reproduced with permission from Ref. [182]. Copyright 2023. Published by Wiley-VCH.

Taejeong et al. demonstrated a composite piezoelectric NPs that can generate direct current under high-intensity focused US for stimulation of deep brain tissues (Fig. 11A) [196]. The composite piezoelectric NP (BTNP-pDA) consisted of N,N′-di-*sec*-butyl-N,N′-dinitroso-1,4-phenylenediamine (BNN6) and piezoelectric barium titanate NPs coated with polydopamine. Subsequently, the piezoelectric behavior of the NPs under ultrasonic stimulation was evaluated by an interconnection-free patch-clamp device. The experimental results showed that the BTNP-pDA possessed excellent current outputs (~3.30 pA, ~4.57 pA, ~11.8 pA, and ~22.4 pA) at different intensities of US (0.4 W $cm^{-2}$, 0.8 W $cm^{-2}$, 1.6 W $cm^{-2}$, and 3.2 W $cm^{-2}$).

US can not only drive the electroactive piezoelectric nanomaterials to generate electrical output, but also modulate the electronic polarization inside the electroactive piezoelectric nanomaterials, thus activating the piezoelectric catalytic performance of the electroactive materials. Cai et al. prepared a piezoelectric NPs based on a hafnium-based UIO-66 and Au NPs [197]. Under US stimulation, UIO-66 could generate a built-in electric field inside the material, thus promoting electron-hole separation and generating catalytic activity (Fig. 11B). The introduction of Au NPs facilitated electron transfer, which inhibited the recombination of electron-hole pairs and improved the piezoelectric properties of UIO-66. Upon deposition of Au NPs, the $d_{33}$ of UIO-66 was increased from 71 $pmV^{-1}$ to 122 $pmV^{-1}$. In addition, the catalytic activity of the piezoelectric NPs was increased by 2-fold under the stimulation of US, which facilitates its further application in the field of catalytic medicine. US has the same potential for development in the field of driving electroactive devices. Based on this, Xu et al. prepared US-responsive oriented piezoelectric nanofiber-derived hydrogels NGC for peripheral nerve regeneration (Fig. 11C) [198]. Specifically, poly (vinylidene fluoride-trifluoroethylene) [BTNPs/P(VDF-TrFE)] nanofibers doped with barium titanate piezoelectric NPs were prepared by electrostatic spinning, which had neat orientation and high β-phase crystallinity, thus ensuring effective piezoelectricity. In order to investigate the piezoelectricity of BTNPs/P(VDF-TrFE) nanofibers, they were encapsulated in two aluminum foil electrodes and a flexible polyurethane film to construct a flexible piezoelectric device. The device showed an open-circuit voltage of about 1.69 V under US stimulation of 0.75 W $cm^{-2}$ in water, demonstrating the potential for in vivo wireless US electrical stimulation.

US stimulation is not only effective in driving piezoelectric-based electroactive materials and devices, but it also plays an important role in the driving process of triboelectric devices. A thin implantable vibratory triboelectric generator (VI-TEG) that can effectively harvest mechanical energy has been demonstrated by Hinchet et al. (Fig. 11D) [157]. In the preparation of the VI-TEG, Hinchet et al. first designed a thin (~50 μm thick) and large perfluoroalkoxy (PFA) membrane as a tribological layer and generated vibrations under US pressure. The PFA membrane was then suspended (with an air gap of 80 μm) on a 3.6 cm × 3.6 cm thin copper electrode (main electrode). The electrode was fabricated on a flexible printed circuit board and covered with gold. The final sealing of the film with a melt adhesive makes the VI-TEG less than 1 mm thick. The VI-TEG is able to efficiently convert US mechanical energy into electrical energy. Under porcine tissue, US energy transfer in vivo produced voltages and currents of 2.4 V and 156 μA, respectively, which were sufficient to charge the battery of a small implant.

In addition to the ultrasound signal, researchers have found that external stimuli, such as magnetic fields and light, also bring about the deformation of materials to produce mechanical force-driven. Zhang et al. developed a magneto-mechanical-electrical (MME) cascade stimulation system based on magnetoelectric nanofiber membranes (Fig. 11E) [181]. The magnetoelectric nanofiber membrane (PLLA/CFO) consists of biodegradable PLLA and cobalt ferrite (CFO). CFO NPs with excellent magnetic properties and biocompatibility were modified with dopamine to enhance their biostability and interfacial coupling with the PLLA matrix. Subsequently, the piezoelectric, magnetic and magnetoelectric properties of PLLA/CFO membranes were explored. The results showed that the PLLA/CFO membrane produced an electrical stimulation of about 53 mV when the magnetic field strength was 80 mT. Wang et al. found that PL can generate large light pressure [182]. A low-power PL (3 W, 355 nm) as a UV light source can trigger piezoelectric photocatalysis of tetragonal BTO (BTO-T) without external force (Fig. 11F). This catalytic performance was generated due to the huge transient light pressure of the 355 nm PL ($5.7 \times 10^7$ Pa, 2.7 W) not only bending the energy bands of the BTO-T to enable the theoretically unavailable reaction to occur, but also inducing a pulsed built-in electric field to determine the effective photo-induced carrier separation. The BTO-T was then assembled into a miniature pressure sensor and the pressure generated by the 355 nm PL was investigated. The pressures generated by different laser powers (2.7, 1.8, and 1.5 W) were $5.35 \times 10^{-3}$, $1.78 \times 10^{-3}$, and $1.24 \times 10^{-3}$ N. Subsequently, the output signal of the BTO-T reached up to 38 mV when the PL pressure was applied to the BTO-T surface.

In the research process of electroactive materials and devices, the driving mode of force determines the application effect and application scenario of electroactive materials and devices. Therefore, clarifying the different driving modes of mechanical forces will further promote the application of electroactive materials and devices in the field of regenerative medicine. It is also worth noting that Molecular Dynamics (MD) simulations resolve dynamic mechanoelectrical coupling and degradation kinetics, while Density Functional Theory (DFT) optimizes triboelectric/piezoelectric properties at atomic scales. Combined with machine learning, these tools enable predictive material screening and defect engineering, accelerating the development of bioactive, high-output PENGs/TENGs for precision regenerative therapies.

## 5. Force-electrical conversion of biomaterials and devices for regenerative medicine

The regulatory role of electric fields in the metabolic processes of organisms has been conclusively demonstrated, with its influence permeating through multiple biological levels, including cells, tissues, and organs. Notably, in cell populations highly sensitive to electrical stimulation, such as bone and neuronal tissues, it exhibits particularly significant regulatory effects. Therefore, electrical stimulation has become an innovative means of tissue regeneration and functional recovery, and is widely used in the field of regenerative medicine. Meanwhile, in terms of the mechanism of tissue regeneration and functional regulation driven by electrical stimulation, electrical stimulation synergistically promotes tissue regeneration and functional regulation through multi-dimensional mechanisms: i) at the level of biologically active molecules, electrical stimulation regulates the release of neurotrophic factors and metabolic small molecules, and reshapes the regenerative microenvironment; ii) at the level of ion channels, electrical stimulation activates voltage-gated and mechanosensitive channels; iii) at the protein expression level, electrical stimulation upregulates cytoskeletal proteins and differentiation markers, and enhances functional protein activity through phosphorylation and acetylation modifications; iv) at the signaling level, electrical stimulation integrates multiple signaling pathways (PI3K/AKT, Wnt/β-catenin, and Hippo-YAP, etc.) to drive cell proliferation, migration, and directional differentiation. Against this backdrop, force-electric conversion biomaterials, which possess the capability to efficiently convert mechanical signals into electrical signals, have demonstrated immense potential and prospects in the realm of regenerative medicine. Based on force-electrically convertible materials, TENGs and PENGs have been extensively integrated into various biomedical application scenarios due to their unique properties [199] (Table 1). These applications primarily focus on three major areas: firstly, regenerative repair following tissue injury, encompassing the repair and regeneration of critical tissues such as nerves, bones, cartilages, tendons, and skin; secondly, electrical stimulation modulation following the loss of specific functions, where precise electrical stimulation techniques are employed to facilitate the

**Table 1**
Force-driven modes and stimulation times of force-electric biomaterials and devices.

| Type | Application | Force-driven mode | Electrical properties | Stimulation time | Ref. |
|---|---|---|---|---|---|
| Piezoelectric biomaterials | Regulation of brain function | Ultrasound | ~3.30 pA | 60 s | 227 |
| | Regulation of muscle function | Biological movement | 120 mV | 10 days | 238 |
| | Regulation of nerve | Ultrasound | 15.29 μV | 4 min | 244 |
| | | Biological movement | 5 V | 3 weeks | 242 |
| TENGs | Bone repair | Biological movement | 35 V<br>3.7 μA | 6 weeks | 212 |
| | Nerve regeneration | Biological movement | 2.7 V<br>0.12 μA | 12 weeks | 203 |
| | Regulation of heart function | Biological movement | 67.5 V<br>5.9 μA | 0.5 ms | 208 |
| PENGs | Nerve regeneration | Ultrasound | 17.9 V<br>2.6 μA | 20 min | 202 |
| | Bone repair | Ultrasound | 220 mV | 2 min | 213 |
| | Skin regeneration | Biological movement | 8.71 V | 10 days | 219 |
| | Regulation of brain function | Biological movement | 13.49 V | 15 min | 226 |
| | Regulation of heart function | Magnetic fields | 559.8 mV<br>314.5 pA | None | 209 |
| | Regulation of muscle function | Magnetic fields | 64 μV | 5 days | 239 |
| | | Ultrasound | ~300 mV | 20 min | 210 |

recovery and regulation of organ functions such as the brain, heart, eyes, and muscles; and thirdly, electrical stimulation therapy for specific diseases, utilizing electric field effects to achieve precise drug delivery, electric field-catalyzed therapy, and electrical stimulation to eliminate diseased cells, thus providing new methods and strategies for tissue function recovery and regeneration.

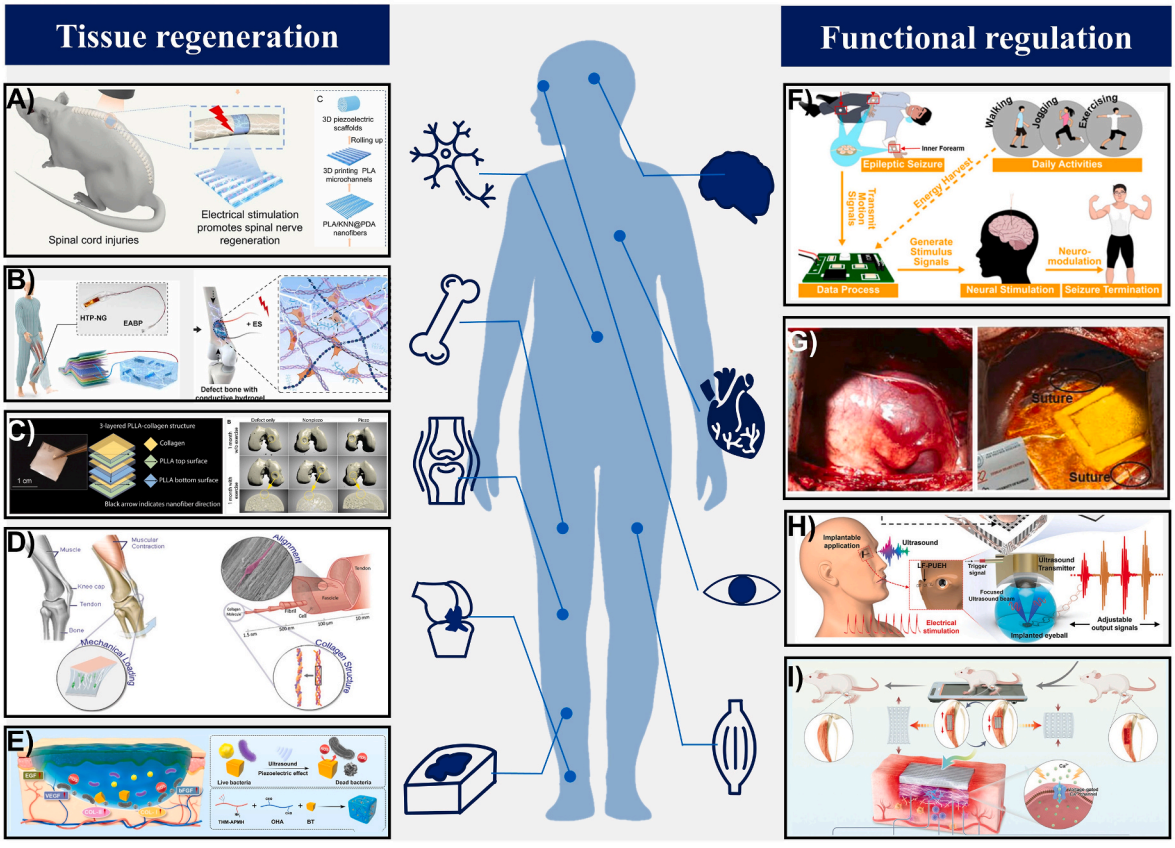


**Fig. 12.** Force-electrical conversion biomaterials for tissue regeneration and functional regulation. A) US-driven piezoelectric degradable spinal cord scaffolds. Reproduced with permission from Ref. [202] Copyright 2022. Published by American Chemical Society. B) Bone regeneration electrical stimulator with combined friction and piezoelectricity. Reproduced with permission from Ref. [204] Copyright 2024. Published by AAAS. C) Exercise-induced piezoelectric stimulation for cartilage regeneration. Reproduced with permission from Ref. [205] Copyright 2024. Published by AAAS. D) A Self-powered piezo-bioelectric device regulates tendon repair Reproduced with permission from Ref. [148] Copyright 2020. Published by Wiley-VCH. E) US-triggered piezocatalytic composite hydrogels for promoting bacterial-infected wound healing Reproduced with permission from Ref. [206] Copyright 2022. Published by Elsevier. F) A self-powered wearable seizure-monitoring/brain-stimulating system for potential epilepsy treatment Reproduced with permission from Ref. [207] Copyright 2022. Published by Elsevier. G) Symbiotic pacemakers based on the TENG. Reproduced with permission from Ref. [208] Copyright 2019. Published by Springer Nature H) Magnetostriction enhanced self-powered nanofiber sheet as cardiac patch. Reproduced with permission from Ref. [209] Copyright 2024. Published by Elsevier. I) Highly stretchable piezoelectric elastomers for skeletal muscle defect repair. Reproduced with permission from Ref. [210] Copyright 2023. Published by Wiley-VCH.

### 5.1. Tissue regeneration

#### 5.1.1. Nerve

Researches have demonstrated that an electrical field environment can effectively promote neuronal differentiation and synaptogenesis, thereby accelerating the recovery of neural function. Specifically, electrical stimulation not only stimulates the regenerative capacity of injured nerves but also significantly enhances the growth of axons at the surgical repair site of nerve transections when applied continuously at a frequency of 20 Hz for 1 h, leading to rapid reinnervation of target muscles [200,201]. However, the percutaneous external wiring required for implantable electrical stimulation devices poses numerous practical inconveniences, limiting their widespread application. To address this issue, self-powered electrical stimulation devices have emerged, aiming to achieve internal treatment through internal energy sources and eliminate the hassle of external wiring.

Piezoelectric electroactive materials, due to their unique property of generating electrical signals in response to external stimuli, thereby promoting the growth and differentiation of neuronal cells, have become a new research direction for treating neural regeneration. These materials provide novel ideas and pathways for solving the challenges of neural regeneration. Notably, Chen et al. have successfully developed a spinal cord repair neural scaffold capable of generating wireless electrical stimulation under ultrasonic driving. This scaffold, composed of biodegradable PLA and piezoelectric KNN nanowires in a three-dimensional multi-channel structure, exhibited excellent effects in promoting neural stem cell differentiation and endogenous angiogenesis in a rat model of spinal cord injury (Fig. 12A) [202]. Furthermore, Jin et al. constructed a fully implantable neural electrical stimulation system by integrating a novel triboelectric/piezoelectric hybrid nanogenerator with a nanoporous neural conduit. This system can generate self-regulating electrical signals utilizing the body's own movements and is highly sensitive to different physiological states, thereby achieving precise regulation of neural regeneration. Experimental data indicate that this system is comparable to autologous grafting in repairing 15 mm-long sciatic nerve defects [203].

It is worth noting that, in designing electrical stimulation neural conduit scaffolds, besides meeting the requirements of electrical stimulation, the structural design of the scaffold is equally crucial. A well-designed structure not only facilitates the directional growth and differentiation of neuronal cells but also provides effective guidance for neural regeneration, further promoting the recovery of neural function. Therefore, in future research, both electrical stimulation and structural design should be considered comprehensively to develop more efficient and reliable neural regeneration treatment strategies.

#### 5.1.2. Bone

Bone tissue stands as the largest natural piezoelectric material in organisms, with its piezoelectricity originating from the oriented arrangement of collagen fibers. The surface of injured bone tissue exhibits electronegativity, which plays a pivotal role in guiding bone regeneration at defective sites. Electrical stimulation, as an effective physical means, can direct the spatial arrangement of cells, promote cell proliferation, and induce differentiation in specific directions. As early as 1981, there were documented cases of successful treatment of tibial nonunion using pulsed electromagnetic fields [211]. The application of direct electrical stimulation with certain parameters to stem cells can also accelerate cell proliferation and osteogenic differentiation. Wang et al. developed a fully implantable bone defect electrical stimulation (BD-ES) system that integrates a hybrid triboelectric/PENG to provide biphasic electrical pulses in response to rehabilitation training, along with a conductive bioactive hydrogel (Fig. 12B). BD-ES enhances various osteogenic-related biological processes, including calcium ion channels and osteogenic differentiation. In a rat model of critical-size femoral defects, BD-ES treatment followed by subsequent bone mineralization reversed the bone defects, resulting in complete healing of the femur within 6 weeks. Compared to direct electrical stimulation, direct contact of the newly formed tissue with the material can more effectively amplify the electrical signals [212]. Cui et al. fabricated a biomimetic mineralized PLLA-based bone scaffold, where PLLA nanofibers provide piezoelectric properties mimicking bone collagen fibers, while hydroxyapatite crystals on the PLLA fiber surface offer bone-like chemical composition. This filled bone scaffold facilitates rapid recruitment of endogenous stem cells and piezoelectric-induced osteogenesis, and it completely degrades as new bone regeneration progresses [213].

Similarly, the growth process of cartilage resembles that of bone cells, and cartilage regeneration poses a crucial challenge in osteoarthritis and cartilage defects. In promoting the regeneration of articular cartilage, piezoelectric materials also demonstrate significant advantages, acting as battery-free electrical stimulators under applied forces or joint loads to enhance cartilage formation. Researchers have prepared a multilayer piezoelectric device that generates controllable piezoelectric charges under stress or joint loads, promoting the adsorption of extracellular proteins, facilitating cell migration or recruitment, and inducing the release of endogenous TGF-β through calcium signaling pathways to promote cartilage formation and regeneration both in vitro and in vivo (Fig. 12C) [205].

Tendon disorders also represent a key challenge in the field of orthopedics. Studies have shown that devices based on piezoelectric conversion can regulate ion channels in tendon cells in vitro and modulate specific tissue regeneration signaling pathways. Moreover, as shown in Fig. 12D, electromechanical stimulation regulates the sensitivity of mechanosensitive ion channels, promoting tendon-specific repair processes over non-tendinous tissues [148]. In summary, these advancements highlight the potential of piezoelectric materials and electrical stimulation in guiding bone and cartilage regeneration, as well as in modulating tendon cell behavior. By leveraging the unique properties of these materials and techniques, researchers are paving the way for more effective and efficient treatment strategies in orthopedic medicine.

#### 5.1.3. Skin

Wound healing is a complex and intricate biological process involving interactions among various cells and molecules. In this process, the guiding role of electric fields has been proven to be crucial. Over a century ago, Emil et al. first recorded the presence of weak currents at wound sites, laying the foundation for subsequent research on the role of electric fields in wound healing [214].

Normal epidermal cells form a transepithelial potential through their internal ion channels, which is the basis for the endogenous electric field in wounds. Cations (such as $Na^+$) are primarily transported to the basal side of the epidermis, while anions (such as $Cl^-$) are transported to the apical side, resulting in an asymmetric ion distribution that generates the transepithelial potential [215,216]. When a wound occurs, the electric field distribution in the wound area changes, with currents being driven out of the wound to form a lateral electric field with the wound edge as the anode and the center as the cathode. This electric field plays a key role in guiding the migration of electrically active key cells (such as epithelial cells) and promoting wound re-epithelialization.

Recent studies have confirmed the impact of the endogenous electric field in wounds on the healing rate. For example, in some disease states (such as diabetes), the absence or weakening of the endogenous electric field in wounds can lead to delayed wound healing [217]. Therefore, assisting in the establishment or supplementation of the electric field in the wound area is of great significance for promoting wound healing.

To leverage electric fields for wound healing, researchers have developed a series of innovative technologies. Luo et al. ingeniously combined TENG with mature wound treatment devices, namely negative pressure wound therapy (NPWT) devices (Fig. 12E). The mechanical force generated by NPWT drives the power generation process of TENG, and the resulting current further supplements the missing electric field in wounds, thereby assisting in wound healing. The electric field

generated by TENG is not only stable and highly safe but also has a significant migratory promotion effect on epithelial cells and drives macrophages to differentiate into the repair-oriented $M_2$ anti-inflammatory phenotype in vitro. Long-term treatment can significantly promote tissue remodeling, mature epithelial cells, order extracellular matrix, and reduce scar formation [218].

Another innovative study by Sun et al. developed a passive and biodegradable piezoelectric suture. The suture is composed of a multilayer coaxial structure, including poly(lactic-co-glycolic acid), polycaprolactone, and magnesium, ensuring safe degradation and excellent mechanical properties. Importantly, the suture has piezoelectric properties, generating an electric field during movement and stretching, which accelerates wound healing and reduces the risk of infection. Experimental results show that wounds treated with this piezoelectric suture heal 50 % faster than those treated with traditional sutures [219].

In summary, electric fields play an important role in the wound healing process, and modern technological applications provide new ways to leverage electric fields for wound healing. By innovatively supplementing or enhancing the electric field in the wound area through technological means, not only can the wound healing process be accelerated, but complications can also be reduced, bringing new hope to the field of wound treatment. In the future, with in-depth research and continuous technological advancements, the application prospects of electric field guidance in wound healing will be broader.

### 5.2. Functional regulation

#### 5.2.1. Brain

Brain electrical stimulation (BES), a pioneering therapeutic and interventional approach in neurology, has been proven to influence neurotransmitter release and synaptic plasticity [220]. The underlying mechanism may involve ion flows induced by electrical stimulation, which promote arterial dilation and increase blood flow in the target region. By delivering precisely controlled electrical currents to specific brain areas, BES exhibits dual effects: on the one hand, it can slowly repair potential neuronal damage caused by diseases; on the other hand, it can instantly modulate sensory, emotional states, and muscular rigidity [221,222]. The mechanisms underlying the effects of BES on neurotransmitter release and synaptic plasticity are complex. Specifically, high-frequency deep brain stimulation, such as using a parameter setting of 100 pulses per second with a pulse width of 0.1 ms, can directly inhibit or activate neural activity, effectively alleviating a variety of pathological symptoms, including Parkinson's disease [223], tremor, epilepsy [224], depression [225], and others.

In terms of technological innovations, Zhao et al. reported a wearable neuromodulation stimulator that does not require an external battery, capable of modulating synaptic plasticity in both long-term potentiation and long-term depression states [226]. Lin et al. designed a closed-loop device that can monitor human movement in real-time and convert it into electrical energy for storage (Fig. 12F). Simultaneously, upon detecting seizures, the device utilizes PVDF doped with zinc oxide to instantly deliver electrical stimulation to the brain. Experimental results show that this device can reduce seizure duration by 40 %–50 % in a mouse model of epilepsy [207]. Furthermore, the Kim team developed a non-invasive, highly safe piezoelectric NPs, BTNP–pDA–BNN6, which can release nitric oxide under US to reversibly open the blood-brain barrier and generate electrical stimulation in the target area under US guidance, providing a potential non-invasive therapy for diseases such as Parkinson's disease [227].

It is worth noting that BES may exhibit different time frames in improving symptoms of various neurological diseases. For example, tremor and rigidity may respond immediately, while long-term issues such as dystonia and emotional changes may take months to resolve. This indicates that the mechanism of action of BES is far more complex than simple neuronal excitation or inhibition. Additionally, BES therapy is associated with a high incidence of side effects, such as adverse reactions caused by lead migration, including motor disorders, speech impairments, cognitive difficulties, and emotional fluctuations. Therefore, the implementation of BES therapy requires strict patient selection, comprehensive assessment, and precise adjustment of stimulation parameters by a professional medical team. Although the use of force-electrically convertible materials for BES eliminates the dependency on external power sources and reduces the risk of infection, precise control of current intensity and stimulation sites remains an urgent issue to be addressed.

#### 5.2.2. Heart

The application of force-electrically convertible materials in cardiac disease treatment primarily focuses on two major areas: cardiac pacemakers and myocardial patches (as shown in Fig. 12G and H). Since the first complete implantation of a cardiac pacemaker in humans in 1958, it has become a crucial treatment method for heart disease [228,229] Force-electrically convertible materials provide a novel power supply approach for cardiac pacemakers, breaking through the life span limitations of traditional commercial pacemakers. Looking ahead, cardiac pacemakers will evolve towards a battery-free, self-powered direction, achieving self-sustaining power supply by harvesting energy within the body. If the energy generated by heartbeat can be effectively captured and utilized, the realization of a one-time implantation, lifelong use cardiac pacemaker will become a reality [230].

As early as 1963, Parsonnet et al. pioneered an attempt to capture in vivo mechanical energy from the pulsatile expansion of the aorta through an implanted piezoelectric device [231]. In Chapter 2 of this paper, we have elaborated on the application of piezoelectric materials in cardiac pacemakers. Additionally, significant progress has been made in the application of TENGs in cardiac pacemakers. For instance, in Fig. 12G, Ouyang et al. prepared an implantable TENG with an open-circuit voltage of up to 65.2 V, harvesting 0.495 μJ of energy per cardiac cycle, which exceeds the required endocardial pacing threshold energy (0.377 μJ), marking an important milestone in the development of symbiotic cardiac pacemakers [208].

On the other hand, myocardial patches primarily address the issue of limited myocardial contractile function following myocardial infarction. Poor electrical conduction between myocardial tissues increases the risk of heart failure. The application of force-electrically convertible materials in this field promotes electrical conduction between myocardial cells by delivering electrical signals to the myocardium. Specifically, in Fig. 12H, Jing et al. innovatively prepared a magneto-electric myocardial patch by adding magneto strictive materials to piezoelectric polymers. [209]. This patch utilizes the driving effect of magneto strictive materials to cause piezoelectric materials to generate electrical signals that act on myocardial cells, thereby triggering myocardial contraction, providing a new possibility for myocardial repair following myocardial infarction.

In summary, force-electrically convertible materials exhibit great potential for application in the field of cardiac disease treatment. Whether by providing a novel self-powering solution for cardiac pacemakers or by promoting electrical conduction between myocardial cells through myocardial patches, force-electrically convertible materials are driving innovation in heart disease treatment technologies. With the deepening of research and continuous technological advancements, force-electrically convertible materials are expected to play a more significant role in the treatment of cardiac diseases, bringing safer and more effective treatment options for patients.

#### 5.2.3. Muscle

Muscle tissue serves as a pivotal component of organisms, accounting for more than half of the body mass and playing a crucial role in force generation, bodily movement, and internal organ support. Its distinctive characteristic lies in its responsiveness to electrical signals and subsequent contraction [232]. Based on function and distribution, muscle tissue is classified into three types: skeletal muscle, cardiac muscle, and

smooth muscle. Skeletal muscle is responsible for bodily activities, cardiac muscle controls heart contraction specifically, while smooth muscle is widely distributed in blood vessels and the digestive system.

When muscle tissue is injured, its regenerative capacity becomes particularly significant. In contrast to skin wound healing, muscle regeneration refers specifically to the repair process of damaged muscle fibers. Healthy muscle possesses a certain regenerative capacity to cope with mild injuries, relying on the activation, proliferation, and differentiation of muscle stem cells. However, severe injuries may lead to insufficient endogenous regenerative capacity, resulting in fibrosis and scar formation, which impair normal muscle function. Currently, surgical reconstruction is the primary means of treating muscle injuries, but this method faces challenges such as low survival rates and scarcity of donor tissue. To overcome these difficulties, researchers are exploring new therapeutic strategies. Additionally, clinical practice has confirmed that electrical stimulation and physical exercise can effectively enhance muscle mass and strength [233–235]. In particular, external electrical stimulation has demonstrated great potential in the treatment of muscle injuries. It not only effectively prevents muscle atrophy due to prolonged inactivity (such as after injury or surgery) but also mimics the role of motor neurons in the physiological environment, influencing muscle cell proliferation rates and hypertrophy characteristics. For instance, the addition of electrical stimulation to two-dimensional cultured muscle precursor cells successfully promoted their myotube formation process [236].

In vitro cultures have also revealed various materials with beneficial effects on the adhesion and proliferation of myoblasts, as well as their myogenic differentiation. For example, negatively charged β-PVDF can promote the adhesion and proliferation of myoblasts, while also exhibiting a positive effect on the myogenic differentiation of human umbilical cord blood mesenchymal stem cells (hUCBMSCs) [237,238]. Ribeiro et al. reported a magneto-electric composite material and studied its impact on myoblast adhesion, proliferation, and differentiation. The deformation caused by magneto strictive materials induced effective electrical signals in the piezoelectric materials, and the results showed that this magneto-electric stimulation significantly improved the maturation index of the cells [239].

Furthermore, Fang et al. prepared piezoelectric elastomer using a copolymerization method of bio-based diacids and diols (Fig. 12I). This material has an elastic modulus matching that of skeletal muscle,

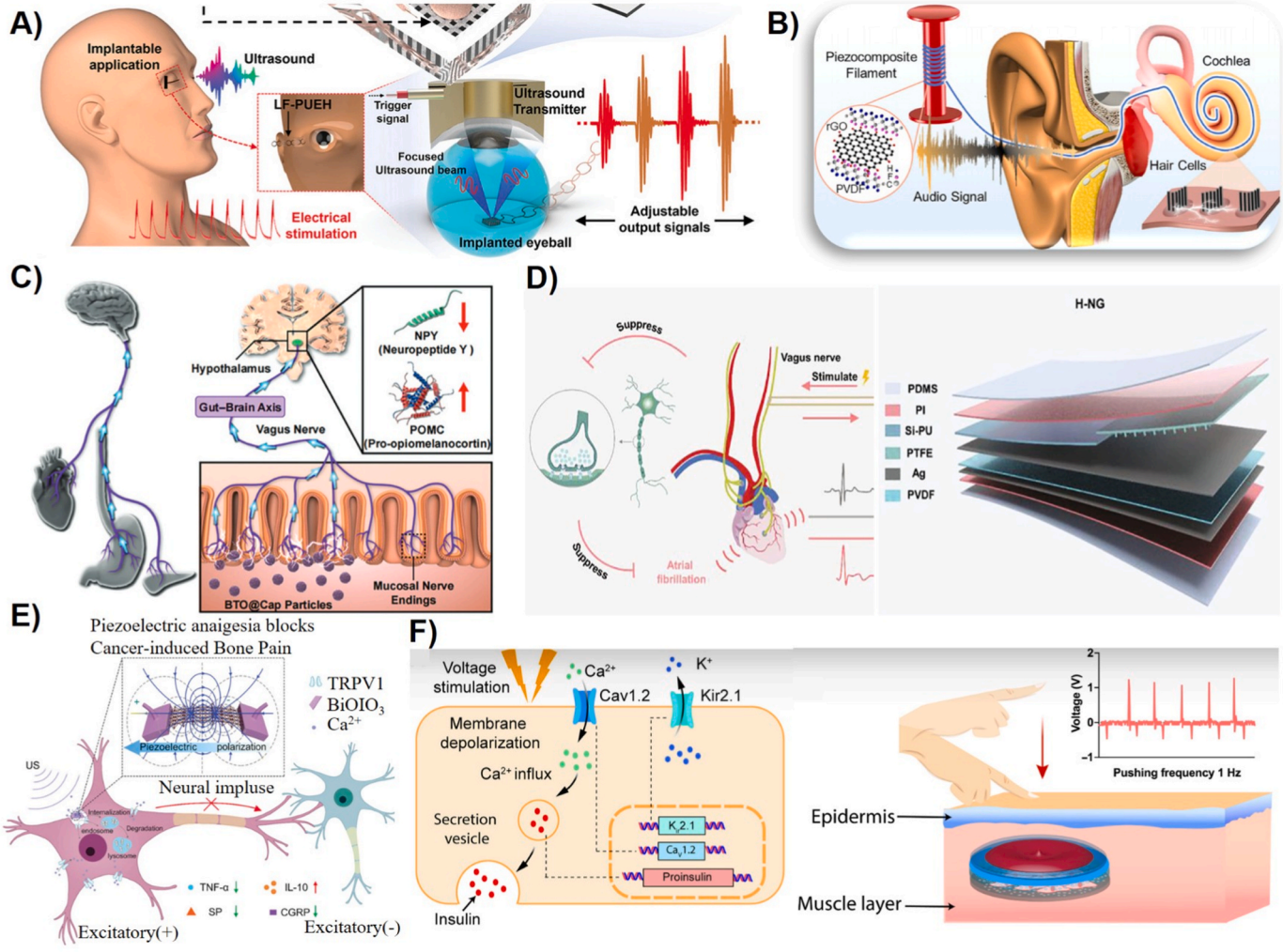


**Fig. 13.** Force-electrical conversion materials in regenerative medicine. A) US-induced wireless energy harvesting for potential retinal electrical stimulation. Reproduced with permission from Ref. [240]. Copyright 2019. Published by Wiley-VCH. B) Self-powered nanostructured piezoelectric filaments for cochlear implants. Reproduced with permission from Ref. [241] Copyright 2024. Published by Wiley-VCH. C) Orally ingested self-powered stimulators for targeted gut–brain axis electrostimulation to treat obesity. Reproduced with permission from Ref. [242] Copyright 2024. Published by Wiley-VCH. D) A closed-loop self-powered low-level vagus nerve stimulation system for atrial fibrillation treatment. Reproduced with permission from Ref. [243] Copyright 2019. Published by Wiley-VCH. E) Piezoelectric analgesia blocks cancer-induced bone pain. Reproduced with permission from Ref. [244] Copyright 2019. Published by Wiley-VCH. F) Autonomously controlled piezoelectricity promotes rapid insulin release. Reproduced with permission from Ref. [245] Copyright 2022. Published by AAAS.

enabling stretching and recovery movements. Under ultrasonic and mechanical stimulation, the piezoelectric charge of the PPBE scaffold can promote myogenic differentiation through the $Ca^{2+}$ signaling pathway, regulate cell function, and thereby improve the morphological and functional properties of skeletal muscle. Therefore, the development of degradable PPBE scaffolds provides a new therapeutic strategy for volumetric muscle loss and holds great potential for other tissue repairs [210].

In summary, the regenerative capacity of muscle tissue is crucial for maintaining the normal function of organisms. Currently, researchers are exploring new therapeutic strategies and materials to improve the treatment outcomes of muscle injuries. Among them, the application of electrical stimulation and novel biomaterials offers new perspectives and methods for the treatment of muscle injuries, potentially leading to more precise and effective treatments in the future.

#### 5.2.4. Other

Besides the aforementioned representative applications of electromechanical conversion materials in tissue regeneration and functional repair, there exist a series of special applications such as electrical stimulation of the retina, cochlea, vagus nerve, gastric muscles, pain relief, and pancreatic cells, which have shown certain therapeutic effects in the treatment of corresponding diseases.

In the field of retinal electrical stimulation, Jiang et al. prepared a lead-free, ultra-thin composite piezoelectric patch (Fig. 13A). Through optimized manufacturing techniques and the addition of microstructural designs on the material surface, they significantly enhanced the device's output power to 45 mW $cm^{-2}$, meeting the average threshold for retinal stimulation, thus providing a potential means for restoring vision [240]. Similarly, given that hair cells in the human ear can convert sound vibrations into electrical potentials, electromechanical conversion materials theoretically possess similar functionalities. Mokhtari et al. investigated a self-powered acoustic sensor based on piezoelectric composite fibers for use after hair cell damage (Fig. 13B). This sensor responds to sounds near the audible range at moderate sound pressure levels (60–95 dB), with an overall sound-to-electricity conversion efficiency of 3.25 % and a sensitivity of 117.5 mV $(Pa\ cm^2)^{-1}$, making it a promising candidate for artificial cochleas [241].

The vagus nerve, as a composite of motor and sensory fibers, has extensive connections with various body systems. Electrical stimulation of the vagus nerve is an effective means of regulating neural activity and organ function. Mac et al. explored a method to reduce food intake by stimulating the gastric vagus nerve, thereby achieving weight loss in obese mice [242]. This oral electrical stimulation device utilizes capsaicin to locate sensory nerve endings in the gastric mucosa and generates electrical signals based on piezoelectric BTO particles under gastric motility, which are then transmitted to the hypothalamus via the brain-gut axis (Fig. 13C). This represents a non-invasive, metabolically non-toxic, and safe weight loss method. Additionally, Sun et al. developed a closed-loop vagus nerve stimulator for the treatment of ventricular fibrillation [243]. This device utilizes hybrid nanogenerators to convert mechanical energy into electrical energy for storage, monitoring the occurrence of ventricular fibrillation while promptly regulating it through electrical stimulation of the vagus nerve (Fig. 13D). Treatment results showed a significant 90 % reduction in ventricular fibrillation duration, accompanied by the discovery of anti-inflammatory properties.

In the field of pain relief, Yin et al. developed an US-driven electrical stimulant for blocking cancer-induced bone pain (CIBP) [244]. They utilized BTO nanosheets to achieve single-cell-level electrical fields, inducing internalization of the TRPV1 on neuronal cells, reducing the secretion of neuropeptides and inflammatory factors, and achieving up to 6 h of CIBP relief (Fig. 13E).

Recently, the construction of electrically sensitive functional cells and the regulation of cell secretion function through electrical stimulation have become research hotspots. Zhao et al. utilized piezoelectric PVDF films to generate suitable electrical stimulation to stimulate electrically sensitive cells derived from the pancreatic β-cell line 1.1E7 [245]. These cells were designed to express insulin, as well as voltage-gated calcium channel CaV1.2 and inward rectifier potassium channel Kir2.1. They found that the piezoelectric-generated charges stimulated the opening of CaV1.2 channels, triggering the release of insulin stored in secretory vesicles (Fig. 13 F). Ultimately, they subcutaneously implanted a button-like device containing these electrically sensitive insulin-producing cells into type 1 diabetic mice. Mice stimulated by directly pushing the skin above the implant showed a rapid decrease in fasting blood glucose levels, while unstimulated mice maintained persistently high blood glucose levels, confirming the effectiveness of finger-push-mediated remote control of insulin release from the implanted cells.

In summary, the application of electromechanical conversion materials in the medical field demonstrates broad prospects and potential. From retinal electrical stimulation to artificial cochleas, from vagus nerve stimulation to pain relief treatments, to the construction of electrically sensitive cells and remote control, these applications not only provide powerful supplements to traditional treatment methods but also open up new directions for the future development of medicine. With continuous technological advancements and in-depth research, the application of electromechanical conversion materials in the medical field will become more extensive and profound, contributing greatly to the cause of human health.

### 5.3. Disease treatment

In recent years, the disease treatment based on tissue regeneration has received increasing attention, and electrical stimulation has been studied to some extent as one of the strategies for disease treatment, which is expected to provide a new approach for the treatment process of diseases based on tissue regeneration. Electroactive materials and devices with force-electric conversion capability have been proved to be an ideal platform for bioelectric therapy. Currently, the therapeutic functions of electroactive materials and devices with force-electric conversion capability in disease treatment are mainly realized through the controlled release of drug molecules [198,246,247], the enhancement of catalytic performance in catalytic therapy [248,249], and the direct interaction between electrical stimulation and cells or tissues [250,251] (Fig. 14).

#### 5.3.1. Drug delivery

Drug delivery systems have become a hot research topic in the biomedical field, driven by the huge clinical demand for targeted therapies, in the hope of bringing more survival benefits to patients. Recently, drug delivery systems have shifted to actively modulate drug release in response to external stimuli. Stimuli-responsive drug delivery systems aim to adjust drug release in response to environmental changes or external stimuli, thus achieving precise control of spatial localization, dose and release rate. With advances in biomechanical energy harvesting technology, self-powered drug delivery has emerged as a type of stimuli-responsive drug delivery. Self-powered drug delivery offers high performance and therapeutic precision as an ideal alternative to oral or injectable drug delivery. Electroactive materials and devices with force-electric conversion capabilities can convert external mechanical energy into electrical energy, enabling self-powered drug delivery without the need for an external power source or complex devices. At the same time, wearable and implantable devices with force-electric conversion capabilities can deliver drugs at specific sites, thus improving efficacy, reducing side effects, and decreasing overall treatment costs.

In stimuli-responsive drug delivery systems, biopolymers, NPs, microneedles, and liposomes are used as common drug carriers that can be electrically stimulated and controlled by electroactive materials and devices. Thus, biomaterial carriers are used in drug delivery systems along with electroactive materials and devices for site-specific

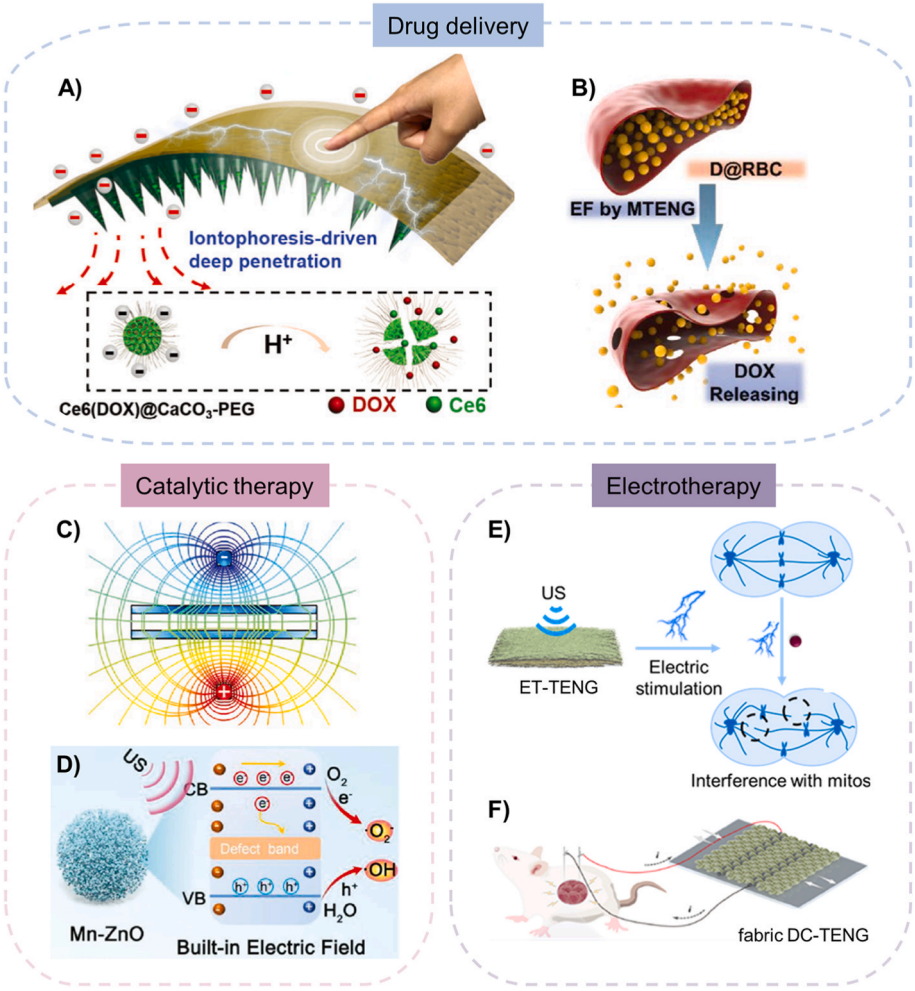


**Fig. 14.** Electroactive materials and devices for disease treatment. A) Working mechanism of the F-MN device composed of F-TENG and dissolving MN patch. Reproduced with permission from Ref. [252]. Copyright 2024. Published by Wiley-VCH. B) Doxorubicin (DOX)-loaded Red blood cells (RBCs) were stimulated by MTENG to achieve controlled release of DOX. Reproduced with permission from Ref. [253]. Copyright 2019. Published by Wiley-VCH. C) The schematic of the electric field distribution, potential distribution, and polarization mode distribution on the surface of the nanocatalyst under electric field stimulation. Reproduced with permission from Ref. [254]. Copyright 2022. Published by Wiley-VCH. D) Schematic illustration of mesoporous Mn–ZnO nanoclusters and its enhanced piezoelectric catalytic mechanism. Reproduced with permission from Ref. [255]. Copyright 2023. Published by Wiley-VCH. E) Schematic diagram of cancer therapy with the US-driven wireless ET-TENG. Reproduced with permission from Ref. [256]. Copyright 2023. Published by Wiley-VCH. F) Schematic illustration of the "Triboelectric Immunotherapy" system. Reproduced with permission from Ref. [257]. Copyright 2023. Published by Elsevier Ltd. (For interpretation of the references to colour in this figure legend, the reader is referred to the Web version of this article.)

controlled drug release. Based on this, Wang et al. proposed a wearable, self-powered MN patch, which was integrated with a flexible friction nanogenerator (F-TENG), aiming at deep tumor therapy [252]. The MNs consisted of a water-soluble polymer mixed with calcium carbonate NPs containing chlorin e6 ($Ce_6$) and DOX. Upon insertion of this integrated patch into the skin, the MNs were rapidly dissolved, which resulted in rapid delivery of drug-loaded negatively charged NPs into the skin. These NPs are then pushed deeper into the skin by electric field stimulation (Fig. 14A). Upon reaching the deep melanoma, the pH-responsive NPs dissociate rapidly due to the acidic microenvironment within the tumor, which allows the loaded $Ce_6$ and DOX to be released directly into the tumor. The integrated patch showed better efficacy in inhibiting deep tumors than the MN patch alone.

In vitro transdermal drug delivery based on electroactive materials and devices mainly relies on electroporation, electrophoresis, and iontophoresis, which impose limitations on drug delivery efficiency. In vivo controlled release of drugs can address to some extent the problems associated with in vitro drug delivery. Therefore, Zhao et al. fabricated a novel magnet TENG (MTENG), which ensures contact and separation cycles between the two tribological layers and can effectively increase the TENG output up to 70 V [253]. RBCs loaded with DOX were used as an antitumor drug delivery system (DDS). After loading DOX, the erythrocyte membrane was very stable with little DOX release. However, under electrical stimulation with MTENG, DOX release increased significantly and returned to normal after the end of the stimulation (Fig. 14B). MTENG-controlled DDS kills cancer cells in vivo with a low DOX dose. This excellent cell killing effect is mainly attributed to the fact that in vivo DDS can realize the precise and effective release of drug molecules under the effect of electrical stimulation. Based on the same advantages, Yao et al. prepared a covalent organic framework nanocage loaded with DOX (hCOF-DOX) to achieve controlled release of drugs in vivo [258]. The covalent organic framework structure was constructed with iron porphyrin as the building block and 2,5-dihydroxyterephthalic acid as the linker. It was found that hCOF-DOX exhibited stimulus-responsive drug release behavior under the electric field stimulation provided by TENG (stimulation frequency of 1.6 Hz, stimulation time of 16 min), and the final cumulative release of DOX reached 34.2 %. This feature provides the basis for controlled drug release in vivo by electrical stimulation.

#### 5.3.2. Catalytic therapy

In the last decade, nanocatalysts designed for localized generation of ROS have been considered as a promising strategy for disease treatment to overcome drug resistance and reduce side effects. However, the catalytic performance of most developed nanocatalysts is still weak, resulting in suboptimal therapeutic effects. Therefore, the development of effective methods to enhance the activity of nanocatalysts possesses important scientific and clinical significance. External stimulation is a viable method to enhance catalytic activity, especially when external stimulation can be easily and safely manipulated. Electric field and US, as two main types of external stimuli, can be used to effectively enhance the catalytic performance of electroactive materials. Thus, electroactive materials with high catalytic activity show great potential for cancer therapy and pathogen removal.

In the process of enhancing the catalytic performance of electroactive materials, electric field stimulation can effectively regulate the electron mobility, electron polarization structure and electron delivery ability of electroactive materials, thus enhancing the catalytic therapeutic effect [248,254,258]. Based on this, Yao et al. developed a human self-driven catalytic promotion system (TENG-CatSystem) inspired by the electrostatic preorganization effect in the natural protease catalytic process in order to improve the effectiveness of the cancer catalytic therapy [254,259,260]. The TENG-CatSystem consists of three main components: the human self-driven TENG acts as an electric field stimulator, which can provide biosafety electric pulse; one-dimensional iron porphyrin covalent organic frameworks coated on carbon nanotubes (COF-CNT) as nanocatalysts for catalytic generation of ROS; conductive hydrogel as a carrier for COF-CNT can be injected into tumor tissue to reduce tissue electrical impedance. The one-dimensional wraparound π-conjugated structure of COF-CNT has a high π-electron delocalization and electron transport capacity, which provides an ideal platform for the rapid movement and separation of electrons under an applied electric field (Fig. 14C). The presence of a conducting hydrogel improves the electron transport ability of COF-CNT under electric field. Under the spontaneous electric field provided by the wearable TENG, the catalytic activity of COF-CNT was four times higher than that in the absence of an electric field, enabling effective tumor therapy. In addition, Shen et al. prepared a carousel-type TENG, and found that the catalytic performance generated by the TENG operation could effectively remove organic pollutants from water [261]. The designed TENG could generate a high voltage of ~510 V and a high-power density of 25.48 W $m^{-2}$. At a rotational speed of 300 r $min^{-1}$ and an operating time of 6 h, the TENG could effectively degrade 59.59 % of triphenylmethane dyes and 59.2 % of azo dyes. Therefore, TENG, as an electroactive device, not only has the catalytic ability, but also can effectively enhance the catalytic performance of electroactive catalysts.

Piezoelectric biomaterials can directly convert mechanical pressure into an electrical response when stimulated by US, thus creating a large dynamic built-in electric field [262,263]. Under the action of the built-in electric field, holes and electrons in the material are separated, activating piezoelectric catalytic reactions. At the same time, the piezoelectric potential generated by piezoelectric biomaterials can tilt the energy bands and change the potentials at the valence and conduction band edges, thus improving the catalytic ability. Tian et al. reported a degradable manganese-doped zinc oxide (Mn–ZnO) piezoelectric nanocluster with multiple catalytic activities for enhanced piezoelectric-catalyzed cancer therapy (Fig. 14D) [255]. Upon manganese doping, the lattice of Mn–ZnO is distorted to form a built-in electric field, which improves the piezoelectric response. In addition, manganese doping produced abundant oxygen vacancies (OVs). The formation of OVs not only promoted the separation of electron-hole pairs under US stimulation, but also inhibited the recombination of electron-hole pairs, leading to the efficient generation of ROS for tumor therapy. The introduction of electroactive materials and devices in catalytic therapy not only provides a new way to enhance the catalytic performance, but also achieves an effective catalytic therapeutic effect.

#### 5.3.3. Electrotherapy

The use of electrical stimulation in the treatment of disease stems from the discovery of the existence of an endogenous electric field in organisms. This electric field is important in embryonic development, tissue generation and a number of important physiological processes. Therefore, electricity has been widely used as an accessible source of physical stimulation to assist in the treatment of diseases, especially for cancer therapy. Many studies have demonstrated that electrical stimulation can be used for cancer therapy not only through mechanisms such as irreversible electroporation (IRE), electroshock or interference with mitosis, but also by mobilizing the immune system to kill tumor cells [250,251,257]. However, the complexity of current electrical stimulation devices and invasive damage to tissues limit their development. Therefore, it is necessary to continuously improve them and develop methods to effectively kill tumors while ensuring safety. The emergence of electroactive materials and devices with force-electricity conversion capability can well solve the problems associated with conventional electrical stimulation devices and promote the further development of the field of electrotherapy. In the area of modulation of mitosis by electrical stimulation, Yao et al. designed an implantable, biodegradable and wirelessly controlled therapeutic TENG (ET-TENG) to wirelessly deliver electrical stimulation to tumor tissues (Fig. 14E) [256]. Under US excitation, the implanted ET-TENG generates an intermediate-frequency voltage (23 kHz, 3.26 V), which inhibits the expression of β-tubulin, γ-tubulin, and β-actin, disrupts the kinetic assembly of microtubules and actin filaments, induces cell-cycle arrest, and ultimately promotes tumor cell death.

In addition, Zulmari et al. used piezoelectric [P(VDF-TrFE)] microparticles (MPs) to induce IRE in 4T1 breast cancer cells and thereby kill the cells [251]. Under US stimulation, MPs located on the cell membrane generate localized voltage in situ. Previous studies have shown that the electric field threshold suitable for IRE is 1000 V/cm, whereas MPs under US stimulation generate an electric field of about 625–1000 V/cm, which is sufficient for IRE. This effective voltage stimulation induces the formation of small pores on the outer surface of the positively charged cells, and these pores allow small molecules to pass through the cellular membrane, which can disrupt the cellular homeostasis. As a result, the lipid bilayer is no longer able to act as a barrier separating the inside and outside of the cell, thus allowing a constant influx of water and ions into the cell, ultimately leading to cell rupture and death.

Electrical stimulation can not only directly induce tumor cell death, but also recruit immune cells for cancer immunotherapy. Li et al. prepared a fabric DC-TENG consisting of eight repetitively woven units (6.8 cm × 7 cm), which could achieve open-circuit voltages ($V_{oc}$), short-circuit currents ($I_{sc}$), and short-circuit charge transfer ($Q_{sc}$) of about 8000 V, 9 μA, and 0.94 μC, respectively, and could lead to immunogenic death of 4T1 tumor cells (Fig. 14F) [257]. After electrical stimulation induced immunogenic death of tumor cells, a large number of tumor antigens and damage-associated molecular patterns were released, which recruited a large number of immune cells and APCs to accumulate at the tumor site, induced dendritic cells to mature and migrate to TDLNs, and demonstrated tumor antigens to the T cells. Subsequently, the activated T cells differentiated into cytotoxic $CD4^+$ and $CD8^+$ T cells and secreted a large number of cytokines, which infiltrated the tumor area along with the blood and lymphatic vessels to further inhibit the tumor growth and effectively prolonged the patient's survival.

## 6. Conclusions and future perspectives

In the field of biomedical science, biomaterials and electrostimulation devices based on force-electric conversion, including PENGs and TENGs, are emerging as novel electrostimulation methods that do not require external power sources, showcasing immense potential. These devices efficiently convert mechanical energy into electrical energy, thereby providing a new and sustainable energy solution for biomedical applications.

From the perspective of materials, optimizing the performance of force-electrically convertible materials is crucial for future advancements. Material selection must comprehensively consider factors such as biocompatibility, hydrophilicity, microstructure, Young's modulus, and special processing techniques like high-voltage polarization, high-temperature annealing, in-situ growth, and electrospinning. These properties not only determine the electrical output performance of the materials but also directly impact their safety and effectiveness in biomedical applications. By optimizing these properties, devices with stronger therapeutic effects tailored to specific diseases can be developed. Considering real-life applications, material and device design should prioritize the potential risks and clinical translational challenges they have, such as biosafety validation (ISO 10993), degradation predictability, GMP-compliant nanofabrication and clinical efficacy benchmarks (Table 2). Interdisciplinary collaboration with organizations to ensure that electromechanical therapies meet safety and functionality requirements for human trials.

In terms of device design, integrating suitable materials into a complete device is a topic that requires in-depth research. This involves structural design, encapsulation strategies, integration, and biodegradability, among other aspects. Especially considering biocompatibility and the biological microenvironment of the application site, device design needs to be more sophisticated and intelligent. Additionally, for some special electroactive materials, such as piezoelectric nanoparticles and piezoelectric nanofibers, their direct contact with tissues or cells significantly reduces the requirements for the electrical output performance of the materials, amplifying the advantages of piezoelectric nanomaterials. However, this also places higher demands on the stability, sustainability, and metabolic pathways of piezoelectric nanomaterials. Future trends in the use of electro-mechanical conversion materials in healthcare should be considered in terms of: therapeutic depth: epidermal sensing, tissue repair and organ-level modulation. Innovations in material forms: injectable piezoelectric microspheres (self-assembling networks), 4D dynamic scaffolds (physiological adaptation) and biohybrid interfaces (cell membrane mimetic coupling). Finally key design principles prioritize biomechanical compatibility (gradient stiffness, degradability) and bioelectrical synergy (impedance matching, dynamic stimulation). Address long-term stability and scalable fabrication challenges through closed-loop systems (self-regulating voltage) and multi-scale fabrication (3D printed nano-architectures). By matching material properties to disease-specific healing stages (acute or remodeling) and functional thresholds (sensing or action), this analysis advances precision electromechanical therapies for tailored regenerative outcomes. Machine learning accelerates biocompatible material discovery and device optimization, while AI-enhanced manufacturing ensures nano-precision. Predictive analytics enable failure prevention and personalized designs, positioning data science as a cornerstone for scalable, high-performance PENGs/TENGs in clinical applications.

Despite the advantages of battery-free and sustainable electrostimulation methods based on force-electricity conversion, the instability and uncontrollability of their tiny mechanical energy conversion efficiency remain major challenges. This may lead to uncertain results when applied to tissues, affecting treatment efficacy. Therefore, achieving controllable electrical stimulation is a significant issue facing current and future research. Future studies need to explore more precise and intelligent electrical stimulation control mechanisms to meet the needs of different treatment locations and purposes.

Moreover, not only the application of force-electric materials in biomedicine but also the entire field of electrostimulation therapy in biomedicine relies on the advancement of basic biological mechanism research. Although electrostimulation has been proven to have significant regulatory effects on various cells or tissues, the specific mechanisms by which it affects cellular activities remain unclear. In future developments, researchers' efforts in this area will be highly meaningful as they aim to reveal the deep-level connections between electrostimulation and cellular activities, thereby providing a theoretical basis for the further optimization and application of electrostimulation therapy.

**Table 2**
Potential risks and clinical translational challenges of force-electric biomaterials and devices.

| Type | | Potential risks | Clinical translation challenges |
|---|---|---|---|
| Piezoelectric material | Piezoelectric ceramics | Chronic inflammatory response | ■ Bioabsorbable<br>■ Standardization of production<br>■ Flexible arrays<br>■ Aseptic treatment<br>■ In vivo charge detection |
| | Piezoelectric polymers | Material fatigue<br>Acute inflammatory response<br>Chemical toxicity | |
| | Piezoelectric hydrogel | Material fatigue | |
| TENG | | Ion homeostasis<br>Acute inflammatory response<br>Electrolytic toxicity<br>Chemical toxicity | |
| PENG | | Material fatigue<br>Acute inflammatory response<br>Chemical toxicity | |

In summary, electrostimulation devices based on force-electric conversion have broad application prospects in the biomedical field. However, to achieve their true clinical application and commercialization, in-depth research and exploration are still needed in multiple areas, including material performance optimization, device design, electrical stimulation control mechanisms, and basic biological mechanism research. We look forward to more breakthroughs and advancements in future research, contributing more wisdom and strength to the development of the biomedical field.

## CRediT authorship contribution statement

**Shuncheng Yao:** Writing – original draft, Conceptualization. **Xi Cui:** Writing – original draft, Conceptualization. **Chao Zhang:** Supervision. **Wenguo Cui:** Supervision. **Zhou Li:** Writing – review & editing, Validation, Supervision.

## Ethics approval and consent to participate

This review article does not require any ethical approval or allied consent for publication.

## Declaration of competing interest

The authors declare that they have no known competing financial interests or personal relationships that could have appeared to influence the work reported in this paper.

## Acknowledgments

S.Y. and X.C. contributed equally to this work. This work was supported by the National Key R&D project from Minister of Science and Technology, China (2022YFB3804700), Beijing Natural Science Foundation (Z240022), the National Natural Science Foundation of China (T2125003), Sponsored by Shanghai Sailing Program (24YF2739400), China Postdoctoral Science Foundation (2024M762011) and The Fundamental Research Funds for the Central Universities.

## Data availability

No data was used for the research described in the article.

## References


[1] K. Cwynarski, G. Iacoboni, E. Tholouli, T. Menne, D.A. Irvine, N. Balasubramaniam, L. Wood, J. Shang, E. Xue, Y. Zhang, S. Basilico, M. Neves, M. Raymond, I. Scott, M. El-Kholy, R. Jha, H. Dainton-Smith, R. Hussain, W. Day, M. Ferrari, S. Thomas, K. Lilova, W. Brugger, T. Marafioti, P. Lao-Sirieix, P. Maciocia, M. Pule, TRBC1-CAR T cell therapy in peripheral T cell lymphoma: a phase 1/2 trial, Nat. Med. (2024), https://doi.org/10.1038/s41591-024-03326-7.

[2] J. Garcia, J. Daniels, Y. Lee, I. Zhu, K. Cheng, Q. Liu, D. Goodman, C. Burnett, C. Law, C. Thienpont, J. Alavi, C. Azimi, G. Montgomery, K.T. Roybal, J. Choi, Naturally occurring T cell mutations enhance engineered T cell therapies, NATURE 626 (2024), https://doi.org/10.1038/s41586-024-07018-7.

[3] A.H. Isaac, S.Y. Recalde Phillips, E. Ruben, M. Estes, V. Rajavel, T. Baig, C. Paleti, K. Landsgaard, R.H. Lee, T. Guda, M.F. Criscitiello, C. Gregory, D.L. Alge, Impact of PEG sensitization on the efficacy of PEG hydrogel-mediated tissue engineering, Nat. Commun. 15 (2024), https://doi.org/10.1038/s41467-024-46327-3.

[4] Y. Zhang, T. Sun, X. Yang, L. Zhou, C.M.J. Tan, M. Lei, H. Bayley, A microscale soft lithium-ion battery for tissue stimulation, Nature chemical engineering 1 (2024) 691–701, https://doi.org/10.1038/s44286-024-00136-z.

[5] A. Calabria, G. Spinozzi, D. Cesana, E. Buscaroli, F. Benedicenti, G. Pais, F. Gazzo, S. Scala, M.R. Lidonnici, S. Scaramuzza, A. Albertini, S. Esposito, F. Tucci, D. Canarutto, M. Omrani, F. De Mattia, F. Dionisio, S. Giannelli, S. Marktel, F. Fumagalli, V. Calbi, S. Cenciarelli, F. Ferrua, B. Gentner, G. Caravagna, F. Ciceri, L. Naldini, G. Ferrari, A. Aiuti, E. Montini, Long-term lineage commitment in haematopoietic stem cell gene therapy, Nature (2024), https://doi.org/10.1038/s41586-024-08250-x.

[6] S. Zhang, F. Huang, Y. Wang, Y. Long, Y. Li, Y. Kang, W. Gao, X. Zhang, Y. Wen, Y. Wang, L. Pan, Y. Xia, Z. Yang, Y. Yang, H. Mo, B. Li, J. Hu, Y. Song, S. Zhang, S. Dong, X. Du, Y. Li, Y. Liu, W. Liao, Y. Gao, Y. Zhang, H. Chen, Y. Liang, J. Chen, H. Weng, H. Huang, NAT10-mediated mRNA $N^4$ acetylcytidine reprograms serine metabolism to drive leukaemogenesis and stemness in acute myeloid leukaemia, Nat. Cell Biol. (2024), https://doi.org/10.1038/s41556-024-01548-y.

[7] J. Li, W. Qiao, Y. Liu, H. Lei, S. Wang, Y. Xu, Y. Zhou, S. Wen, Z. Yang, W. Wan, J. Shi, N. Dong, Y. Wu, Facile engineering of interactive double network hydrogels for heart valve regeneration, Nat. Commun. 15 (2024), https://doi.org/10.1038/s41467-024-51773-0.

[8] J. He, L. Qian, Z. Li, Y. Wang, K. Liu, H. Wei, Y. Sun, J. He, K. Yao, J. Weng, X. Hu, D. Zhang, Y. He, A tissue bandage for pelvic ganglia injury, Nat. Commun. 15 (2024), https://doi.org/10.1038/s41467-024-53302-5.

[9] Y. Wang, X. Han, Z. Cui, D. Shi, Bioelectricity, its fundamentals, characterization methodology, and applications in nano-bioprobing and cancer diagnosis, Adv. Biosyst. 3 (2019), https://doi.org/10.1002/adbi.201900101.

[10] H. Wu, Y. Wang, H. Li, Y. Hu, Y. Liu, X. Jiang, H. Sun, F. Liu, A. Xiao, T. Chang, L. Lin, K. Yang, Z. Wang, Z. Dong, Y. Li, S. Dong, S. Wang, J. Chen, Y. Liu, D. Yin, H. Zhang, M. Liu, S. Kong, Z. Yang, X. Yu, Y. Wang, Y. Fan, L. Wang, C. Yu, L. Chang, Accelerated intestinal wound healing via dual electrostimulation from a soft and biodegradable electronic bandage, Nat. Electron. (2024), https://doi.org/10.1038/s41928-024-01138-8.

[11] M. Li, C. Wang, Q. Yu, H. Chen, Y. Ma, L. Wei, M.X. Wu, M. Yao, M. Lu, A wearable and stretchable dual-wavelength LED device for home care of chronic infected wounds, Nat. Commun. 15 (2024), https://doi.org/10.1038/s41467-024-53579-6, 9380-9380.

[12] L. Wang, J. Du, Q. Liu, D. Wang, W. Wang, M. Lei, K. Li, Y. Li, A. Hao, Y. Sang, F. Yi, W. Zhou, H. Liu, C. Mao, J. Qiu, Wrapping stem cells with wireless electrical nanopatches for traumatic brain injury therapy, Nat. Commun. 15 (2024), https://doi.org/10.1038/s41467-024-51098-y, 7223-7223.

[13] B. Wang, G. Li, Q. Zhu, W. Liu, W. Ke, W. Hua, Y. Zhou, X. Zeng, X. Sun, Z. Wen, C. Yang, Y. Pan, Bone repairment via mechanosensation of Piezo1 using wearable pulsed triboelectric nanogenerator, Small 18 (2022), https://doi.org/10.1002/smll.202201056.

[14] P. Sun, C. Li, C. Yang, M. Sun, H. Hou, Y. Guan, J. Chen, S. Liu, K. Chen, Y. Ma, Y. Huang, X. Li, H. Wang, L. Wang, S. Chen, H. Cheng, W. Xiong, X. Sheng, M. Zhang, J. Peng, S. Wang, Y. Wang, L. Yin, A biodegradable and flexible neural interface for transdermal optoelectronic modulation and regeneration of peripheral nerves, Nat. Commun. 15 (2024), https://doi.org/10.1038/s41467-024-49166-4.

[15] F. Qi, Y. Wang, T. Ma, S. Zhu, W. Zeng, X. Hu, Z. Liu, J. Huang, Z. Luo, Electrical regulation of olfactory ensheathing cells using conductive polypyrrole/chitosan polymers, Biomaterials 34 (2013) 1799–1809, https://doi.org/10.1016/j.biomaterials.2012.11.042.

[16] X. Ju, J. Kong, G. Qi, S. Hou, X. Diao, S. Dong, Y. Jin, A wearable electrostimulation-augmented ionic-gel photothermal patch doped with MXene for skin tumor treatment, Nat. Commun. 15 (2024), https://doi.org/10.1038/s41467-024-45070-z.

[17] S. Zhong, Z. Zhang, Q. Zhao, Z. Yue, C. Xiong, G. Chen, J. Wang, L. Li, Lattice expansion in ruthenium nanozymes improves catalytic activity and electro-responsiveness for boosting cancer therapy, Nat. Commun. 15 (2024), https://doi.org/10.1038/s41467-024-52277-7.

[18] Z. Li, D. He, B. Guo, Z. Wang, H. Yu, Y. Wang, S. Jin, M. Yu, L. Zhu, L. Chen, C. Ding, X. Wu, T. Wu, S. Gong, J. Mao, Y. Zhou, D. Luo, Y. Liu, Self-promoted electroactive biomimetic mineralized scaffolds for bacteria-infected bone regeneration, Nat. Commun. 14 (2023), https://doi.org/10.1038/s41467-023-42598-4.

[19] W. Liu, H. Zhao, C. Zhang, S. Xu, F. Zhang, L. Wei, F. Zhu, Y. Chen, Y. Chen, Y. Huang, M. Xu, Y. He, B.C. Heng, J. Zhang, Y. Shen, X. Zhang, H. Huang, L. Chen, X. Deng, In situ activation of flexible magnetoelectric membrane enhances bone defect repair, Nat. Commun. 14 (2023), https://doi.org/10.1038/s41467-023-39744-3.

[20] S. Bairagi, I. Shahid ul, C. Kumar, A. Babu, A.K. Aliyana, G. Stylios, S.C. Pillai, D. M. Mulvihill, Wearable nanocomposite textile-based piezoelectric and triboelectric nanogenerators: progress and perspectives, Nano Energy 118 (2023) 108962, https://doi.org/10.1016/j.nanoen.2023.108962.

[21] W. Deng, Y. Zhou, A. Libanori, G. Chen, W. Yang, J. Chen, Piezoelectric nanogenerators for personalized healthcare, Chem. Soc. Rev. 51 (2022) 3380–3435, https://doi.org/10.1039/d1cs00858g.

[22] R. Qiu, X. Zhang, C. Song, K. Xu, H. Nong, Y. Li, X. Xing, K. Mequanint, Q. Liu, Q. Yuan, X. Sun, M. Xing, L. Wang, E-cardiac patch to sense and repair infarcted myocardium, Nat. Commun. 15 (2024), https://doi.org/10.1038/s41467-024-48468-x.

[23] S. Chen, X. Tong, Y. Huo, S. Liu, Y. Yin, M.-L. Tan, K. Cai, W. Ji, Piezoelectric biomaterials inspired by nature for applications in biomedicine and nanotechnology, Adv. Mater. 36 (2024), https://doi.org/10.1002/adma.202406192.

[24] A. Khan, R. Joshi, M.K. Sharma, A. Ganguly, P. Parashar, T.-W. Wang, S. Lee, F.-C. Kao, Z.-H. Lin, Piezoelectric and triboelectric nanogenerators: promising technologies for self-powered implantable biomedical devices, Nano Energy 119 (2024) 109051, https://doi.org/10.1016/j.nanoen.2023.109051.

[25] W. Zhang, X. Qin, G. Li, X. Zhou, H. Li, D. Wu, Y. Song, K. Zhao, K. Wang, X. Feng, L. Tan, B. Wang, X. Sun, Z. Wen, C. Yang, Self-powered triboelectric-responsive microneedles with controllable release of optogenetically engineered extracellular vesicles for intervertebral disc degeneration repair, Nat. Commun. 15 (2024), https://doi.org/10.1038/s41467-024-50045-1.

[26] Y. Wang, H. Du, H. Yang, Z. Xi, C. Zhao, Z. Qian, X. Chuai, X. Peng, H. Yu, Y. Zhang, X. Li, G. Hu, H. Wang, M. Xu, A rolling-mode triboelectric nanogenerator with multi-tunnel grating electrodes and opposite-charge-enhancement for wave energy harvesting, Nat. Commun. 15 (2024), https://doi.org/10.1038/s41467-024-51245-5.

[27] X. Wei, Y. Wang, B. Tan, E. Zhang, B. Wang, H. Su, L. Yu, Y. Yin, Z.L. Wang, Z. Wu, Triboelectric nanogenerators stimulated electroacupuncture (EA) treatment for promoting the functional recovery after spinal cord injury, Mater. Today 60 (2022) 41–51, https://doi.org/10.1016/j.mattod.2022.09.010.

[28] D.-M. Lee, M. Kang, I. Hyun, B.-J. Park, H.J. Kim, S.H. Nam, H.-J. Yoon, H. Ryu, H.-m. Park, B.-O. Choi, S.-W. Kim, An on-demand bioresorbable neurostimulator, Nat. Commun. 14 (2023), https://doi.org/10.1038/s41467-023-42791-5.

[29] H. Ouyang, Z. Liu, N. Li, B. Shi, Y. Zou, F. Xie, Y. Ma, Z. Li, H. Li, Q. Zheng, X. Qu, Y. Fan, Z.L. Wang, H. Zhang, Z. Li, Symbiotic cardiac pacemaker, Nat. Commun. 10 (2019), https://doi.org/10.1038/s41467-019-09851-1.

[30] J. Curie, P. Curie, Développement par compression de l'électricité polaire dans les cristaux hémièdres à faces inclinées, Bull. Mineral. 3 (4) (1880) 90–93.

[31] I. Katsouras, K. Asadi, M. Li, T.B. van Driel, K.S. Kjær, D. Zhao, T. Lenz, Y. Gu, P. W.M. Blom, D. Damjanovic, M.M. Nielsen, D.M. de Leeuw, The negative piezoelectric effect of the ferroelectric polymer poly(vinylidene fluoride), Nat. Mater. 15 (2016) 78–84, https://doi.org/10.1038/nmat4423.

[32] M. Xie, Y. Zhang, M.J. Kraśny, C. Bowen, H. Khanbareh, N. Gathercole, Flexible and active self-powered pressure, shear sensors based on freeze casting ceramic–polymer composites, Energy Environ. Sci. 11 (2018) 2919–2927, https://doi.org/10.1039/C8EE01551A.

[33] X. Liao, Z. Qiu, T. Jiang, M.R. Sadiq, Z. Huang, C.E.M. Demore, S. Cochran, Functional piezocrystal characterisation under varying conditions, Materials 8 (2015) 8304–8326, https://doi.org/10.3390/ma8125456.

[34] M.T. Chorsi, E.J. Curry, H.T. Chorsi, R. Das, J. Baroody, P.K. Purohit, H. Ilies, T. D. Nguyen, Piezoelectric biomaterials for sensors and actuators, Adv. Mater. 31 (2019) 1802084, https://doi.org/10.1002/adma.201802084.

[35] M.T. Chorsi, E.J. Curry, H.T. Chorsi, R. Das, J. Baroody, P.K. Purohit, H. Ilies, T. D. Nguyen, Piezoelectric biomaterials for sensors and actuators, Adv. Mater. 31 (2019), https://doi.org/10.1002/adma.201802084.

[36] N. Sinha, G.E. Wabiszewski, R. Mahameed, V.V. Felmetsger, S.M. Tanner, R. W. Carpick, G. Piazza, Piezoelectric aluminum nitride nanoelectromechanical actuators, Appl. Phys. Lett. 95 (2009), https://doi.org/10.1063/1.3194148.

[37] Y. Qin, X. Wang, Z.L. Wang, Erratum: microfibre–nanowire hybrid structure for energy scavenging, Nature 457 (2009), https://doi.org/10.1038/nature07628, 340-340.

[38] P. Zhu, Y. Chen, J. Shi, Piezocatalytic tumor therapy by ultrasound-triggered and BaTiO3-mediated piezoelectricity, Adv. Mater. 32 (2020) 2001976, https://doi.org/10.1002/adma.202001976.

[39] Y. Shan, E. Wang, X. Cui, Y. Xi, J. Ji, J. Yuan, L. Xu, Z. Liu, Z. Li, A biodegradable piezoelectric sensor for real-time evaluation of the motor function recovery after nerve injury, Adv. Funct. Mater. 34 (2024) 2400295, https://doi.org/10.1002/adfm.202400295.

[40] L. Tan, X. Wang, W. Zhu, A. Li, Y. Wang, Excellent piezoelectric performance of KNNS-based lead-free piezoelectric ceramics through powder pretreatment by hydrothermal method, J. Alloys Compd. 874 (2021) 159770, https://doi.org/10.1016/j.jallcom.2021.159770.

[41] H. Wang, M. Godara, Z. Chen, H. Xie, A one-step residue-free wet etching process of ceramic PZT for piezoelectric transducers, Sensor Actuator Phys. 290 (2019) 130–136, https://doi.org/10.1016/j.sna.2019.03.028.
[42] Q. Zhu, X. Song, X. Chen, D. Li, X. Tang, J. Chen, Q. Yuan, A high performance nanocellulose-PVDF based piezoelectric nanogenerator based on the highly active CNF@ZnO via electrospinning technology, Nano Energy 127 (2024) 109741, https://doi.org/10.1016/j.nanoen.2024.109741.
[43] Y. Shan, S. Liu, B. Wang, Y. Hong, C. Zhang, C.W. Lim, G. Zhang, Z. Yang, A gravity-driven sintering method to fabricate geometrically complex compact piezoceramics, Nat. Commun. 12 (2021) 6066, https://doi.org/10.1038/s41467-021-26373-x.
[44] Q. Xu, Y. Tao, Z. Wang, H. Zeng, J. Yang, Y. Li, S. Zhao, P. Tang, J. Zhang, M. Yan, Q. Wang, K. Zhou, D. Zhang, H. Xie, Y. Zhang, C. Bowen, Highly flexible, high-performance, and stretchable piezoelectric sensor based on a hierarchical droplet-shaped ceramics with enhanced damage tolerance, Adv. Mater. 36 (2024) 2311624, https://doi.org/10.1002/adma.202311624.
[45] Y. Liu, L. Ding, L. Dai, X. Gao, H. Wu, S. Wang, C. Zhuang, L. Cai, Z. Liu, L. Liu, J. Zhang, Y. Wang, All-ceramic flexible piezoelectric energy harvester, Adv. Funct. Mater. 32 (2022) 2209297, https://doi.org/10.1002/adfm.202209297.
[46] Y. Purusothaman, H. Leng, A. Nanda, I. Levine, S. Priya, Textured lead-free piezoelectric ceramics for flexible energy harvesters, ACS Appl. Mater. Interfaces 15 (2023) 6584–6593, https://doi.org/10.1021/acsami.2c15640.
[47] C. Li, W. Guo, Y. Kong, H. Gao, Size-dependent piezoelectricity in zinc oxide nanofilms from first-principles calculations, Appl. Phys. Lett. 90 (2007) 033108, https://doi.org/10.1063/1.2430686.
[48] E. Fukada, History and recent progress in piezoelectric polymers, IEEE Trans. Ultrason. Ferroelectr. Freq. Control 47 (2000) 1277–1290, https://doi.org/10.1109/58.883516.
[49] E. Fukada, Recent developments of polar piezoelectric polymers, IEEE Trans. Dielect Elect. Insul. 13 (2006) 1110–1119, https://doi.org/10.1109/TDEI.2006.247839.
[50] M. Smith, S. Kar-Narayan, Piezoelectric polymers: theory, challenges and opportunities, Int. Mater. Rev. 67 (2022) 65–88, https://doi.org/10.1080/09506608.2021.1915935.
[51] X. Yan, X. Li, Z. Long, Z. Peng, J. Fu, Z. Zhang, S. Liu, Y. Hong, Q. Li, S. Zhang, D. Damjanovic, Z. Yang, Induced polarization imparts piezoelectricity in noncrystalline polymer films, Phys. Rev. Appl. 22 (2024) 014077, https://doi.org/10.1103/PhysRevApplied.22.014077.
[52] S. Yao, Q. Wu, S. Wang, Y. Zhao, Z. Wang, Q. Hu, L. Li, H. Liu, Self-driven electric field control of orbital electrons in AuPd alloy nanoparticles for cancer catalytic therapy, Small 20 (2024) 2307087, https://doi.org/10.1002/smll.202307087.
[53] S. Yao, Y. Zhao, Z. Wang, S. Wang, M. Zheng, Q. Hu, L. Li, Covalent organic framework nanocages with enhanced carrier utilization and cavitation effect for cancer sonodynamic therapy, ACS Appl. Mater. Interfaces 15 (2023) 34488–34496, https://doi.org/10.1021/acsami.3c04911.
[54] S. Yao, M. Zheng, S. Wang, T. Huang, Z. Wang, Y. Zhao, W. Yuan, Z. Li, Z.L. Wang, L. Li, Self-driven electrical stimulation promotes cancer catalytic therapy based on fully conjugated covalent organic framework nanocages, Adv. Funct. Mater. 32 (2022) 2209142, https://doi.org/10.1002/adfm.202209142.
[55] Y. Gong, K. Zhang, I.M. Lei, Y. Wang, J. Zhong, Advances in piezoelectret materials-based bidirectional haptic communication devices, Adv. Mater. 36 (2024) 2405308, https://doi.org/10.1002/adma.202405308.
[56] J. Zhang, Q. Shi, W. Zhang, Y. Wu, R. Liu, Y. Jin, A new theory, Nanoscale Confinement Polarization Pinning effect for enhancing piezoelectricity of PVDF-HFP, to fabricate piezoelectric sensor for exercise assistance, Chem. Eng. J. 500 (2024) 157399, https://doi.org/10.1016/j.cej.2024.157399.
[57] J. Huang, M.S. Lisowski, J. Runt, E.S. Hall, R.T. Kean, N. Buehler, J.S. Lin, Crystallization and microstructure of poly(L-lactide-co-meso-lactide) copolymers, Macromolecules 216 (1998), https://doi.org/10.1021/ma9714629.
[58] P.-H. Ducrot, I. Dufour, C. Ayela, Optimization of PVDF-TrFE processing conditions for the fabrication of organic MEMS resonators, Sci. Rep. 6 (2016) 19426, https://doi.org/10.1038/srep19426.
[59] J. He, R. Wei, S. Ge, W. Wu, J. Guo, J. Tao, R. Wang, C. Wang, C. Pan, Artificial visual-tactile perception array for enhanced memory and neuromorphic computations, InfoMat 6 (2024) e12493, https://doi.org/10.1002/inf2.12493.
[60] F.Y. Jiang, Y.Z. Shan, J.Y. Tian, L.L. Xu, C.H. Li, F. Yu, X. Cui, C.W. Wang, Z. Li, K. L. Ren, Poly(l-Lactic acid) nanofiber-based multilayer film for the electrical stimulation of nerve cells, Adv. Mater. Interfaces 10 (2023), https://doi.org/10.1002/admi.202202474.
[61] Z. Zhang, M.H. Litt, L. Zhu, Unified understanding of ferroelectricity in n-nylons: is the polar crystalline structure a prerequisite? Macromolecules 49 (2016) 3070–3082, https://doi.org/10.1021/acs.macromol.5b02739.
[62] T. Itoh, M. Takano, T. Yanagisawa, M. Hashimoto, Ferroelectricity in odd- and even-numbered nylons, Ferroelectrics 216 (1998) 35–51, https://doi.org/10.1080/00150199808018226.
[63] Y. Dobashi, D. Yao, Y. Petel, N. Tan Ngoc, M.S. Sarwar, Y. Thabet, C.L.W. Ng, E. S. Glitz, N. Giao Tran Minh, C. Plesse, F. Vidal, C.A. Michal, J.D.W. Madden, Piezoionic mechanoreceptors: force-induced current generation in hydrogels, SCIENCE 376 (2022) 502, https://doi.org/10.1126/science.aaw1974.
[64] J. Odent, N. Baleine, V. Biard, Y. Dobashi, C. Vancaeyzeele, G.T.M. Nguyen, J.D. W. Madden, C. Plesse, J.-M. Raquez, 3D-Printed stacked ionic assemblies for iontronic touch sensors, Adv. Funct. Mater. 33 (2023) 2210485, https://doi.org/10.1002/adfm.202210485.
[65] H. Wei, Z. Wang, H. Zhang, Y. Huang, Z. Wang, Y. Zhou, B.B. Xu, S. Halila, J. Chen, Ultrastretchable, highly transparent, self-adhesive, and 3D-printable ionic hydrogels for multimode tactical sensing, Chem. Mater. 33 (2021) 6731–6742, https://doi.org/10.1021/acs.chemmater.1c01246.
[66] S. Wang, T. Yang, D. Zhang, Q. Hua, Y. Zhao, Unveiling gating behavior in piezoionic effect: toward neuromimetic tactile sensing, Adv. Mater. 36 (2024) 2405391, https://doi.org/10.1002/adma.202405391.
[67] K. Yang, B. Li, Z. Ma, J. Xu, D. Wang, Z. Zeng, D. Ho, Ion-selective mobility differential amplifier: enhancing pressure-induced voltage response in hydrogels, Angew. Chem. Int. Ed. (2024) e202415000, https://doi.org/10.1002/anie.202415000.
[68] X. Guan, S. Zheng, J. Luo, X. Liu, X. Wang, B. Zhang, Y. Zhu, D. Li, Q. Han, M. Ueda, M. An, Spider webs-inspired aluminum coordination hydrogel piezoionic sensors for tactile nerve systems, Adv. Funct. Mater. (2024) 2414016, https://doi.org/10.1002/adfm.202414016 n/a.
[69] E. Fukada, R.L. Zimmerman, S. Mascarenhas, Denaturation of horn keratin observed by piezoelectric measurements, Biochem. Biophys. Res. Commun. 62 (1975) 415–418, https://doi.org/10.1016/S0006-291X(75)80154-9.
[70] H.K. Ravi, F. Simona, J. Hulliger, M. Cascella, Molecular origin of piezo- and pyroelectric properties in collagen investigated by molecular dynamics simulations, J. Phys. Chem. B 116 (2012) 1901–1907, https://doi.org/10.1021/jp208436j.
[71] D. Vasilescu, R. Cornillon, G. Mallet, Piezoelectric resonances in amino-acids, Nature 225 (1970), https://doi.org/10.1038/225635a0, 635-635.
[72] F. Yang, J. Li, Y. Long, Z. Zhang, L. Wang, J. Sui, Y. Dong, Y. Wang, R. Taylor, D. Ni, W. Cai, P. Wang, T. Hacker, X. Wang, Wafer-scale heterostructured piezoelectric bio-organic thin films, Science 373 (2021) 337–342, https://doi.org/10.1126/science.abf2155.
[73] J. Sui, J. Li, L. Gu, C.A. Schmidt, Z. Zhang, Y. Shao, E. Gazit, P.U.P.A. Gilbert, X. Wang, Orientation-controlled crystallization of γ-glycine films with enhanced piezoelectricity, J. Mater. Chem. B 10 (2022) 6958–6964, https://doi.org/10.1039/D2TB00997H.
[74] J.O. Donnell, S.M. Sarkar, S. Guerin, G.G. Borda, C. Silien, T. Soulimane, D. Thompson, E.O. Reilly, S.A.M. Tofail, Piezoelectricity in the proteinogenic amino acid L-leucine: a novel piezoactive bioelectret, IEEE Trans. Dielect Elect. Insul. 27 (2020) 1465–1468, https://doi.org/10.1109/TDEI.2020.008908.
[75] X. Wang, H. Zhang, P.J. Quinn, Production of l-valine from metabolically engineered Corynebacterium glutamicum, Appl. Microbiol. Biotechnol. 102 (2018) 4319–4330, https://doi.org/10.1007/s00253-018-8952-2.
[76] S. Guerin, J. O'Donnell, E.U. Haq, C. McKeown, C. Silien, F.M.F. Rhen, T. Soulimane, S.A.M. Tofail, D. Thompson, Racemic amino acid piezoelectric transducer, Phys. Rev. Lett. 122 (2019) 047701, https://doi.org/10.1103/PhysRevLett.122.047701.
[77] A. Kholkin, N. Amdursky, I. Bdikin, E. Gazit, G. Rosenman, Strong piezoelectricity in bioinspired peptide nanotubes, ACS Nano 4 (2010) 610–614, https://doi.org/10.1021/nn901327v.
[78] R.M.F. Baptista, E. de Matos Gomes, M.M.M. Raposo, S.P.G. Costa, P.E. Lopes, B. Almeida, M.S. Belsley, Self-assembly of dipeptide Boc-diphenylalanine nanotubes inside electrospun polymeric fibers with strong piezoelectric response, Nanoscale Adv. 1 (2019) 4339–4346, https://doi.org/10.1039/C9NA00464E.
[79] M. Minary-Jolandan, M.-F. Yu, Nanoscale characterization of isolated individual type I collagen fibrils: polarization and piezoelectricity, Nanotechnology 20 (2009) 085706, https://doi.org/10.1088/0957-4484/20/8/085706.
[80] M. Minary-Jolandan, M.-F. Yu, Uncovering nanoscale electromechanical heterogeneity in the subfibrillar structure of collagen fibrils responsible for the piezoelectricity of bone, ACS Nano 3 (2009) 1859–1863, https://doi.org/10.1021/nn900472n.
[81] E. Kar, M. Barman, S. Das, A. Das, P. Datta, S. Mukherjee, M. Tavakoli, N. Mukherjee, N. Bose, Chicken feather fiber-based bio-piezoelectric energy harvester: an efficient green energy source for flexible electronics, Sustain. Energy Fuels 5 (2021) 1857–1866, https://doi.org/10.1039/D0SE01433H.
[82] V. Sencadas, C. Garvey, S. Mudie, J.J.K. Kirkensgaard, G. Gouadec, S. Hauser, Electroactive properties of electrospun silk fibroin for energy harvesting applications, Nano Energy 66 (2019) 104106, https://doi.org/10.1016/j.nanoen.2019.104106.
[83] S.K. Karan, S. Maiti, O. Kwon, S. Paria, A. Maitra, S.K. Si, Y. Kim, J.K. Kim, B. B. Khatua, Nature driven spider silk as high energy conversion efficient bio-piezoelectric nanogenerator, Nano Energy 49 (2018) 655–666, https://doi.org/10.1016/j.nanoen.2018.05.014.
[84] L. Su, Y. Feng, K. Wei, X. Xu, R. Liu, G. Chen, Carbohydrate-based macromolecular biomaterials, Chem. Rev. 121 (2021) 10950–11029, https://doi.org/10.1021/acs.chemrev.0c01338.
[85] N.A. Hoque, P. Thakur, P. Biswas, M.M. Saikh, S. Roy, B. Bagchi, S. Das, P.P. Ray, Biowaste crab shell-extracted chitin nanofiber-based superior piezoelectric nanogenerator, J. Mater. Chem. A 6 (2018) 13848–13858, https://doi.org/10.1039/C8TA04074E.
[86] G. de Marzo, V.M. Mastronardi, L. Algieri, F. Vergari, F. Pisano, L. Fachechi, S. Marras, L. Natta, B. Spagnolo, V. Brunetti, F. Rizzi, F. Pisanello, M. De Vittorio, Sustainable, flexible, and biocompatible enhanced piezoelectric chitosan thin film for compliant piezosensors for human health, Advanced Electronic Materials 9 (2023) 2200069, https://doi.org/10.1002/aelm.202200069.
[87] J. Wang, C. Carlos, Z. Zhang, J. Li, Y. Long, F. Yang, Y. Dong, X. Qiu, Y. Qian, X. Wang, Piezoelectric nanocellulose thin film with large-scale vertical crystal alignment, ACS Appl. Mater. Interfaces 12 (2020) 26399–26404, https://doi.org/10.1021/acsami.0c05680.
[88] T. Li, Y. Yuan, L. Gu, J. Li, Y. Shao, S. Yan, Y. Zhao, C. Carlos, Y. Dong, H. Qian, X. Wang, W. Wu, S. Wang, Z. Wang, X. Wang, Ultrastable piezoelectric biomaterial

nanofibers and fabrics as an implantable and conformal electromechanical sensor patch, Sci. Adv., 10 eadn8706, https://doi.org/10.1126/sciadv.adn8706.
[89] Y. Su, W. Li, X. Cheng, Y. Zhou, S. Yang, X. Zhang, C. Chen, T. Yang, H. Pan, G. Xie, G. Chen, X. Zhao, X. Xiao, B. Li, H. Tai, Y. Jiang, L.-Q. Chen, F. Li, J. Chen, High-performance piezoelectric composites via β phase programming, Nat. Commun. 13 (2022) 4867, https://doi.org/10.1038/s41467-022-32518-3.
[90] J. Liu, S. Zeng, M. Zhang, J. Xiong, H. Gu, Z. Wang, Y. Hu, X. Zhang, Y. Du, L. Ren, Giant piezoelectric output and stability enhancement in piezopolymer composites with liquid metal nanofillers, Adv. Sci. 10 (2023) 2304096, https://doi.org/10.1002/advs.202304096.
[91] X. Cui, Y. Shan, J. Li, M. Xiao, Y. Xi, J. Ji, E. Wang, B. Zhang, L. Xu, M. Zhang, Z. Li, Y. Zhang, Bifunctional piezo-enhanced PLLA/ZA coating prevents aseptic loosening of bone implants, Adv. Funct. Mater. 34 (2024) 2403759, https://doi.org/10.1002/adfm.202403759.
[92] Y. Park, Y.-E. Shin, J. Park, Y. Lee, M.P. Kim, Y.-R. Kim, S. Na, S.K. Ghosh, H. Ko, Ferroelectric multilayer nanocomposites with polarization and stress concentration structures for enhanced triboelectric performances, ACS Nano 14 (2020) 7101–7110, https://doi.org/10.1021/acsnano.0c01865.
[93] Q. Yu, Y. Bai, Z. Li, F. Jiang, R. Luo, Y. Gai, Z. Liu, L. Zhou, Y. Wang, C. Li, K. Ren, D. Luo, H. Meng, Z. Li, Interface-induced high piezoelectric γ-glycine-based flexible biodegradable films, Nano Energy 121 (2024), https://doi.org/10.1016/j.nanoen.2023.109196.
[94] D. Choi, Y. Lee, Z.-H. Lin, S. Cho, M. Kim, C.K. Ao, S. Soh, C. Sohn, C.K. Jeong, J. Lee, M. Lee, S. Lee, J. Ryu, P. Parashar, Y. Cho, J. Ahn, I.-D. Kim, F. Jiang, P. S. Lee, G. Khandelwal, S.-J. Kim, H.S. Kim, H.-C. Song, M. Kim, J. Nah, W. Kim, H. G. Menge, Y.T. Park, W. Xu, J. Hao, H. Park, J.-H. Lee, D.-M. Lee, S.-W. Kim, J. Y. Park, H. Zhang, Y. Zi, R. Guo, J. Cheng, Z. Yang, Y. Xie, S. Lee, J. Chung, I.-K. Oh, J.-S. Kim, T. Cheng, Q. Gao, G. Cheng, G. Gu, M. Shim, J. Jung, C. Yun, C. Zhang, G. Liu, Y. Chen, S. Kim, X. Chen, J. Hu, X. Pu, Z.H. Guo, X. Wang, J. Chen, X. Xiao, X. Xie, M. Jarin, H. Zhang, Y.-C. Lai, T. He, H. Kim, I. Park, J. Ahn, N.D. Huynh, Y. Yang, Z.L. Wang, J.M. Baik, D. Choi, Recent advances in triboelectric nanogenerators: from technological progress to commercial applications, ACS Nano 17 (2023) 11087–11219, https://doi.org/10.1021/acsnano.2c12458.
[95] X. Guo, M. Chen, Y. Zheng, H. Cui, X. Li, Triboelectric nanogenerators: theoretical calculations, materials, and applications in net-zero emissions, JOURNAL OF PHYSICS D-APPLIED PHYSICS 56 (2023), https://doi.org/10.1088/1361-6463/acf770.
[96] C. Bao, M. He, J. Li, Y. Hu, Y. Wang, J. Ma, J. Wen, Study on the surface charge transfer mechanism induced by dual-electric field mutual inductance, JOURNAL OF Materials CHEMISTRY A 12 (2024) 16636–16647, https://doi.org/10.1039/d4ta02651a.
[97] L. Wang, X. Yang, W.A. Daoud, High power-output mechanical energy harvester based on flexible and transparent Au nanoparticle-embedded polymer matrix, Nano Energy 55 (2019) 433–440, https://doi.org/10.1016/j.nanoen.2018.10.030.
[98] J. Chun, J.W. Kim, W.-s. Jung, C.-Y. Kang, S.-W. Kim, Z.L. Wang, J.M. Baik, Mesoporous pores impregnated with Au nanoparticles as effective dielectrics for enhancing triboelectric nanogenerator performance in harsh environments, Energy Environ. Sci. 8 (2015) 3006–3012, https://doi.org/10.1039/c5ee01705j.
[99] M. Wang, J. Duan, X. Yang, Y. Wang, Y. Duan, Q. Tang, Interfacial electric field enhanced charge density for robust triboelectric nanogenerators by tailoring metal/perovskite Schottky junction, Nano Energy 73 (2020), https://doi.org/10.1016/j.nanoen.2020.104747.
[100] S. Du, S. Fu, W. He, Q. Li, K. Li, H. Wu, J. Wang, C. Shan, Q. Mu, C. Hu, High durable rotary triboelectric nanogenerator enabled by ferromagnetic metal particles as a friction material, Adv. Funct. Mater. 33 (2023), https://doi.org/10.1002/adfm.202306491.
[101] M. Lai, B. Du, H. Guo, Y. Xi, H. Yang, C. Hu, J. Wang, Z.L. Wang, Enhancing the output charge density of TENG via building longitudinal paths of electrostatic charges in the contacting layers, ACS Appl. Mater. Interfaces 10 (2018) 2158–2165, https://doi.org/10.1021/acsami.7b15238.
[102] S. Gao, Q. Han, X. Zhang, P. Pennacchi, F. Chu, Ultra-high-speed hybrid ceramic triboelectric bearing with real-time dynamic instability monitoring, Nano Energy 103 (2022), https://doi.org/10.1016/j.nanoen.2022.107759.
[103] B. Xie, R. Yin, S. Miao, H. Jia, Y. Ma, Y. Liu, Thermal-stable and high-dielectric $BaTiO_3$-based ceramic Powder/PMDS films for triboelectric nanogenerator, Ceram. Int. 50 (2024) 12778–12786, https://doi.org/10.1016/j.ceramint.2024.01.182.
[104] X. Liu, Z. Zhao, Y. Gao, Y. Nan, Y. Hu, Z. Guo, W. Qiao, J. Wang, L. Zhou, Z. L. Wang, J. Wang, Triboelectric nanogenerators exhibiting ultrahigh charge density and energy density, Energy Environ. Sci. 17 (2024) 3819–3831, https://doi.org/10.1039/d4ee00895b.
[105] S. Kuntharin, V. Harnchana, J. Sintusiri, P. Thongbai, A. Klamchuen, K. Sinthiptharakoon, V. Amornkitbamrung, P. Chindaprasirt, Smart triboelectric floor based on calcium silicate-carbon composite for energy harvesting and motion sensing applications, Sens. Actuators A Phys. 358 (2023), https://doi.org/10.1016/j.sna.2023.114423.
[106] W. Seung, H.-J. Yoon, T.Y. Kim, H. Ryu, J. Kim, J.-H. Lee, J.H. Lee, S. Kim, Y. K. Park, Y.J. Park, S.-W. Kim, Boosting power-generating performance of triboelectric nanogenerators via artificial control of ferroelectric polarization and dielectric properties, Adv. Energy Mater. 7 (2017), https://doi.org/10.1002/aenm.201600988.
[107] P. Zhang, W. Zhang, L. Deng, H. Zhang, A triboelectric nanogenerator based on temperature-stable high dielectric $BaTiO_3$-based ceramic powder for energy harvesting, Nano Energy 87 (2021), https://doi.org/10.1016/j.nanoen.2021.106176.
[108] B. Xie, Y. Ma, K. Nie, Y. Liu, J. Su, R. Yin, Y. Liu, Advanced functionalities of Gd 0.1 Ta 0.1 Ti 0.1 O 2 ceramic powder/P (VDF-TrFE) films for enhanced triboelectric performance, Sens. Actuators A Phys. 373 (2024), https://doi.org/10.1016/j.sna.2024.115438.
[109] J. Chi, C. Liu, L. Che, D. Li, K. Fan, Q. Li, W. Yang, L. Dong, G. Wang, Z.L. Wang, Harvesting water-evaporation-induced electricity based on liquid-solid triboelectric nanogenerator, Adv. Sci. 9 (2022), https://doi.org/10.1002/advs.202201586.
[110] M. Kaur, A. Alagumalai, O. Mahian, S.M. Osman, T. Nagao, Z.L. Wang, Harvesting energy via water movement and surface ionics in microfibrous ceramic wools, Energy Environ. Mater. (2024), https://doi.org/10.1002/eem2.12760.
[111] S. Gupta, R. Bhunia, B. Fatma, D. Maurya, D. Singh, Prateek, R. Gupta, S. Priya, R. K. Gupta, A. Garg, Multifunctional and flexible polymeric nanocomposite films with improved ferroelectric and piezoelectric properties for energy generation devices, ACS Appl. Energy Mater. 2 (2019) 6364–6374, https://doi.org/10.1021/acsaem.9b01000.
[112] K.A. Lazar, K.V. Vijoy, T. Joseph, H. John, K.J. Saji, Vertically integrated triboelectric nanogenerators using PDMS/LSCO composite, Mater. Sci. Eng. B 292 (2023), https://doi.org/10.1016/j.mseb.2023.116388.
[113] P. Manchi, S.A. Graham, M.V. Paranjape, A. Kurakula, V.S. Kavarthapu, J.S. Yu, Calcium copper titanate incorporated polydimethylsiloxane flexible composite film-based triboelectric nanogenerator for energy harvesting and self-powered sensing applications, J. Mater. Sci. Technol. 190 (2024) 56–66, https://doi.org/10.1016/j.jmst.2023.11.059.
[114] X. Tao, X. Chen, Z.L. Wang, Design and synthesis of triboelectric polymers for high performance triboelectric nanogenerators, Energy Environ. Sci. 16 (2023) 3654–3678, https://doi.org/10.1039/d3ee01325a.
[115] M. Zhu, Z. Yi, B. Yang, C. Lee, Making use of nanoenergy from human - nanogenerator and self-powered sensor enabled sustainable wireless IoT sensory systems, Nano Today 36 (2021), https://doi.org/10.1016/j.nantod.2020.101016.
[116] Z. Liu, X. Chen, Z.L. Wang, Biopolymer and biomimetic techniques for triboelectric nanogenerators (TENGs), Adv. Mater. (2024), https://doi.org/10.1002/adma.202409440.
[117] A. Sutka, L. Lapcinskis, D. He, H. Kim, J.D. Berry, J. Bai, M. Knite, A.V. Ellis, C. K. Jeong, P.C. Sherrell, Engineering polymer interfaces: a review toward controlling triboelectric surface charge, Adv. Mater. Interfaces 10 (2023), https://doi.org/10.1002/admi.202300323.
[118] M. Shanbedi, H. Ardebili, A. Karim, Polymer-based triboelectric nanogenerators: materials, characterization, and applications, Prog. Polym. Sci. 144 (2023), https://doi.org/10.1016/j.progpolymsci.2023.101723.
[119] S. Zhou, X. Tao, Z. Liu, H. Wu, Z. Guan, L. Liu, J. Li, X. Chen, W. Ou-Yang, Regulation of dihedral angle on molecular engineering for enhancing triboelectric performance, Adv. Funct. Mater. 34 (2024), https://doi.org/10.1002/adfm.202405443.
[120] Z. Liu, Y.-z. Huang, Y. Shi, X. Tao, P. Yang, X. Dong, J. Hu, Z.-X. Huang, X. Chen, J.-P. Qu, Creating ultrahigh and long-persistent triboelectric charge density on weak polar polymer via quenching polarization, Adv. Funct. Mater. 33 (2023), https://doi.org/10.1002/adfm.202302164.
[121] N. Meng, Y. Zhang, W. Liu, Q. Chen, N. Soykeabkaew, Y. Liao, Monolithic conjugated microporous polymer aerogel for triboelectric nanogenerator, Adv. Funct. Mater. 34 (2024), https://doi.org/10.1002/adfm.202313534.
[122] H. Wu, J. Li, L. Liu, Z. Guan, S. Zhou, Z. Tian, X. Chen, Y. Zhu, W. Ou-Yang, A fast electron-injection strategy for enhancing triboelectric surface charge density of polymers, Nano Energy 122 (2024), https://doi.org/10.1016/j.nanoen.2024.109351.
[123] Z. Liu, Y. Huang, Y. Shi, X. Tao, H. He, F. Chen, Z.-X. Huang, Z.L. Wang, X. Chen, J.-P. Qu, Fabrication of triboelectric polymer films via repeated rheological forging for ultrahigh surface charge density, Nat. Commun. 13 (2022), https://doi.org/10.1038/s41467-022-31822-2.
[124] J. Qi, A.C. Wang, W. Yang, M. Zhang, C. Hou, Q. Zhang, Y. Li, H. Wang, Hydrogel-based hierarchically wrinkled stretchable nanofibrous membrane for high performance wearable triboelectric nanogenerator, Nano Energy 67 (2020), https://doi.org/10.1016/j.nanoen.2019.104206.
[125] Y. Shao, G. Du, B. Luo, T. Liu, J. Zhao, S. Zhang, J. Wang, M. Chi, C. Cai, Y. Liu, X. Meng, Z. Liu, S. Wang, S. Nie, A tough monolithic-integrated triboelectric bioplastic enabled by dynamic covalent chemistry, Adv. Mater. (2024), https://doi.org/10.1002/adma.202311993.
[126] M. Kang, M.S.B.M. Khusrin, Y.-J. Kim, B. Kim, B.J. Park, I. Hyun, I.M. Imani, B.-O. Choi, S.-W. Kim, Nature-derived highly tribopositive κ-carrageenan-agar composite-based fully biodegradable triboelectric nanogenerators, Nano Energy 100 (2022), https://doi.org/10.1016/j.nanoen.2022.107480.
[127] M.-Z. Huang, P. Parashar, A.-R. Chen, S.-C. Shi, Y.-H. Tseng, K.C. Lim, H.-Y. Yeh, A. Pal, D.-Y. Kang, Z.-H. Lin, Snake-scale stimulated robust biomimetic composite triboelectric layer for energy harvesting and smart health monitoring, Nano Energy 122 (2024), https://doi.org/10.1016/j.nanoen.2024.109266.
[128] D. Kumar, D.W. Jin, D.G. Jeong, D.S. Kong, Y.C. Hu, S. Ko, K.-T. Lee, S. Yoon, J. Y. Park, J.H. Kim, J.H. Jung, Boosted triboelectric output performance in g-$C_3N_4$ embedded P(VDF-TrFE) composite via a coupling of photocarrier and ferroelectric dipole, Nano Energy 122 (2024), https://doi.org/10.1016/j.nanoen.2024.109320.
[129] F. Wang, S. Wang, Y. Liu, S. Ouyang, D. Sun, X. Yang, J. Li, Z. Wu, J. Qian, Z. Zhao, L. Wang, C. Jia, S. Ma, Cellulose nanofiber-based triboelectric nanogenerators for efficient air filtration in harsh environments, Nano Lett. 24 (2024) 2861–2869, https://doi.org/10.1021/acs.nanolett.3c05089.

[130] W. Zhang, Y. Lu, T. Liu, J. Zhao, Y. Liu, Q. Fu, J. Mo, C. Cai, S. Nie, Spheres multiple physical network-based triboelectric materials for self-powered contactless sensing, Small 18 (2022), https://doi.org/10.1002/smll.202200577.
[131] V.P. Kallupadi, H. Varghese, U.N.S. Hareesh, A. Chandran, Modulating contact electrification with metal-organic frameworks in flexible triboelectric nanogenerators for kinetic energy harvesting and self-powered humidity sensing applications, Adv. Funct. Mater. (2024), https://doi.org/10.1002/adfm.202411855.
[132] F. Wang, S. Wang, Y. Liu, T. Hou, Z. Wu, J. Qian, Z. Zhao, L. Wang, C. Jia, S. Ma, Improved electrical output performance of cellulose-based triboelectric nanogenerators enabled by negative triboelectric materials, Small 20 (2024), https://doi.org/10.1002/smll.202308195.
[133] A. Mahapatra, R.S. Ajimsha, D. Deepak, Sumit, R. Aggarwal, S. Kumar, R. Venkatesh, S.S. Roy, P. Misra, Textile-integrated MoS2-PDMS single electrode triboelectric nanogenerator for vibrational energy harvesting and biomechanical motion sensing, Nano Energy 116 (2023), https://doi.org/10.1016/j.nanoen.2023.108829.
[134] J. He, R. Wei, X. Ma, W. Wu, X. Pan, J. Sun, J. Tang, Z. Xu, C. Wang, C. Pan, Contactless user-interactive sensing display for human–human and human–machine interactions, Adv. Mater. 36 (2024) 2401931, https://doi.org/10.1002/adma.202401931.
[135] W. Cho, S. Kim, H. Lee, N. Han, H. Kim, M. Lee, T.H. Han, J.J. Wie, High-performance yet sustainable triboelectric nanogenerator based on sulfur-rich polymer composite with MXene segregated structure, Adv. Mater. 36 (2024), https://doi.org/10.1002/adma.202404163.
[136] Z. Fang, W. Lou, W. Zhang, X. Guan, J. He, J. Lin, Modulating crystallinity and dielectric constant of chitosan film for triboelectric polarity shift and performance enhancement in triboelectric nanogenerators, Nano Energy 117 (2023), https://doi.org/10.1016/j.nanoen.2023.108923.
[137] X. Zhao, Z. Ounaies, A facile method to enhance the flexibility and triboelectric output of PDMS using ionic liquid-coated single-wall carbon nanotubes, Nano Energy 94 (2022), https://doi.org/10.1016/j.nanoen.2021.106908.
[138] P. Pandey, D.-H. Jung, G.-J. Choi, M.-K. Seo, S. Lee, J.M. Kim, I.-K. Park, J.I. Sohn, Nafion-mediated barium titanate-polymer composite nanofibers-based triboelectric nanogenerator for self-powered smart street and home control system, Nano Energy 107 (2023), https://doi.org/10.1016/j.nanoen.2022.108134.
[139] X.-X. Wu, J.-J. Zhang, C.-H. Lee, M.-F. Lin, Enhanced triboelectric properties of Eu2O3-doped BaTiO3/PVDF-HFP nanofibers, Nanoscale 15 (2023) 3823–3831, https://doi.org/10.1039/d2nr05990h.
[140] Z.L. Wang, J. Song, Piezoelectric nanogenerators based on zinc oxide nanowire arrays, Science 312 (2006) 242–246, https://doi.org/10.1126/science.1124005.
[141] G.Y. Zhu, T.X. Zhang, M. Chen, K. Yao, X.Q. Huang, B. Zhang, Y.Z. Li, J. Liu, Y. B. Wang, Z.H. Zhao, Bone physiological microenvironment and healing mechanism: basis for future bone-tissue engineering scaffolds, Bioact. Mater. 6 (2021) 4110–4140, https://doi.org/10.1016/j.bioactmat.2021.03.043.
[142] H.P. Wei, J.J. Cui, K.L. Lin, J. Xie, X.D. Wang, Recent advances in smart stimuli-responsive biomaterials for bone therapeutics and regeneration, Bone Res. 10 (2022), https://doi.org/10.1038/s41413-021-00180-y.
[143] G.L. Koons, M. Diba, A.G. Mikos, Materials design for bone-tissue engineering, Nat. Rev. Mater. 5 (2020) 584–603, https://doi.org/10.1038/s41578-020-0204-2.
[144] Z. Li, G. Zhu, R. Yang, A.C. Wang, Z.L. Wang, Muscle-driven in vivo nanogenerator, Adv. Mater. 22 (2010) 2534–2537, https://doi.org/10.1002/adma.200904355.
[145] D.H. Kim, H.J. Shin, H. Lee, C.K. Jeong, H. Park, G.-T. Hwang, H.-Y. Lee, D.J. Joe, J.H. Han, S.H. Lee, J. Kim, B. Joung, K.J. Lee, In vivo self-powered wireless transmission using biocompatible flexible energy harvesters, Adv. Funct. Mater. 27 (2017) 1700341, https://doi.org/10.1002/adfm.201700341.
[146] L. Dong, A.B. Closson, M. Oglesby, D. Escobedo, X. Han, Y. Nie, S. Huang, M. D. Feldman, Z. Chen, J.X.J. Zhang, In vivo cardiac power generation enabled by an integrated helical piezoelectric pacemaker lead, Nano Energy 66 (2019) 104085, https://doi.org/10.1016/j.nanoen.2019.104085.
[147] Y. Zhang, L. Zhou, C. Liu, X. Gao, Z. Zhou, S. Duan, Q. Deng, L. Song, H. Jiang, L. Yu, S. Guo, H. Zheng, Self-powered pacemaker based on all-in-one flexible piezoelectric nanogenerator, Nano Energy 99 (2022) 107420, https://doi.org/10.1016/j.nanoen.2022.107420.
[148] M.A. Fernandez-Yague, A. Trotier, S. Demir, S.A. Abbah, A. Larrañaga, A. Thirumaran, A. Stapleton, S.A.M. Tofail, M. Palma, M. Kilcoyne, A. Pandit, M. J. Biggs, A self-powered piezo-bioelectric device regulates tendon repair-associated signaling pathways through modulation of mechanosensitive ion channels, Adv. Mater. 33 (2021) 2008788, https://doi.org/10.1002/adma.202008788.
[149] Y.Z. Zhang, L.L. Xu, Z. Liu, X. Cui, Z. Xiang, J.Y. Bai, D.J. Jiang, J.T. Xue, C. Wang, Y.X. Lin, Z. Li, Y.Z. Shan, Y. Yang, L. Bo, Z. Li, X.Z. Zhou, Self-powered pulsed direct current stimulation system for enhancing osteogenesis in $MC_3T_3$-E1, Nano Energy 85 (2021), https://doi.org/10.1016/j.nanoen.2021.106009.
[150] T. Vinikoor, G.K. Dzidotor, T.T. Le, Y. Liu, H.M. Kan, S. Barui, M.T. Chorsi, E. J. Curry, E. Reinhardt, H.Z. Wang, P. Singh, M.A. Merriman, E. D'Orio, J. Park, S. Y. Xiao, J.H. Chapman, F. Lin, C.S. Truong, S. Prasadh, L. Chuba, S. Killoh, S. W. Lee, Q. Wu, R.M. Chidambaram, K.W.H. Lo, C.T. Laurencin, T.D. Nguyen, Injectable and biodegradable piezoelectric hydrogel for osteoarthritis treatment, Nat. Commun. 14 (2023), https://doi.org/10.1038/s41467-023-41594-y.
[151] S. Wang, L. Lin, Z.L. Wang, Triboelectric nanogenerators as self-powered active sensors, Nano Energy 11 (2015) 436–462, https://doi.org/10.1016/j.nanoen.2014.10.034.
[152] T. Zheng, G. Li, L. Zhang, Y. Lei, Breathable, transparent, waterproof, flexible and high-output triboelectric nanogenerators for sport monitoring and speech recognition, JOURNAL OF Materials CHEMISTRY A 12 (2023) 495–508, https://doi.org/10.1039/d3ta05954e.
[153] J. Wan, S. Wang, Y. Liu, Y. Zong, H. Li, W. Chen, P. Li, Z. Chen, J. Huang, Highly flexible and transparent triboelectric nanogenerators toward reliable energy harvesting and recognition, Nano Energy 123 (2024), https://doi.org/10.1016/j.nanoen.2024.109377.
[154] S. Mishra, P. Supraja, D. Haranath, R.R. Kumar, S. Pola, Effect of surface and contact points modification on the output performance of triboelectric nanogenerator, Nano Energy 104 (2022), https://doi.org/10.1016/j.nanoen.2022.107964.
[155] D.-M. Lee, N. Rubab, I. Hyun, W. Kang, Y.-J. Kim, M. Kang, B.O. Choi, S.-W. Kim, Ultrasound-mediated triboelectric nanogenerator for powering on-demand transient electronics, Sci. Adv. 8 (2022), https://doi.org/10.1126/sciadv.abl8423.
[156] X. Hui, L. Tang, D. Zhang, S. Yan, D. Li, J. Chen, F. Wu, Z.L. Wang, H. Guo, Acoustically enhanced triboelectric stethoscope for ultrasensitive cardiac sounds sensing and disease diagnosis, Adv. Mater. 36 (2024), https://doi.org/10.1002/adma.202401508.
[157] R. Hinchet, H.-J. Yoon, H. Ryu, M.-K. Kim, E.-K. Choi, D.-S. Kim, S.-W. Kim, Transcutaneous ultrasound energy harvesting using capacitive triboelectric technology, SCIENCE 365 (2019), https://doi.org/10.1126/science.aan3997.
[158] S. Yao, M. Zheng, Z. Wang, Y. Zhao, S. Wang, Z. Liu, Z. Li, Y. Guan, Z.L. Wang, L. Li, Self-powered, implantable, and wirelessly controlled NO generation system for intracranial neuroglioma therapy, Adv. Mater. 34 (2022), https://doi.org/10.1002/adma.202205881.
[159] H. Li, Z. Wang, Y. Hu, G. He, L. Huang, Y. Liu, Z.L. Wang, P. Jiang, Enhancing CAR-T cell therapy against solid tumor by drug-free triboelectric immunotherapy, Biomaterials 314 (2025), https://doi.org/10.1016/j.biomaterials.2024.122871.
[160] L. Liu, X. Yang, L. Zhao, H. Hong, H. Cui, J. Duan, Q. Yang, Q. Tang, Nodding duck structure multi-track directional freestanding triboelectric nanogenerator toward low-frequency ocean wave energy harvesting, ACS Nano 15 (2021) 9412–9421, https://doi.org/10.1021/acsnano.1c00345.
[161] B. Meng, W. Tang, Z.-h. Too, X. Zhang, M. Han, W. Liu, H. Zhang, A transparent single-friction-surface triboelectric generator and self-powered touch sensor, Energy Environ. Sci. 6 (2013) 3235–3240, https://doi.org/10.1039/c3ee42311e.
[162] Y. Wu, Y. Luo, J. Qu, W.A. Daoud, T. Qi, Sustainable and shape-adaptable liquid single-electrode triboelectric nanogenerator for biomechanical energy harvesting, Nano Energy 75 (2020), https://doi.org/10.1016/j.nanoen.2020.105027.
[163] J. Liu, L. Zhou, Y. Gao, P. Yang, D. Liu, W. Qiao, B. Zhang, Z. Zhao, Z.L. Wang, J. Wang, Achieving ultra-high voltage (≈10 kV) triboelectric nanogenerators, Adv. Energy Mater. 13 (2023), https://doi.org/10.1002/aenm.202300410.
[164] S. Wang, L. Lin, Y. Xie, Q. Jing, S. Niu, Z.L. Wang, Sliding-triboelectric nanogenerators based on in-plane charge-separation mechanism, Nano Lett. 13 (2013) 2226–2233, https://doi.org/10.1021/nl400738p.
[165] Y. Gao, L. He, D. Liu, J. Zhang, L. Zhou, Z.L. Wang, J. Wang, Spontaneously established reverse electric field to enhance the performance of triboelectric nanogenerators via improving Coulombic efficiency, Nat. Commun. 15 (2024), https://doi.org/10.1038/s41467-024-48456-1.
[166] S. Yang, C. Zhang, Z. Du, Y. Tu, X. Dai, Y. Huang, J. Fan, Z. Hong, T. Jiang, Z. L. Wang, Fluid oscillation-driven Bi-directional air turbine triboelectric nanogenerator for ocean wave energy harvesting, Adv. Energy Mater. 14 (2024), https://doi.org/10.1002/aenm.202304184.
[167] X. Wang, L. Chen, Z. Xu, P. Chen, C. Ye, B. Chen, T. Jiang, Z. Hong, Z.L. Wang, High-durability stacked disc-type rolling triboelectric nanogenerators for environmental monitoring around charging buoys of unmanned ships, Small 20 (2024), https://doi.org/10.1002/smll.202310809.
[168] S. Wang, Y. Xie, S. Niu, L. Lin, Z.L. Wang, Freestanding triboelectric-layer-based nanogenerators for harvesting energy from a moving object or human motion in contact and non-contact modes, Adv. Mater. 26 (2014) 2818–2824, https://doi.org/10.1002/adma.201305303.
[169] H. Wang, J. Wang, R. Liao, L. Yang, H. Wu, Z.L. Wang, Detrapping current measurement system driven by triboelectric nanogenerators for mapping electron trap states in dielectrics, Adv. Funct. Mater. 31 (2021), https://doi.org/10.1002/adfm.202103463.
[170] S. Fu, S. Yi, Q. Ke, K. Liu, H. Xu, A self-powered hydrogel/nanogenerator system accelerates wound healing by electricity-triggered on-demand phosphatase and tensin homologue (PTEN) inhibition, ACS Nano 17 (2023) 19652–19666, https://doi.org/10.1021/acsnano.3c02561.
[171] W. Li, Z. Liu, X. Tan, N. Yang, Y. Liang, D. Feng, H. Li, R. Yuan, Q. Zhang, L. Liu, L. Ge, All-in-One self-powered microneedle device for accelerating infected diabetic wound repair, Adv. Healthcare Mater. 13 (2024), https://doi.org/10.1002/adhm.202304365.
[172] L. Zhao, Z. Gao, W. Liu, C. Wang, D. Luo, S. Chao, S. Li, Z. Li, C. Wang, J. Zhou, Promoting maturation and contractile function of neonatal rat cardiomyocytes by self-powered implantable triboelectric nanogenerator, Nano Energy 103 (2022), https://doi.org/10.1016/j.nanoen.2022.107798.
[173] D. Liu, X. Wang, C. Gao, Z. Zhang, Q. Wang, Y. Pei, H. Wang, Y. Tang, K. Li, Y. Yu, Q. Cai, X. Zhang, Biodegradable piezoelectric-conductive integrated hydrogel scaffold for repair of osteochondral defects, Adv. Mater. 36 (2024), https://doi.org/10.1002/adma.202409400.
[174] G. Li, Z. Li, Y. Min, S. Chen, R. Han, Z. Zhao, 3D-Printed piezoelectric scaffolds with shape memory polymer for bone regeneration, Small 19 (2023), https://doi.org/10.1002/smll.202302927.

[175] Q. Zheng, M. Peng, Z. Liu, S. Li, R. Han, H. Ouyang, Y. Fan, C. Pan, W. Hu, J. Zhai, Z. Li, Z.L. Wang, Dynamic real-time imaging of living cell traction force by piezo-phototronic light nano-antenna array, Sci. Adv. 7 (2021), https://doi.org/10.1126/sciadv.abe7738.
[176] Z. Che, S. O'Donovan, X. Xiao, X. Wan, G. Chen, X. Zhao, Y. Zhou, J. Yin, J. Chen, Implantable triboelectric nanogenerators for self-powered cardiovascular healthcare, Small 19 (2023), https://doi.org/10.1002/smll.202207600.
[177] H. Guo, D.-M. Lee, P. Zhao, S.-H. Kim, I. Hyun, B.-J. Park, J.-H. Lee, H. Sun, S.-W. Kim, Cell activity manipulation through optimizing piezoelectricity and polarization of diphenylalanine peptide nanotube-based nanocomposite, Chem. Eng. J. 468 (2023), https://doi.org/10.1016/j.cej.2023.143597.
[178] X. Meng, X. Xiao, S. Jeon, D. Kim, B.-J. Park, Y.-J. Kim, N. Rubab, S. Kim, S.-W. Kim, An ultrasound-driven bioadhesive triboelectric nanogenerator for instant wound sealing and electrically accelerated healing in emergencies, Adv. Mater. 35 (2023), https://doi.org/10.1002/adma.202209054.
[179] P. Chen, C. Cheng, X. Yang, T.-t. Sha, X. Zou, F. Zhang, W. Jiang, Y. Xu, X. Cao, Y.-M. You, Z. Luo, Wireless deep brain stimulation by ultrasound-responsive molecular piezoelectric nanogenerators, ACS Nano 17 (2023) 25625–25637, https://doi.org/10.1021/acsnano.3c10227.
[180] C. Xiao, L. Fan, S. Zhou, X. Kang, P. Guan, R. Fu, C. Li, J. Ren, Z. Wang, P. Yu, Y. Wang, C. Deng, L. Zhou, C. Ning, One-dimensional ferroelectric nanoarrays with wireless switchable static and dynamic electrical stimulation for selective regulating osteogenesis and antiosteosarcoma, ACS Nano 16 (2022) 20770–20785, https://doi.org/10.1021/acsnano.2c07900.
[181] Q. Zhang, J. Zhu, H. Liu, X. Fei, M. Zhu, Magneto-mechano-electric cascade stimulation system accelerates wound healing constructed by biodegradable magnetoelectric nanofibers, Adv. Funct. Mater. 34 (2024), https://doi.org/10.1002/adfm.202309968.
[182] Y. Wang, X. Li, Y. Chen, Y. Li, Z. Liu, C. Fang, T. Wu, H. Niu, Y. Li, W. Sun, W. Tang, W. Xia, K. Song, H. Liu, W. Zhou, Pulsed-laser-triggered piezoelectric photocatalytic $CO_2$ reduction over tetragonal $BaTiO_3$ nanocubes, Adv. Mater. 35 (2023), https://doi.org/10.1002/adma.202305257.
[183] Y. Chen, Y. Wang, J. Yu, G. Xiong, H. Niu, Y. Li, D. Sun, X. Zhang, H. Liu, W. Zhou, Underfocus laser induced Ni nanoparticles embedded metallic Mon microrods as patterned electrode for efficient overall water splitting, Adv. Sci. 9 (2022), https://doi.org/10.1002/advs.202105869.
[184] X. Qin, H. Shi, Z. Wen, B. Chu, H. Li, H. Wang, Y. He, X. Sun, Triboelectric-responsive drug delivery hydrogel for accelerating infected wound healing, Adv. Healthcare Mater. 13 (2024), https://doi.org/10.1002/adhm.202303474.
[185] Y. Yang, R. Luo, S. Chao, J. Xue, D. Jiang, Y.H. Feng, X.D. Guo, D. Luo, J. Zhang, Z. Li, Z.L. Wang, Improved pharmacodynamics of epidermal growth factor via microneedles-based self-powered transcutaneous electrical stimulation, Nat. Commun. 13 (2022), https://doi.org/10.1038/s41467-022-34716-5.
[186] H. Liu, M. Zhang, L. Zu, J. Wen, H. Li, F. Xing, M. Yan, Z.L. Wang, B. Chen, A biodegradable, triboelectric self-stimulated herbal transdermal therapeutic dressing for healing massive chronic wound, Nano Energy 125 (2024), https://doi.org/10.1016/j.nanoen.2024.109585.
[187] Z. Liu, Y. Hu, X. Qu, Y. Liu, S. Cheng, Z. Zhang, Y. Shan, R. Luo, S. Weng, H. Li, H. Niu, M. Gu, Y. Yao, B. Shi, N. Wang, W. Hua, Z. Li, Z.L. Wang, A self-powered intracardiac pacemaker in swine model, Nat. Commun. 15 (2024), https://doi.org/10.1038/s41467-023-44510-6.
[188] M. Zhou, M. Huang, H. Zhong, C. Xing, Y. An, R. Zhu, Z. Jia, H. Qu, S. Zhu, S. Liu, L. Wang, H. Ma, Z. Qu, G. Ning, S. Feng, Contact separation triboelectric nanogenerator based neural interfacing for effective sciatic nerve restoration, Adv. Funct. Mater. 32 (2022), https://doi.org/10.1002/adfm.202200269.
[189] T. Wang, H. Ouyang, Y. Luo, J. Xue, E. Wang, L. Zhang, Z. Zhou, Z. Liu, X. Li, S. Tan, Y. Chen, L. Nan, W. Cao, Z. Li, F. Chen, L. Zheng, Rehabilitation exercise-driven symbiotic electrical stimulation system accelerating bone regeneration, Sci. Adv. 10 (2024), https://doi.org/10.1126/sciadv.adi6799.
[190] X. Cui, Y. Shan, J. Li, M. Xiao, Y. Xi, J. Ji, E. Wang, B. Zhang, L. Xu, M. Zhang, Z. Li, Y. Zhang, Bifunctional piezo-enhanced PLLA/ZA coating prevents aseptic loosening of bone implants, Adv. Funct. Mater. 34 (2024), https://doi.org/10.1002/adfm.202403759.
[191] G. Murillo, A. Blanquer, C. Vargas-Estevez, L. Barrios, E. Ibáñez, C. Nogués, J. Esteve, Electromechanical nanogenerator–cell interaction modulates cell activity, Adv. Mater. 29 (2017) 1605048, https://doi.org/10.1002/adma.201605048.
[192] M. Kitsara, A. Blanquer, G. Murillo, V. Humblot, S. De Bragança Vieira, C. Nogués, E. Ibáñez, J. Esteve, L. Barrios, Permanently hydrophilic, piezoelectric PVDF nanofibrous scaffolds promoting unaided electromechanical stimulation on osteoblasts, Nanoscale 11 (2019) 8906–8917, https://doi.org/10.1039/C8NR10384D.
[193] M. Polak, K. Berniak, P.K. Szewczyk, J.E. Karbowniczek, M.M. Marzec, U. Stachewicz, PLLA scaffolds with controlled surface potential and piezoelectricity for enhancing cell adhesion in tissue engineering, Appl. Surf. Sci. 621 (2023) 156835, https://doi.org/10.1016/j.apsusc.2023.156835.
[194] Z. Liu, M. Cai, X. Zhang, X. Yu, S. Wang, X. Wan, Z.L. Wang, L. Li, Cell-traction-triggered on-demand electrical stimulation for neuron-like differentiation, Adv. Mater. 33 (2021) 2106317, https://doi.org/10.1002/adma.202106317.
[195] L. Sun, X. Chen, K. Ma, R. Chen, Y. Mao, R. Chao, H. Wang, B. Yu, J. Wang, S. Zhang, Novel titanium implant: a 3D multifunction architecture with charge-trapping and piezoelectric self-stimulation, Adv. Healthcare Mater. 12 (2023), https://doi.org/10.1002/adhm.202202620.
[196] T. Kim, H.J. Kim, W. Choi, Y.M. Lee, J.H. Pyo, J. Lee, J. Kim, J. Kim, J.-H. Kim, C. Kim, W.J. Kim, Deep brain stimulation by blood-brain-barrier-crossing piezoelectric nanoparticles generating current and nitric oxide under focused ultrasound, Nat. Biomed. Eng. 7 (2023), https://doi.org/10.1038/s41551-022-00965-4.
[197] L. Cai, J. Du, F. Han, T. Shi, H. Zhang, Y. Lu, S. Long, W. Sun, J. Fan, X. Peng, Piezoelectric metal-organic frameworks based sonosensitizer for enhanced nanozyme catalytic and sonodynamic therapies, ACS Nano 17 (2023) 7901–7910, https://doi.org/10.1021/acsnano.3c01856.
[198] D. Xu, S. Fu, H. Zhang, W. Lu, J. Xie, J. Li, H. Wang, Y. Zhao, R. Chai, Ultrasound-responsive aligned piezoelectric nanofibers derived hydrogel conduits for peripheral nerve regeneration, Adv. Mater. 36 (2024), https://doi.org/10.1002/adma.202307896.
[199] X. Cui, L. Wu, C. Zhang, Z. Li, Implantable self-powered systems for electrical stimulation medical devices, Adv. Sci. (2024) 2412044, https://doi.org/10.1002/advs.202412044 n/a.
[200] B. Singh, Q.-G. Xu, C.K. Franz, R. Zhang, C. Dalton, T. Gordon, V.M.K. Verge, R. Midha, D.W. Zochodne, Accelerated axon outgrowth, guidance, and target reinnervation across nerve transection gaps following a brief electrical stimulation paradigm: laboratory investigation, Journal of Neurosurgery JNS 116 (2012) 498–512, https://doi.org/10.3171/2011.10.JNS11612.
[201] Y. Shan, L. Xu, X. Cui, E. Wang, F. Jiang, J. Li, H. Ouyang, T. Yin, H. Feng, D. Luo, Y. Zhang, Z. Li, A responsive cascade drug delivery scaffold adapted to the therapeutic time window for peripheral nerve injury repair, Mater. Horiz. 11 (2024) 1032–1045, https://doi.org/10.1039/d3mh01511d.
[202] P. Chen, C. Xu, P. Wu, K. Liu, F. Chen, Y. Chen, H. Dai, Z. Luo, Wirelessly powered electrical-stimulation based on biodegradable 3D piezoelectric scaffolds promotes the spinal cord injury repair, ACS Nano 16 (2022) 16513–16528, https://doi.org/10.1021/acsnano.2c05818.
[203] F. Jin, T. Li, T. Yuan, L. Du, C. Lai, Q. Wu, Y. Zhao, F. Sun, L. Gu, T. Wang, Z.-Q. Feng, Physiologically self-regulated, fully implantable, battery-free system for peripheral nerve restoration, Adv. Mater. 33 (2021) 2104175, https://doi.org/10.1002/adma.202104175.
[204] T. Wang, H. Ouyang, Y. Luo, J. Xue, E. Wang, L. Zhang, Z. Zhou, Z. Liu, X. Li, S. Tan, Y. Chen, L. Nan, W. Cao, Z. Li, F. Chen, L. Zheng, Rehabilitation exercise–driven symbiotic electrical stimulation system accelerating bone regeneration, Sci. Adv.,10 eadi6799, https://doi.org/10.1126/sciadv.adi6799.
[205] Y. Liu, G. Dzidotor, T.T. Le, T. Vinikoor, K. Morgan, E.J. Curry, R. Das, A. McClinton, E. Eisenberg, L.N. Apuzzo, K.T.M. Tran, P. Prasad, T.J. Flanagan, S.-W. Lee, H.-M. Kan, M.T. Chorsi, K.W.H. Lo, C.T. Laurencin, T.D. Nguyen, Exercise-induced piezoelectric stimulation for cartilage regeneration in rabbits,Sci. Transl. Med., 14 eabi7282, https://doi.org/10.1126/scitranslmed.abi7282.
[206] D. Liu, L. Li, B.-L. Shi, B. Shi, M.-D. Li, Y. Qiu, D. Zhao, Q.-D. Shen, Z.-Z. Zhu, Ultrasound-triggered piezocatalytic composite hydrogels for promoting bacterial-infected wound healing, Bioact. Mater. 24 (2023) 96–111, https://doi.org/10.1016/j.bioactmat.2022.11.023.
[207] R. Lin, Y. Fan, Y. Xie, D. Ge, S. Liang, H. Guan, M. Chen, Y. Zhang, L. Xing, X. Xue, Y. Zhan, A self-powered wearable seizure-monitoring/brain-stimulating system for potential epilepsy treatment, Nano Energy 107 (2023) 108121, https://doi.org/10.1016/j.nanoen.2022.108121.
[208] H. Ouyang, Z. Liu, N. Li, B. Shi, Y. Zou, F. Xie, Y. Ma, Z. Li, H. Li, Q. Zheng, X. Qu, Y. Fan, Z.L. Wang, H. Zhang, Z. Li, Symbiotic cardiac pacemaker, Nat. Commun. 10 (2019) 1821, https://doi.org/10.1038/s41467-019-09851-1.
[209] T. Jing, X. Tao, T. Li, Z. Li, H. Zhang, G. Huang, Z. Jin, J. Xu, C. Xie, S. Qu, Magnetostriction enhanced self-powered nanofiber sheet as cardiac patch with magnetoelectric synergistic effect on actuating Na+ k+-ATPase, Chem. Eng. J. 490 (2024) 151791, https://doi.org/10.1016/j.cej.2024.151791.
[210] Q. Fang, D. Wang, W. Lin, Z. Ge, X. Deng, R. Zhao, Y. Tang, W. Liu, Z. Xiong, A. Duan, Z. Zhang, Y. Xiang, X. Hu, G. Wang, Highly stretchable piezoelectric elastomer for accelerated repairing of skeletal muscles loss, Adv. Funct. Mater. 34 (2024) 2313055, https://doi.org/10.1002/adfm.202313055.
[211] C.A.L. Bassett, S.N. Mitchell, S.R. Gaston, Treatment of ununited tibial diaphyseal fractures with pulsing electromagnetic-fields, J. Bone Joint Surg. 63 (1981) 511–523, https://doi.org/10.2106/00004623-198163040-00001.
[212] T. Wang, H. Ouyang, Y. Luo, J. Xue, E. Wang, L. Zhang, Z. Zhou, Z. Liu, X. Li, S. Tan, Y. Chen, L. Nan, W. Cao, Z. Li, F. Chen, L. Zheng, Rehabilitation exercise-driven symbiotic electrical stimulation system accelerating bone regeneration, Sci. Adv. 10 (2024), https://doi.org/10.1126/sciadv.adi6799, 6799-6799.
[213] X. Cui, L. Xu, Y. Shan, J. Li, J. Ji, E. Wang, B. Zhang, X. Wen, Y. Bai, D. Luo, C. Chen, Z. Li, Piezocatalytically-induced controllable mineralization scaffold with bone-like microenvironment to achieve endogenous bone regeneration, Sci. Bull. 69 (2024) 1895–1908, https://doi.org/10.1016/j.scib.2024.04.002.
[214] C.D. McCaig, A.M. Rajnicek, B. Song, M. Zhao, Controlling cell behavior electrically: current views and future potential, Physiol. Rev. 85 (2005) 943–978, https://doi.org/10.1152/physrev.00020.2004.
[215] C. Martin-Granados, C.D. McCaig, Harnessing the electric spark of life to cure skin wounds, Adv. Wound Care 3 (2013) 127–138, https://doi.org/10.1089/wound.2013.0451.
[216] R. Luo, J. Dai, J. Zhang, Z. Li, Accelerated skin wound healing by electrical stimulation, Adv. Healthcare Mater. 10 (2021) 2100557, https://doi.org/10.1002/adhm.202100557.
[217] B. Reid, M. Zhao, The electrical response to injury: molecular mechanisms and wound healing, Adv. Wound Care 3 (2013) 184–201, https://doi.org/10.1089/wound.2013.0442.
[218] R. Luo, Y. Liang, J. Yang, H. Feng, Y. Chen, X. Jiang, Z. Zhang, J. Liu, Y. Bai, J. Xue, S. Chao, Y. Xi, X. Liu, E. Wang, D. Luo, Z. Li, J. Zhang, Reshaping the endogenous electric field to boost wound repair via electrogenerative dressing, Adv. Mater. 35 (2023) 2208395, https://doi.org/10.1002/adma.202208395.

[219] Z. Sun, Y. Jin, J. Luo, L. Li, Y. Ding, Y. Luo, Y. Qi, Y. Li, Q. Zhang, K. Li, H. Shi, S. Yin, H. Wang, H. Wang, C. Hou, A bioabsorbable mechanoelectric fiber as electrical stimulation suture, Nat. Commun. 15 (2024) 8462, https://doi.org/10.1038/s41467-024-52354-x.
[220] S.R. Patel, C.M. Lieber, Precision electronic medicine in the brain, Nat. Biotechnol. 37 (2019) 1007–1012, https://doi.org/10.1038/s41587-019-0234-8.
[221] R. Sitaram, T. Ros, L. Stoeckel, S. Haller, F. Scharnowski, J. Lewis-Peacock, N. Weiskopf, M.L. Blefari, M. Rana, E. Oblak, N. Birbaumer, J. Sulzer, Closed-loop brain training: the science of neurofeedback, Nat. Rev. Neurosci. 18 (2017) 86–100, https://doi.org/10.1038/nrn.2016.164.
[222] X. Cui, L. Wu, C. Zhang, Z. Li, Implantable self-powered systems for electrical stimulation medical devices, Adv. Sci. (2024), https://doi.org/10.1002/advs.202412044.
[223] A.M. Lozano, N. Lipsman, H. Bergman, P. Brown, S. Chabardes, J.W. Chang, K. Matthews, C.C. McIntyre, T.E. Schlaepfer, M. Schulder, Y. Temel, J. Volkmann, J.K. Krauss, Deep brain stimulation: current challenges and future directions, Nat. Rev. Neurol. 15 (2019) 148–160, https://doi.org/10.1038/s41582-018-0128-2.
[224] M. Dümpelmann, Early seizure detection for closed loop direct neurostimulation devices in epilepsy, J. Neural. Eng. 16 (2019) 041001, https://doi.org/10.1088/1741-2552/ab094a.
[225] O.G. Sani, Y. Yang, M.B. Lee, H.E. Dawes, E.F. Chang, M.M. Shanechi, Mood variations decoded from multi-site intracranial human brain activity, Nat. Biotechnol. 36 (2018) 954–961, https://doi.org/10.1038/nbt.4200.
[226] T. Zhao, Y. Han, L. Qin, H. Guan, L. Xing, X. Li, X. Xue, G. Li, Y. Zhan, Bidirectional modulation of neural plasticity by self-powered neural stimulation, Nano Energy 85 (2021) 106006, https://doi.org/10.1016/j.nanoen.2021.106006.
[227] T. Kim, H.J. Kim, W. Choi, Y.M. Lee, J.H. Pyo, J. Lee, J. Kim, J. Kim, J.-H. Kim, C. Kim, W.J. Kim, Deep brain stimulation by blood–brain-barrier-crossing piezoelectric nanoparticles generating current and nitric oxide under focused ultrasound, Nat. Biomed. Eng. 7 (2023) 149–163, https://doi.org/10.1038/s41551-022-00965-4.
[228] S.K. Mulpuru, M. Madhavan, C.J. McLeod, Y.-M. Cha, P.A. Friedman, Cardiac pacemakers: function, troubleshooting, and management Part 1 of a 2-Part Series, J. Am. Coll. Cardiol. 69 (2017) 189–210, https://doi.org/10.1016/j.jacc.2016.10.061.
[229] M. Madhavan, S.K. Mulpuru, C.J. McLeod, Y.-M. Cha, P.A. Friedman, Advances and future directions in cardiac pacemakers Part 2 of a 2-Part Series, J. Am. Coll. Cardiol. 69 (2017) 211–235, https://doi.org/10.1016/j.jacc.2016.10.064.
[230] A. Pfenniger, M. Jonsson, A. Zurbuchen, V.M. Koch, R. Vogel, Energy harvesting from the cardiovascular system, or how to get a little help from yourself, Ann. Biomed. Eng. 41 (2013) 2248–2263, https://doi.org/10.1007/s10439-013-0887-2.
[231] V. Parsonnet, M.M. Asa, H. Lotman, I.R. Zucker, G.H. Myers, The potentiality of the use of biologic energy as A power source for implantable pacemakers, Ann. N. Y. Acad. Sci. 9 (1963), https://doi.org/10.1111/j.1749-6632.1963.tb00033.x, 174-&.
[232] S. Jin, H. Choi, D. Seong, C.-L. You, J.-S. Kang, S. Rho, W.B. Lee, D. Son, M. Shin, Injectable tissue prosthesis for instantaneous closed-loop rehabilitation, Nature 623 (2023) 58–65, https://doi.org/10.1038/s41586-023-06628-x.
[233] S. Derhambakhsh, J. Mohammadi, M.A. Shokrgozar, H. Rabbani, N. Sadeghi, H. Nekounam, S. Mohammadi, K.-B. Lee, M. Khakbiz, Investigation of electrical stimulation on phenotypic vascular smooth muscle cells differentiation in tissue-engineered small-diameter vascular graft, Tissue Cell 81 (2023) 101996, https://doi.org/10.1016/j.tice.2022.101996.
[234] T. Dvir, B.P. Timko, M.D. Brigham, S.R. Naik, S.S. Karajanagi, O. Levy, H. Jin, K. K. Parker, R. Langer, D.S. Kohane, Nanowired three-dimensional cardiac patches, Nat. Nanotechnol. 6 (2011) 720–725, https://doi.org/10.1038/nnano.2011.160.
[235] H. Sun, J. Tang, Y. Mou, J. Zhou, L. Qu, K. Duval, Z. Huang, N. Lin, R. Dai, C. Liang, Z. Chen, L. Tang, F. Tian, Carbon nanotube-composite hydrogels promote intercalated disc assembly in engineered cardiac tissues through β1-integrin mediated FAK and RhoA pathway, Acta Biomater. 48 (2017) 88–99, https://doi.org/10.1016/j.actbio.2016.10.025.
[236] J.H. Lee, W.-Y. Jeon, H.-H. Kim, E.-J. Lee, H.-W. Kim, Electrical stimulation by enzymatic biofuel cell to promote proliferation, migration and differentiation of muscle precursor cells, Biomaterials 53 (2015) 358–369, https://doi.org/10.1016/j.biomaterials.2015.02.062.
[237] P.M. Martins, S. Ribeiro, C. Ribeiro, V. Sencadas, A.C. Gomes, F.M. Gama, S. Lanceros-Méndez, Effect of poling state and morphology of piezoelectric poly (vinylidene fluoride) membranes for skeletal muscle tissue engineering, RSC Adv. 3 (2013) 17938–17944, https://doi.org/10.1039/C3RA43499K.
[238] J.-K. Yoon, M. Misra, S.J. Yu, H.Y. Kim, S.H. Bhang, S.Y. Song, J.-R. Lee, S. Ryu, Y. W. Choo, G.-J. Jeong, S.P. Kwon, S.G. Im, T.I. Lee, B.-S. Kim, Thermosensitive, stretchable, and piezoelectric substrate for generation of myogenic cell sheet fragments from human mesenchymal stem cells for skeletal muscle regeneration, Adv. Funct. Mater. 27 (2017) 1703853, https://doi.org/10.1002/adfm.201703853.
[239] S. Ribeiro, C. Ribeiro, E.O. Carvalho, C.R. Tubio, N. Castro, N. Pereira, V. Correia, A.C. Gomes, S. Lanceros-Méndez, Magnetically activated electroactive microenvironments for skeletal muscle tissue regeneration, ACS Appl. Bio Mater. 3 (2020) 4239–4252, https://doi.org/10.1021/acsabm.0c00315.
[240] L. Jiang, Y. Yang, R. Chen, G. Lu, R. Li, J. Xing, K.K. Shung, M.S. Humayun, J. Zhu, Y. Chen, Q. Zhou, Ultrasound-induced wireless energy harvesting for potential retinal electrical stimulation application, Adv. Funct. Mater. 29 (2019) 1902522, https://doi.org/10.1002/adfm.201902522.
[241] F. Mokhtari, S. Danti, B. Azimi, F. Hellies, E. Zanoletti, G. Albertin, L. Astolfi, R. J. Varley, J.M. Razal, Self-powered nanostructured piezoelectric filaments as advanced transducers for new cochlear implants, Energy Environ. Mater. (2024) e12807, https://doi.org/10.1002/eem2.12807 n/a.
[242] C.-H. Mac, H.-M. Tai, S.-M. Huang, H.-H. Peng, A.K. Sharma, G.L.T. Nguyen, P.-J. Chang, J.-T. Wang, Y. Chang, Y.-J. Lin, H.-W. Sung, Orally ingested self-powered stimulators for targeted gut–brain Axis electrostimulation to treat obesity and metabolic disorders, Adv. Mater. 36 (2024) 2310351, https://doi.org/10.1002/adma.202310351.
[243] Y. Sun, S. Chao, H. Ouyang, W. Zhang, W. Luo, Q. Nie, J. Wang, C. Luo, G. Ni, L. Zhang, J. Yang, H. Feng, G. Mao, Z. Li, Hybrid nanogenerator based closed-loop self-powered low-level vagus nerve stimulation system for atrial fibrillation treatment, Sci. Bull. 67 (2022) 1284–1294, https://doi.org/10.1016/j.scib.2022.04.002.
[244] Y. Yin, P. Zhao, X. Xu, B. Zhou, J. Chen, X. Jiang, Y. Liu, Y. Wu, W. Yue, H. Xu, W. Bu, Piezoelectric analgesia blocks cancer-induced bone pain, Adv. Mater. 36 (2024) 2403979, https://doi.org/10.1002/adma.202403979.
[245] H. Zhao, S. Xue, M.-D. Hussherr, A.P. Teixeira, M. Fussenegger, Autonomous push button–controlled rapid insulin release from a piezoelectrically activated subcutaneous cell implant, Sci. Adv. 8 eabm4389, https://doi.org/10.1126/sciadv.abm4389.
[246] P. Adhikary, M.A.P. Mahmud, T. Solaiman, Z. Lin, Recentadvances on biomechanical motion-driven triboelectric nanogenerators for drug delivery, Nano Today 45 (2022), https://doi.org/10.1016/j.nantod.2022.101513.
[247] Y. Yang, L. Xu, D. Jiang, B.Z. Chen, R. Luo, Z. Liu, X. Qu, C. Wang, Y. Shan, Y. Cui, H. Zheng, Z. Wang, Z.L. Wang, X.D. Guo, Z. Li, Self-powered controllable transdermal drug delivery system, Adv. Funct. Mater. 31 (2021), https://doi.org/10.1002/adfm.202104092.
[248] S. Yao, Q. Wu, S. Wang, Y. Zhao, Z. Wang, Q. Hu, L. Li, H. Liu, Self-driven electric field control of orbital electrons in AuPd alloy nanoparticles for cancer catalytic therapy, Small 20 (2024), https://doi.org/10.1002/smll.202307087.
[249] T. Zhang, Y. Zheng, H. Xiang, Y. Chen, R. Wu, Cascade piezocatalytic nanoprodrug for synergistic piezocatalytic therapy and sono-activated chemotherapy-augmented immunotherapy, Nano Today 58 (2024), https://doi.org/10.1016/j.nantod.2024.102453.
[250] S. Zhong, S. Yao, Q. Zhao, Z. Wang, Z. Liu, L. Li, Z.L. Wang, Electricity-assisted cancer therapy: from traditional clinic applications to emerging methods integrated with nanotechnologies, Advanced NanoBiomed Research 3 (2023) 2200143, https://doi.org/10.1002/anbr.202200143.
[251] Z.S. Pedraza, Y. Wang, C. Carlos, Z. Tang, J. Li, W. Cai, X. Wang, Development of ferroelectric P(VDF-TrFE) microparticles for ultrasound-driven cancer cell killing, ACS Appl. Mater. Interfaces 15 (2023) 54304–54311, https://doi.org/10.1021/acsami.3c13410.
[252] C. Wang, G. He, H. Zhao, Y. Lu, P. Jiang, W. Li, Enhancing deep-seated melanoma therapy through wearable self-powered microneedle patch, Adv. Mater. 36 (2024), https://doi.org/10.1002/adma.202311246.
[253] C. Zhao, H. Feng, L. Zhang, Z. Li, Y. Zou, P. Tan, H. Ouyang, D. Jiang, M. Yu, C. Wang, H. Li, L. Xu, W. Wei, Z. Li, Highly efficient in vivo cancer therapy by an implantable magnet triboelectric nanogenerator, Adv. Funct. Mater. 29 (2019), https://doi.org/10.1002/adfm.201808640.
[254] S. Yao, X. Zhao, X. Wang, T. Huang, Y. Ding, J. Zhang, Z. Zhang, Z.L. Wang, L. Li, Bioinspired electron polarization of nanozymes with a human self-generated electric field for cancer catalytic therapy, Adv. Mater. 34 (2022), https://doi.org/10.1002/adma.202109568.
[255] B. Tian, R. Tian, S. Liu, Y. Wang, S. Gai, Y. Xie, D. Yang, F. He, P. Yang, J. Lin, Doping engineering to modulate lattice and electronic structure for enhanced piezocatalytic therapy and ferroptosis, Adv. Mater. 35 (2023), https://doi.org/10.1002/adma.202304262.
[256] S. Yao, S. Wang, M. Zheng, Z. Wang, Z. Liu, Z.L. Wang, L. Li, Implantable, biodegradable, and wireless triboelectric devices for cancer therapy through disrupting microtubule and actins dynamics, Adv. Mater. 35 (2023), https://doi.org/10.1002/adma.202303962.
[257] H. Li, C. Chen, Z. Wang, Y. Huang, G. He, Y. Liu, P. Jiang, Z.L. Wang, Triboelectric immunotherapy using electrostatic-breakdown induced direct-current, Mater. Today 64 (2023) 40–51, https://doi.org/10.1016/j.mattod.2023.02.026.
[258] S. Yao, M. Zheng, S. Wang, T. Huang, Z. Wang, Y. Zhao, W. Yuan, Z. Li, Z.L. Wang, L. Li, Self-driven electrical stimulation promotes cancer catalytic therapy based on fully conjugated covalent organic framework nanocages, Adv. Funct. Mater. 32 (2022), https://doi.org/10.1002/adfm.202209142.
[259] S. Yao, X. Zhao, X. Wan, X. Wang, T. Huang, J. Zhang, L. Li, π–π conjugation promoted nanocatalysis for cancer therapy based on a covalent organic framework, Mater. Horiz. 8 (2021) 3457–3467, https://doi.org/10.1039/D1MH01273H.
[260] S. Yao, Z. Liu, L. Li, Recent progress in nanoscale covalent organic frameworks for cancer diagnosis and therapy, Nano-Micro Lett. 13 (2021) 176, https://doi.org/10.1007/s40820-021-00696-2.
[261] S. Shen, J. Fu, J. Yi, L. Ma, F. Sheng, C. Li, T. Wang, C. Ning, H. Wang, K. Dong, Z. L. Wang, High-efficiency wastewater purification system based on coupled

photoelectric-catalytic action provided by triboelectric nanogenerator, Nano-Micro Lett. 13 (2021), https://doi.org/10.1007/s40820-021-00695-3.
[262] Q. Truong Hoang, D.Y. Kim, H.S. Park, W. Jang, T.G. Nguyen Cao, J.H. Kang, Y. T. Ko, S.J. Mun, S.H. Bhang, M.S. Shim, K.W. Bang, Oxygen-supplying piezocatalytic therapy of hypoxic tumors by intratumoral delivery of pH-responsive multicompartmental carriers with sequential drug release capability, Adv. Funct. Mater. 34 (2024), https://doi.org/10.1002/adfm.202306078.
[263] H. Quan Truong, V. Ravichandran, C. Thuy Giang Nguyen, J.H. Kang, Y.T. Ko, T. I. Lee, M.S. Shim, Piezoelectric Au-decorated ZnO nanorods: ultrasound-triggered generation of ROS for piezocatalytic cancer therapy, Chem. Eng. J. 435 (2022), https://doi.org/10.1016/j.cej.2022.135039.